Computational Studies of Some Pericyclic Reactions

HO Ho-On

A Thesis Submitted in Partial Fulfilment

of the Requirements for the Degree of

Master of Philosophy

in

Chemistry

August 2004

Thesis Examination Committee

Internal Examiners

Professor W. K. Li (Supervisor)
Department of Chemistry
The Chinese University of Hong Kong
Hong Kong SAR, China

Professor K. S. Chan (Chairman)
Department of Chemistry
The Chinese University of Hong Kong
Hong Kong SAR, China

Professor T. C. W. Mak
Department of Chemistry
The Chinese University of Hong Kong
Hong Kong SAR, China

External Examiner

Professor G. H. Chen
Department of Chemistry
The University of Hong Kong
Hong Kong SAR, China

Computational Studies of Some Pericyclic Reactions

Abstract

The Gaussian-3 (G3) model and its variant G3(MP2) have been applied to investigate the following pericylic reactions: (i) the cycloaddition reaction between ethylene and butadiene; (ii) the cycloaddition reaction between ethylene and hexatriene; (iii) the electrocyclic reaction of hexatriene; (iv) the electrocyclic reactions of [12]annulene and (v) the concerted cycloaddition reactions between ethylene and azines as well as other related heterocyclic aromatic systems.

In the appendices, we also report the structural, energetics, and bonding studies of phosphabenzene and arsabenzene, as well as those of hexamethylenetetramine (HMT) and related systems. These studies have also been carried out using the G3/G3(MP2) levels of theory.

Most of our calculated results are in excellent agreement with available experimental data. This excellent agreement lends confidence and reliability to those results which have no experimental data available as well as to the reaction pathways proposed.

Submitted by HO Ho-On

for the degree of Master of Philosophy in Chemistry

at The Chinese University of Hong Kong in (August 2004)

一些周環反應的理論計算研究

論文摘要

本論文採用Gaussian-3(G3)和G3(MP2)理論計算方法系統地研究以下的化學反應 (1)乙烯與丁二烯的環加成反應；(2)乙烯與己三烯的環加成反應；(3)己三烯的電環化反應；(4)[12]輪烯的電環化反應，及(5)乙烯與連氮系列和其他相關體系的環加成反應。此外，我們在附錄中研究了(1)磷苯和砷苯化合物，及(2)環六甲基四胺及其相關體系的結構 、穩定性和化學鍵。

我們計算得的結果與實驗數據有令人滿意的符合。本論文的研究表明對某些缺乏實驗數據的反應和體系，我們可通過類似的理論取得可靠的數值結果。此外， 本論文的結果對周環反應途徑的設計具有指導作用。

Acknowledgments

I am very much indebted to my supervisor, Professor Wai–Kee Li, whose guidance, invaluable advises and encouragement have made this thesis possible.

I also wish to thank my fellow students and colleagues in Rooms 225A and 225B, Science Center (North Block), at the Chinese University of Hong Kong, for their helpful discussions and support.

Table of Contents

Thesis Committee		i
Abstract		ii
Acknowledgements		iv
Table of Contents		v
Chapter 1	**Introduction**	1
	1.1 The Gaussian-3 Method	1
	1.2 The G3 Method with Reduced Mϕller-Plesset Order and Basis Set	2
	1.3 Calculation of Thermodynamical Data	2
	1.4 Remark on the Location of Transition Structures	3
	1.5 Natural Bond Orbital (NBO) Analysis	3
	1.6 Scope of the Thesis	4
	1.7 References	4
Chapter 2	**The Important Basic Concepts of Ab Initio Calculations and Their Application to Pericyclic Reactions**	6
	2.1 Potential Energy Surfaces	6
	2.2 Ab Initio Method	6
	2.2.1 Basic Sets	7
	2.2.2 Correlation Methods	8
	2.3 Pericyclic Reaction	10
	2.4 The Perturbation Theory of Reactivity	10
	2.5 References	11
Chapter 3	**Ab Initio Study of the Cycloaddition Reaction between Ethylene and Butadiene as well as That between Ethylene and Hexatriene**	13
	3.1 Introduction	13
	3.2 Methods of Calculation	15
	3.3 Results and Discussion	15
	3.3.1 Reaction between ethylene and butadiene	30
	3.3.2 Reaction between ethylene and hexatriene	34
	3.3.3 Electrocyclic reaction of hexatriene	37
	3.4 Conclusion	40
	3.5 References	41
Chapter 4	**A G3(MP2) Study on the Electrocyclic Reactions of [12]annulene**	43
	4.1 Introduction	43
	4.2 Methods of Calculation	44
	4.3 Results and Discussion	45
	4.4 Summary	51
	4.5Conclusion	52
	4.6 References	52

Chapter 5	**A G3(MP2) Study on the Cycloaddition Reactions between Ethylene and Azines as well as Other Related Systems**	54
	5.1 Introduction	54
	5.2 Methods of Calculation	55
	5.3 Results and Discussion	55
	5.3.1 Addition of ethylene to azines	55
	5.3.2 Addition of ethylene to quinolene, isoquinolene and 1,8-naphthyridine	64
	5.4 Conclusion	70
	5.5 References	70
Chapter 6	**Conclusion**	72
Appendix A	**Energetic and Bonding Investigation of Phosphabenzene and Arsabenzene: A Gaussian-3 Study**	73
	A.1 Introduction	73
	A.2 Methods of Calculation	73
	A.3 Results and Discussion	74
	A.4 Conclusion	77
	A.5 References	77
Appendix B	**Energetic and Bonding Study of Hexamethylenetetramine (HMT) and Fourteen Related Cage Molecules: A G3(MP2) Investigation**	79
	B.1 Introduction	79
	B.2 Methods of Calculation	80
	B.3 Results and Discussion	80
	B.4 Conclusion	87
	B.5 References	87
Appendix C	**The Gaussian-3 Theoretical Models**	89
	C.1 The G3 Theory	89
	C.2 The G3(MP2) Theory	90
Appendix D	**Calculation of Enthalpy at 298 K, H_{298}**	91

Chapter 1
Introduction

Providing an accurate and reliable prediction of energetics for molecular systems and reaction mechanisms are the main objectives in computational chemistry. In order to achieve these goals, a number of theoretical procedures have been proposed. In recent years, Pople and his co-workers introduced a series of ab initio methods, the Gaussian-n (Gn) models,[1-11] to achieve these purposes. Their aim is to develop a general procedure for accurate energies applicable for a variety of molecular systems. The Gn models, based on a series of additivity approximations,[8,9] consist of a sequence of well-defined single-point calculations to provide an accurate prediction on the energetics of a given molecular system. The theoretical Gn models include: Gaussian-1 (G1),[1,2] Gaussian- (G2),[3,4] and Gaussian-3 (G3)[5-7] levels of theory and their less expensive variants. Applying these theoretical procedures, the calculated energies of the molecular systems are expected to have an average absolute deviation from experiment of the order of 10-15 kJ mol^{-1} (or ~2-3 kcal mol^{-1}).

Since the G1 and G2 models are more computationally demanding and yield less accurate results than G3, these methods have not been applied to the selected chemical systems presented in this thesis. In this thesis, we employ only the G3 method and its variant G3(MP2)[6] to study the structures and energetics of some selected reactions and chemical systems.

1.1 The Gaussian-3 Method

The G3 energy is an approximation of the molecular energy at the QCISD(T)/G3large level, where G3large is a modified 6-311+G(3df,2p) basis set. In the G3 model, structures are optimized at the second-order Møller-Plesset theory (MP2) using the 6-31G(d) basis set with all electrons included, i.e., at the MP2(Full)/6-31G(d) level. Based on these optimized structures, single-point calculations at the QCISD(T)/6-31G(d), MP4/6-31G(d), MP4/6-31+G(d), MP4/6-31G(2df,p), and MP2(Full)/G3large levels are required. Also, this model requires higher level correction (HLC) in the calculation of total electronic energies (E_e). The

HLC is $-6.386 \times 10^{-3} n_\beta - 2.977 \times 10^{-3}(n_\alpha - n_\beta)$ for molecules and $-6.219 \times 10^{-3} n_\beta - 1.185 \times 10^{-3}(n_\alpha - n_\beta)$ for atoms, in which n_α and n_β are the number of α and β electrons, respectively, with $n_\alpha \geq n_\beta$. The MP2(Full)/6-31G(d) harmonic vibrational frequencies, scaled by a factor of 0.9661, are applied for the zero-point vibrational energy (ZPVE) correction at 0 K ($E_0 = E_e + \text{ZPVE}$).

The G3 theory has been used to calculate molecular energies, such as atomization energies,[2-9] ionization energies,[2,10] proton affinities,[2,10] and electron affinities[2] of 125 molecules for which these quantities have been well established experimentally. The average absolute deviation is about 1.02 kcal mol^{-1} (or ~4 kJ mol^{-1}).[5] According to the previous studies,[12-14] the error bar of this method for medium size systems is about 10 kJ mol^{-1}. Detailed methodology of the G3 theory is given in Appendix C.

1.2 The G3 Method with Reduced Mϕller-Plesset Order and Basis Set

An economical variant of the G3 theory, G3(MP2),[6] has been introduced by Pople et al. recently. The G3(MP2) model involves only two single-point energy calculations at the QCISD(T)/6-31G(d) and MP2/G3MP2large levels, based on the geometry optimized at the MP2(Full)/6-31G(d) level. The G3MP2large basis set is the same as the aforementioned G3large basis set, except the core polarization functions have been removed.[6] Also, HLC is included to yield the E_e of the molecule, where HLC = $-9.729 \times 10^{-3} n_\beta - 4.471 \times 10^{-3}(n_\alpha - n_\beta)$. Similar to the G3 method, the MP2(Full)/6-31G(d) vibrational frequencies, scaled by 0.9661, are applied for the ZPVE correction at 0 K to give the total energy of (E_0) for the molecule.

It is noted that the G3(MP2) method is able to yield results with average absolute deviations of 1.3 kcal mol^{-1} (or ~5.4 kJ mol^{-1}), when compared with the aforementioned 299 energies determined by experiments.[5] According to the previous studies,[12-14] the error bar of this method for medium size systems is about 15 kJ mol^{-1}.

1.3 Calculation of Thermodynamical Data

The heats of formation at temperature T (ΔH°_{fT}) in this work were calculated in the following manner. For molecule AB, its Gn ΔH°_{fT} was calculated from the

corresponding heat of reaction $\Delta H^{\circ}_{rT}(A + B \rightarrow AB)$ and the respective experimental $\Delta H^{\circ}_{fT}(A)$ and $\Delta H^{\circ}_{fT}(B)$ for elements A and B.

1.4 Remark on the Location of Transition Structures

In this thesis, all stationary points on the potential energy surface (PES) were characterized by frequency calculation. In other words all stable species possess real vibrational frequencies only, while transition structures (TSs) have one and only one imaginary vibrational frequency. For each TS, the "reactant(s)" and "product(s)" were confirmed by intrinsic reaction coordinate (IRC) calculations.

1.5 Natural Bond Orbital (NBO) Analysis

The Natural Bond Orbital (NBO) analysis has been carried out for a number of species in order to study the bonding and interactions in the phosphabenzene and arsabenzene in Appendix A. This analysis allows us to isolate the interaction energies in low-order perturbative expressions of easily interpretable form and to relate these expressions to chemical explanations. The bond interaction in various systems is discussed in terms of stabilization energies, $\Delta E_{(2)}$, which is calculated by the second-order perturbation analysis of the Fock matrix obtained in the NBO analysis.[15] By this perturbational approach, the donor-acceptor interaction involving a filled orbital φ (donor) and an unfilled antibonding orbital φ^* (acceptor) can be quantitatively described. Specifically, this stabilization energy is calculated by the following expression:

$$\Delta_{\varphi\varphi^*} E_{(2)} = -2\frac{(<\varphi \mid F \mid \varphi^* >)^2}{\varepsilon_{\varphi^*} - \varepsilon_{\varphi}}$$

where F is the Fock operator and ε_{φ} and ε_{φ^*} are the NBO energies of the donor and acceptor orbitals, respectively.[16]

1.6 Scope of the Thesis

In this thesis, the G3 and G3(MP2) methods are applied to study a number of pericyclic reactions. The important basic concepts of ab initio calculations and their application to pericyclic reactions will be briefly introduced in Chapter 2. In Chapter 3, the cycloaddition reactions between butadiene and ethylene are studied at both the

G3 and G3(MP2) methods. In addition, the cycloaddition reactions between hexatriene and ethylene as well as the electrocyclic reaction of hexatriene are investigated at the G3(MP2) level. The electrocyclic reactions of [12]annulene, the concerted cycloadditon reactions between ethylene and azines as well as other related systems will be discussed in Chapters 4 and 5 respectively. The method employed in these two projects is the G3(MP2) method. Finally, a conclusion will be given in Chapter 6. In Appendices A and B, the structures, energetics and bonding studies of, phosphabenzene and arsabenzene as well as hexamethylenetetramine (HMT) and related systems are investigated with the G3 and G3(MP2) levels of theory.

Editorial Note: Each chapter of this thesis should be treated as separate entity. In other words, each chapter has its own numbering system for molecular species, equations, tables, figures and references.

1.6 References

1. Pople, J. A.; Head-Gordon, M.; Fox, D. J.; Raghavachari, K.; Curtiss, L. A. *J. Chem. Phys.* **1989**, *90*, 5622.
2. Curtiss, L. A.; Jones, C.; Trucks, G. W.; Raghavachari, K.; Pople, J. A. *J. Chem Phys.* **1990**, *93*, 2537.
3. Curtiss, L. A.; Raghavachari, K.; Trucks, G. W.; Pople, J. A. *J. Chem. Phys.* **1991**, *94*, 7221.
4. Curtiss, L. A.; Raghavachari, K.; Pople, J. A. *J. Chem. Phys.* **1993**, *98*, 1293.
5. Curtiss, L. A.; Raghavachari, K.; Redfern, P. C.; Rassolov, V. R.; Pople, J. A. *J. Chem. Phys.* **1998**, *109*, 7764.
6. Curtiss, L. A.; Redfern, P. C.; Raghavachari, K.; Rassolov, V. R.; Pople, J. A. *J. Chem. Phys.* **1999**, *110*, 4703.
7. Curtiss, L. A.; Redfern, P. C.; Raghavachari, K.; Pople, J. A. *J. Chem. Phys.* **2001**, *114*, 108.
8. Curtiss, L. A.; Carpenter, J. E.; Raghavachari, K.; Pople, J. A. *J. Chem. Phys.* **1992**, *96*, 9030.
9. Curtiss, L. A.; Raghavachari, K.; Pople, J. A. *Chem. Phys. Lett.* **1993**, *214*, 183.
10. Curtiss, L. A.; Raghavachari, K.; Redfern, P. C.; Pople, J. A. *J. Chem. Phys.* **1997**, *106*, 1063.
11. Curtiss, L. A.; Raghavachari, K.; Redfern, P. C.; Pople, J. A. *J. Chem. Phys.*

1998, *109*, 42.

12. Cheng, M.-F.; Ho, H.-O.; Lam, C.-S.; Li, W.-K. *J. Serb. Chem. Soc.* **2002**, *67*, 257.
13. Cheung, T.-S.; Law, C.-K.; Li, W.-K. *J. Mol. Struct. (THEOCHEM)* **2001**, *572*, 243.
14. Cheng, M.-F.; Ho, H.-O.; Lam, C.-S.; Li, W.-K. *Chem. Phys. Lett.* **2002**, *356*, 109.
15. Reed, A. E.; Curtiss, L. A.; Weinhold, F. *Chem. Rev.* **1988**, *88*, 899.
16. Klaptke, T. M.; Schulz, A. *Quantum Chemical Methods in Main-Group Chemistry*; Wiley: Chichester, 1998.

Chapter 2

The Important Basic Concepts of Ab Initio Calculations and Their Application to Pericyclic Reactions

2.1 Potential Energy Surfaces

As mentioned in Chapter 1, an accurate and reliable prediction of molecular structures, energetics and mechanisms is one of the main objectives in computational chemistry. Understanding the potential energy surfaces (PES), the potential energy of a molecule or assembly of molecules as a function of geometry, is an important step in achieving these goals. For most purposes, it is sufficient to examine two types of stationary points on the surfaces: minima, which correspond to stable structures, and first-order saddle points, which correspond to transition structures through which stable species transform to another.

The basic requirement of constructing a potential energy surface is a theoretical method which determines the energy of the molecule at a given geometry. Theorists have developed a number of methods of different accuracy to calculate the energy of a molecule as a function of its geometry.

2.2 Ab Initio Method

Most theoretical methods calculate the energy of a chemical system by firstly constructing its wavefunction Ψ. Once the wavefunction is constructed, the energy of the system can be determined using the following equation:

$$E = \frac{<\Psi | \hat{H} | \Psi>}{<\Psi | \Psi>}$$

where $\hat{H}$ is the Hamiltonian operator. The calculation involves many computational expressions. The ab initio method fully calculates all the mathematical expressions without referring to or neglecting the experimental data.

The simplest approach in ab initio method is the Hartree-Fock (HF) method. It constructs the wavefunction Ψ which is an antisymmetrized product of orthogonal spin-orbital wavefunctions ϕ_i. These spin-orbitals are referred to as molecular orbitals (MO), each of which can accommodate one electron. The wavefunction Ψ is

substituted into the previous equation. Using variational principle, the lowest energy E and the best wavefunction Ψ (subject to the constraint of the form of Ψ) can be obtained if the MO wavefunctions are varied to obtain a minimum value of the energy. Actually, the spin-orbitals ϕ_i are linear combinations of a set of basis functions, χ_μ, as

$$\phi_i = \sum_\mu c_{\mu i} \chi_\mu$$

in which the χ_μ are fixed (they are not varied in the HF calculation). Only the coefficients $c_{\mu i}$ are varied. The procedure of varying $c_{\mu i}$ to obtain the minimum energy is implemented in the form of matrix manipulation. The final result is a set of ϕ_i in terms of χ_μ. Each ϕ_i is associated with an orbital energy.

Electrons may be distributed among these MOs and each combination of MOs chosen to accommodate the electrons is called configuration. The wavefunction of each configuration, the configuration state function (CSF), is constructed as the antisymmetrized product of wavefunctions of the MOs occupied in that configuration. Among all possible configurations, the one in which the n (number of electrons) MOs of lowest orbital energies are occupied is called the ground state configuration. The corresponding CSF is the HF wavefunction and is substituted for Ψ in the previous equation to obtain the HF energy of the system. The MOs occupied in the ground state configuration are referred to as occupied MOs, while the remaining orbitals as virtual MOs. Other CSFs are called substituted configuration wavefunctions as they can be generated from the HF wavefunction by substituting the virtual MO(s) for the occupied MO(s).

2.2.1 Basis Sets

From the above, it can be seen that to do a HF calculation, one must select a basis set. Since the basis functions are not varied in the HF calculation, they must be specified explicitly. A number of basis sets have been developed. A larger basis set gives more accurate results but requires more computational resources. Hence, it is necessary for one to choose a basis set carefully. The explicit forms of the basis sets developed are usually determined for free atoms or small representative molecules and then used without further modification for larger systems. Commonly used basis sets are of the Gaussian type (GTFs) with radial dependence $\exp(-\zeta r^2)$. The simpler sets of basis functions bear some relation to the atomic orbitals ($1s$, $2s$, $2p$, $3s$, ...,

etc.). They can be broadly classified as minimal, extended, polarization and diffuse-augmented basis sets.

A minimal basis includes one function (GTF or fixed linear combination of GTFs) for each orbital which is occupied in the electronic ground state of the atoms. For example, $1s$, $2s$, $2p_x$, $2p_y$ and $2p_z$ functions are used for carbon while a single $1s$ function is employed for hydrogen. A common basis of this type is STO-3G.[1-5] Extended basis sets employ more than one basis function per atomic orbital. A common practice is to have two functions per atomic orbital, leading to a double-zeta basis set. An alternative is to employ two or more functions for the valence atomic orbitals ($2s$, $2p_x$, $2p_y$ and $2p_z$ for carbon and $1s$ for hydrogen) but a single function for each inner-shell atomic orbital. Such a basis set is termed split-valence. Examples include the 3-21G [6,7] and 6-311G [8] sets.

Polarization basis sets are derived from the extended sets by adding basis functions with higher orbital angular momentum quantum numbers such as d, f, ... on carbon, p, d, ... on hydrogen. The popular ones are 6-31G(d) [9-11] (also written as 6-31G*), formed from the split-valence 6-31G representation by adding a single set of d functions to non-hydrogen atoms, 6-31G(d,p) (sometimes written as 6-31G**) which has, in addition, a single set of p functions on hydrogen atoms. Diffuse-augmented basis sets are derived from extended or polarization sets by adding one or several diffuse functions with small exponents ζ. Commonly used sets are 3-21+G [12] and 6-31+G(d) [13] which include diffuse functions for non-hydrogen atoms. The diffuse-augmented basis sets are usually employed in the calculation of anionic systems.

2.2.2 Correlation Methods

In the HF method, the interactions between electrons are only taken into account in an average way. To improve the result, the instantaneous electron-electron interactions, usually referred to as correlations, should be included, in addition to employing larger basis set. The treatments that takes correlation into consideration are collectively termed correlation methods.

A commonly used correlation method is the Mϕller-Plesset (MP) perturbation theory[14] which takes the HF wavefunction as the zeroth-order wavefunction. The HF energy is identical to the energy corrected to first-order in the perturbation theory. The MP method is further classified according to the order to which the energy is

corrected, i.e., second-order as MP2, third-order as MP3, and so forth. Popular treatments include MP2, MP3 and MP4 methods.

Instead of perturbation theory, the HF energy may be improved with the variational method. The HF wavefunction does come from variational method, but it is only the best wavefunction in the form of an antisymmetrized product of one-electron spin-orbitals. Better results is obtained if we use a more flexible wavefunction, such as

$$\Psi = \Psi_0 + \sum_k a_k \Psi_k$$

where Ψ_0 is the HF wavefunction, a_k are adjustable parameters and Ψ_k are some unadjustable functions.

In the configuration interaction (CI) method, Ψ_k are substituted CSFs produced by the HF calculation. By including different CSFs into the wavefunction Ψ expressed as above, the interaction between different configurations can be taken into account. When all possible substituted CSFs are included, the treatment is called full configuration interaction (FCI) method. Though the number of all possible substituted CSFs is finite for an incomplete basis set, it is usually very large. Hence, the FCI method is rarely employed and only possible for some relatively small systems.[15]

For larger systems, a practical approach is the truncated CI method which includes some types of substituted CSFs only. The substituted CSFs may be classified according to the number of occupied MO wavefunction(s) substituted by virtual MO wavefunction(s). One with an occupied MO wavefunction substituted is called a single-substitution CSF, one with two occupied MO wavefunctions substituted is called a double-substitution CSF, and so forth. Two common CI methods are: configuration interaction with doubles (CID), where only double-substitution CSFs are considered, as well as configuration interaction with singles and doubles (CISD), where both single- and double-substitution CSFs are included.

The CI method is usually much more expensive but more reliable than the MP method. However, the truncated CI method is size-inconsistent. To restore the size-consistence, different variations of CI method such as quadratic configuration interaction (QCI)[16] and coupled cluster (CC)[17] methods are developed. These two methods are not variational but are more popular than the original truncated CI

method as size-consistence is usually considered to be more important than being variational.

2.3 Pericyclic Reaction

A pericyclic reaction is one that takes place in a single step through a cyclic transition state, with a concerted movement of electrons simultaneously breaking bonds and making bonds, with no intermediates being involved. There are four major classes of pericyclic processes: cycloaddition reaction, electrocyclic reaction, sigmatropic rearrangement and group transfer reaction. In this thesis, we focus on the first two. The stereochemistry of these reactions is dictated by the symmetry of the orbitals involved in bond reorganization.

Cycloaddition reactions are those in which two unsaturated molecules add together to yield a cyclic product. Cycloaddition can take place by either suprafacial or antarafacial pathways. Suparafacial cycloaddition involves reaction between lobes on the same face of one component and on the same face of the second component. Antarafacial cycloaddition involves reaction between lobes on the same face of one component and on the opposite faces of the other component. The reaction course in a specific case can be found by inspecting the symmetry of the Highest Occupied Molecular Orbital (HOMO) of one reactant and the Lowest Unoccupied Molecular Orbital (LUMO) of the other reactant.

Electrocyclic reactions involve the cyclization of conjugated polyenes. These reactions can occur by either conrotatory or disrotatory paths, depending on the symmetry of the terminal lobes of the π system. Conrotatory cyclization requires that both lobes rotate in the same direction, whereas disrotatory cyclization requires that the lobes rotate in opposite directions. The reaction course for any specific case can be found by examining the symmetry of the HOMO.

Other than the stereochemistry of pericyclic reaction, the chemical reactivity of this reaction is also a subject of interest. A number of approximate quantum mechanical theories of reactivity have been developed. One of these approximate methods, frontier molecular orbital theory, has been particular successful.

2.4 The Perturbation Theory of Reactivity

In order to approach the problem of chemical reactivity, a number of different perturbation expressions for calculation of the energy change which occurs upon the

interaction of two molecules have been published. The expression, derived by Kolpman[18] and Salem[19], for the energy (ΔE) gained and lost when the orbitals of one reactant overlap with those of another is

$$\Delta E = -\sum_{ab}(q_a + q_b)\beta_{ab}S_{ab} + \sum_{k<l}\frac{Q_k Q_l}{\varepsilon \mathrm{R}_{kl}} + \sum_{r}^{occ.}\sum_{s}^{unocc.} - \sum_{s}^{occ.}\sum_{r}^{unocc.}\frac{2(\sum_{ab} c_{ra}c_{rb}\beta_{ab})^2}{E_r - E_s}$$

where,

q_a and q_b are the electron populations (often loosely called electron densities) in atomic orbitals a and b.

β and S are the resonance and overlap integrals.

Q_k and Q_l are the total charges on atoms k and l.

ε is the local dielectric constant.

R_{kl} is the distance between the atoms k and l.

c_{ra} is the coefficient of atomic orbital a in molecular orbital r, where r refers to the molecular orbitals on one molecule and s refers to those on the other.

E_r is the energy of molecular orbital r.

The first term of this expression is the first-order closed-shell repulsion term, and comes from the interaction of the filled orbitals of the one molecule with the filled orbitals of the other. Overall it is antibonding in effect. The second term is simply the Coulombic repulsion or attraction. This term, which contains the total charge, Q, on each atom, is obviously important when ions or polar molecules are reacting together. The third term represents the interaction of all the filled orbitals (especially the HOMOs) with all the unfilled (especially the LUMOs) of correct symmetry. It is the second-order perturbation term and is only true if $E_r \neq E_s$. [When $E_r \approx E_s$, the interaction is better described in charge-transfer term, and the perturbation is then a first-order one of the form $\sum_{ab} 2c_{ra}c_{sb}\beta_{ab}$.] Thus, the HOMO and the LUMO are the most important ones, as they are the ones with the smallest value of $E_r - E_s$, and hence they make the largest contribution to the third term.

2.5 References

1. Hehre, W. J.; Stewart, R. F.; Pople, J. A. *J. Chem. Phys.* **1969**, *51*, 2657.
2. Hehre, W. J.; Ditchfield, R.; Stewart, R. F.; Pople, J. A. *J. Chem. Phys.* **1970**, *52*,

2769.

3. Pietro, W. J.; Levi, B. A.; Hehre, W. J.; Stewart, R. F. *Inorg. Chem.*, **1980**, *19*, 2225.
4. Pietro, W. J.; Blurock, E. S.; Hout, R. F.; Jr,; Hehre, W. J.; Defress, D. J.; Stewart, R. F. *Inorg. Chem.*, **1981**, *20*, 3650.
5. Pietro, W. J.; Hehre, W. J. *J.Comput. Chem.*, **1983**, *4*, 241.
6. Binkley, J. S.; Pople, J. A.; Hehre, W. J. *J. Am. Chem. Soc.*, **1980**, *102*, 939.
7. Gorden, M. S.; Binkley, J. S.; Pople, J. A.; Pietro, W. J.; Hehre, W. J. *J. Am. Chem. Soc.*, **1982**, *104*, 2797.
8. Krishnsn, R.; Binkley, J. S.; Seeger, R.; Pople, J. A. *J. Chem. Phys.* **1980**, *72*, 650.
9. Binkley, J. S.; Pople, J. A. *J. Chem. Phys.* **1977**, *66*, 879.
10. Francl, M. M.; Pietro, W. J.; Hehre, W. J.; Binkley, J. S.; Gorden, M. S.; Defress, D. J.; Pople, J. A. *J. Chem. Phys.* **1982**, *77*, 3654.
11. Hariharan, P. C.; Pople, J. A. *Theori. Chom. Acta* **1973**, *28*, 213.
12. Clark, T.; Chandrasekhar, J.; Spitznagel G. W.; Schleyer, P. v. R. *J. Comput. Chem.*, **1983**, *4*, 294.
13. Spitznagel G. W.; Clark, T.; Chandrasekhar, J.; Schleyer, P. v. R. *J. Comput. Chem.*, **1982**, *3*, 363.
14. Mϕller, C.; Plesset, M. S. *Phys. Rev.*, **1934**, *46*, 318.
15. (a) Bauschlicher, C, W.; Jr.; Langhoff, S. R.; Taylor, P. R.; Partidge, H. Chem. Phys. Lett., **1986**, *126*, 436; (b) Bauschlicher, C, W.; Jr.; Langhoff, S. R.; Taylor, P. R.; Handy, N. C.; Knowles, P. J. *J. Chem. Phys.* **1986**, *85*, 1469; (c) Bauschlicher, C, W.; Jr.; Taylor, P. R. *ibid.*, **1986**, *85*, 2779; (d) Bauschlicher, C, W.; Jr.; Taylor, P. R. *ibid.*, **1986**, *85*, 6510.
16. Pople, J. A.; Head-Gordon, M. Raghavachari, K. *J. Chem. Phys.* **1987**, *87*, 5968.
17. Cizek, J. *J. Chem. Phys.* **1966**, *45*, 4256.
18. Klopman, G. *J. Am. Chem. Soc.*, **1968**, *90*, 223.
19. Salem, L. *J. Am. Chem. Soc.*, **1968**, *90*, 543.

Chapter 3

Ab Initio Study of the Cycloaddition Reaction between Ethylene and Butadiene and as well as That between Ethylene and Hexatriene

Abstract

The [2+2] and [2+4] cycloaddition reactions between butadiene and ethylene have been studied using the Gaussian-3 (G3) and G3(MP2) methods. In this study, both of the concerted and stepwise pathways have been investigated. It is found that the most favorable mechanism is, as expected, the concerted [2+4] pathway. The G3 and G3(MP2) barriers are in very good agreement with the experimental estimate. On the other hand, the reaction between *cZc*-hexatriene and ethylene has three possible processes: the [2+2], [2+4], and [2+6] cycloadditions. Once again, the concerted and stepwise pathways of these three reactions have been studied by the G3(MP2) method. Other than these three possible cycloaddition reactions, the well-known electrocyclic formation of cyclohexadiene, is another competitive reaction. This reaction has also been studied by the same method in the present work. It is found that the most favorable pathway is the concerted [2+4] mechanism, while the barrier of the ring closing process of *cZc*-hexatriene itself is about 5 kJ mol^{-1} higher. A detailed discussion on the pathways of the three cycloadditions and the electrocyclic reaction is given.

3.1 Introduction

Electrocyclic addition reaction is one of the most useful methods in organic synthesis. The most famous one, the Diels-Alder reaction between butadiene and ethylene, has been the subject of intense interest and debate.[1-9] Both the concerted and stepwise mechanisms of this reaction have been studied in detail with different computational methods by many chemists. They have successfully located the transition states (TSs) and intermediates of both the concerted and the stepwise pathways. However, in many instances, the computed energy barrier height of the concerted pathway does not always agree well with the experimental data. For example, Sakai calculated both the concerted and stepwise pathways by CASSCF and CAS-MP2 methods. He found that the activation energies, calculated at the

CAS-MP2/6-311+G(d,p) level, of the concerted and stepwise pathways are 171.1 and 174.4 kJ mol^{-1},[1] respectively, while the experimental barrier has been found to be 105.0 kJ mol^{-1} [10] [It is noted that, in the experimental study of this reaction, the investigation was carried out at 800 K with an energy barrier 27.5 ±2 kcal mol^{-1} (165.1 ±8.4 kJ mol^{-1}).] Based on the computational results obtained, Sakai thus was not able to conclude whether the reaction proceeds via a concerted or stepwise pathway.

In 1993, Houk and Li also studied the concerted pathway of this reaction[8] and calculated the activation energies at the levels of CASSCF/3-21G and QCISD(T)/6-31G(d) to be 156.1 and 106.7 kJ mol^{-1}, respectively. At about the same time, Carpenter and Sosa located the concerted TS at the MP2/6-31G(d) level and calculated the barrier heights at the LDF/DZVP and NLDF/DZVP levels. The activation energies were found to be 25.1 and 85.4 kJ mol^{-1}, respectively.[9] Three years later, Houk and co-workers studied the reaction again with DFT methods: the barrier height at the B3LYP/6-31G(d) level was calculated to be 103.8 kJ mol^{-1}. [2]

In the present work, we report the potential energy profiles for the concerted and stepwise [2+2] and [2+4] addition reactions between butadiene and ethylene (Scheme 1) obtained by the Gaussian-3 (G3)[11] method as well as its variant, G3(MP2)[12].

Scheme 1

The two G3 methods mentioned above have been shown to give satisfactory results which agree well with experimental data.[13,14] In addition, the less time consuming G3(MP2) method is applied to the main interest of this work: cycloaddition between hexatriene and ethylene, which has not yet been studied theoretically or experimentally. For this reaction, there are three possible processes: [2+2], [2+4], and [2+6] cycloadditions (Scheme 2).

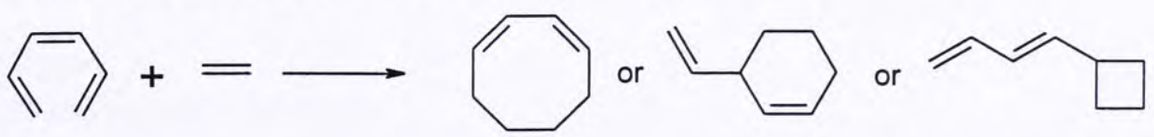

Scheme 2

Upon studying these cycloaddition reactions, the energy needed to overcome the symmetry forbidden [2+2] pathway can be reliably calculated. Also, a comparison between the two symmetry allowed processes: [2+4] and [2+6] additions, will be made. Finally, these addition reaction pathways will be compared with the electrocyclic reaction of hexatriene (Scheme 3).

Scheme 3

In this work, we will report the energy profiles of both the concerted and stepwise reaction pathways of these three cycloadditions. Furthermore, the disrotatory reaction pathway of the formation of cyclohexadiene is also reported. It is noted that the all-*cis* hexatriene is taken as the reactant for Schemes 2 and 3.

3.2 Methods of Calculation

All calculations reported here have been carried out using the Gaussian 98 package of programs.[15] The methods of calculation employed, G3 and G3(MP2), have been described in Chapter 1.

In this work, for each reaction studied, we have identified a number of TSs. For each TS found, its "reactant(s)" and "product(s)" have been confirmed by intrinsic reaction coordinate (IRC) calculations.[16,17] In addition, all the species along the concerted pathway are taken to be closed-shell entities, while those along the stepwise pathways are open-shell ones. For these open-shell species, the subsequent single-point calculations for the G3 and G3(MP2) energies were carried out with the unrestricted formalism.

In this work, the notation **1**, **2**, ..., etc. are used to label the stable species found, while the identified TSs of the reactions are denoted as **TSa**, **TSb**, ..., etc. In the following discussion, all the energetic results refer to those obtained at 0 K.

3.3 Results and Discussion

The profiles of all the addition reactions studied at 0 K are displayed in Figures 1, 3, 5, 7, 9, and 11, while the structures (with selected parameters in Å and

degrees) of the TSs and intermediates involved in the corresponding reactions are displayed in Figures 2, 4, 6, 8, 10, and 12, respectively.

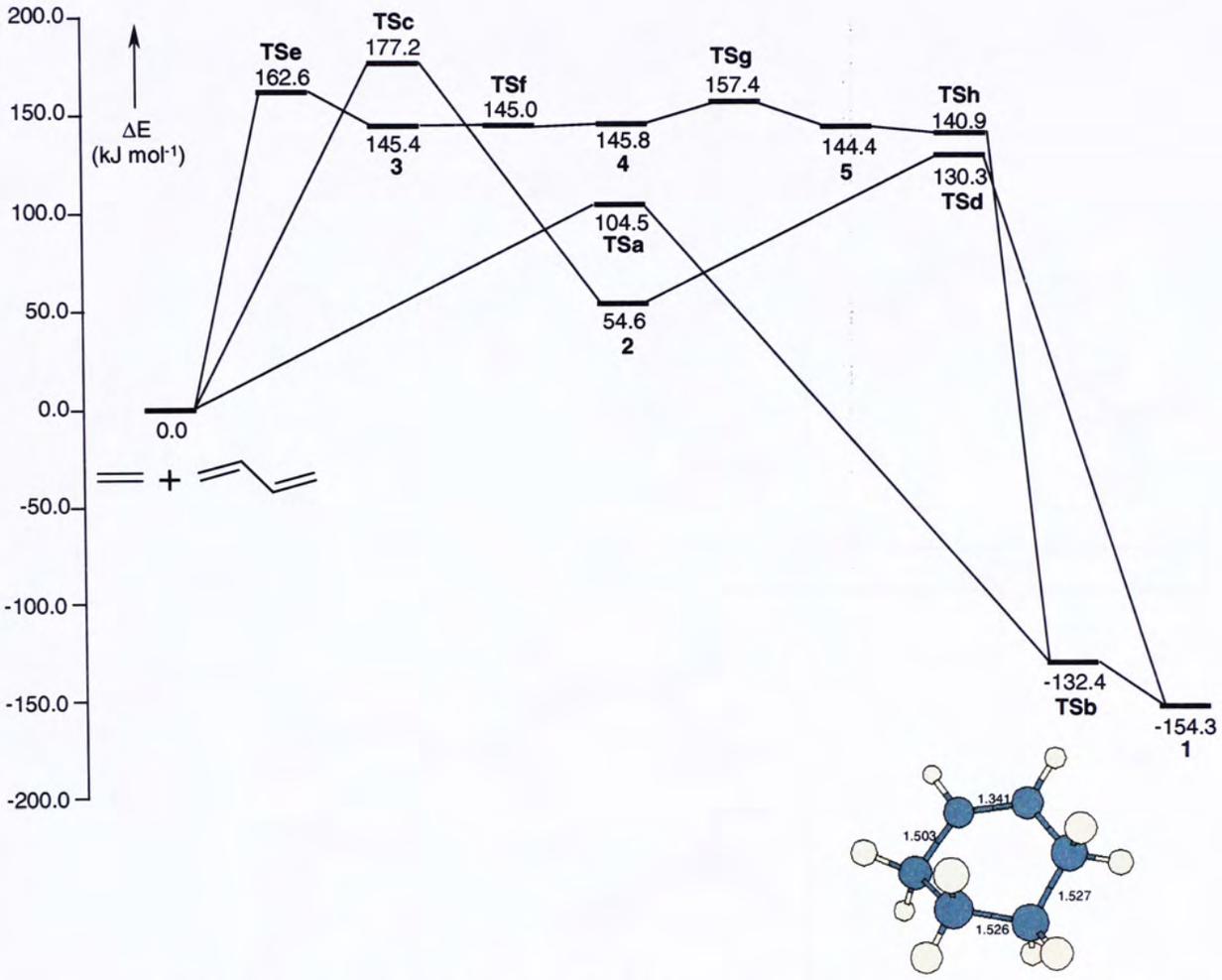

Figure 1. The G3 energy profiles showing three possible pathways for the Diels-Alder reaction between butadiene and ethylene.

Transition Structures

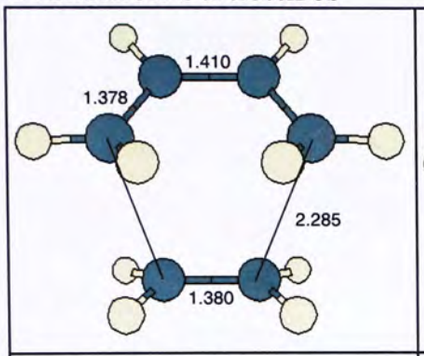

TSa

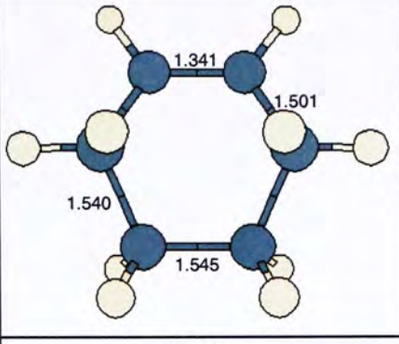

TSb

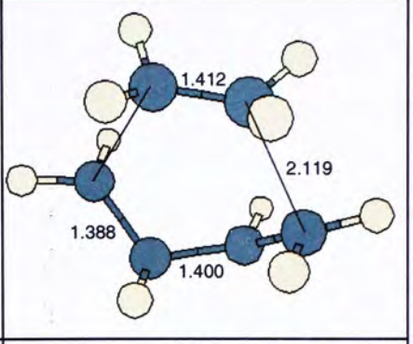

TSc

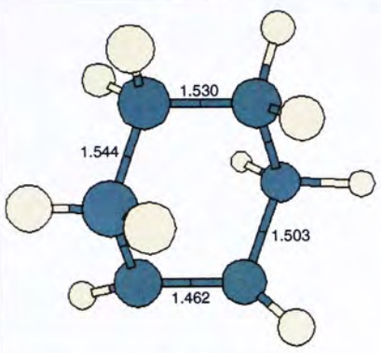

TSd

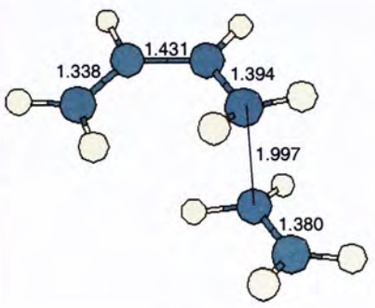

TSe

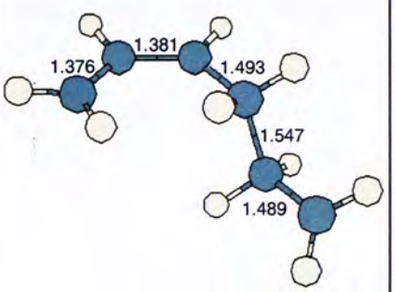

TSf

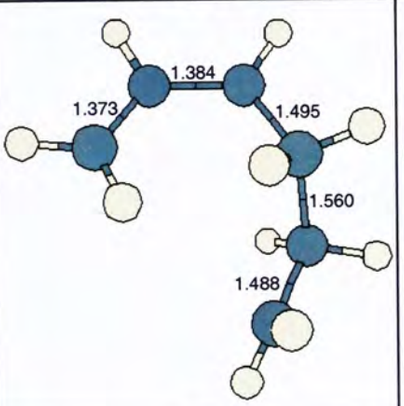

TSg

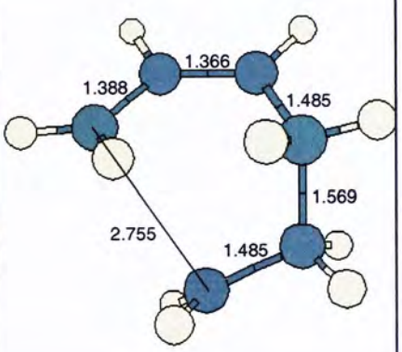

TSh

Intermediates

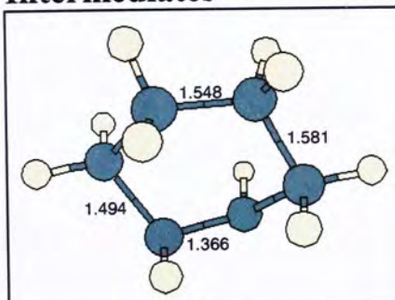

2

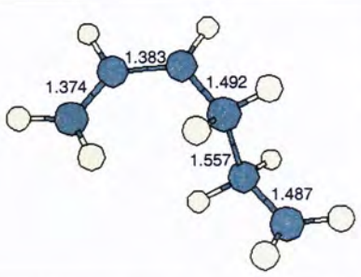

3

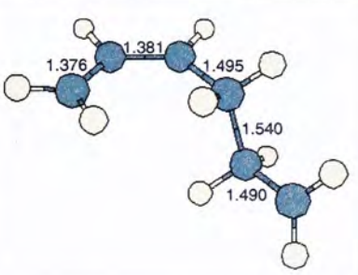

4

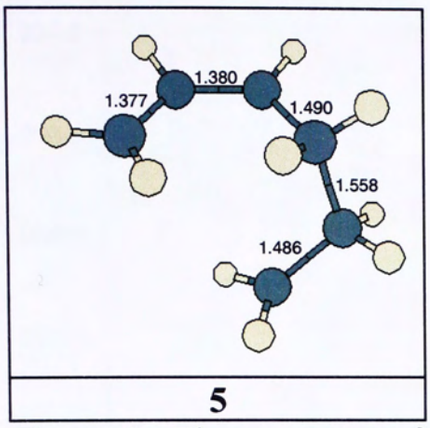

5

Figure 2. The structures of all TSs and intermediates involved in the three possible pathways for the Diels-Alder reaction between butadiene and ethylene.

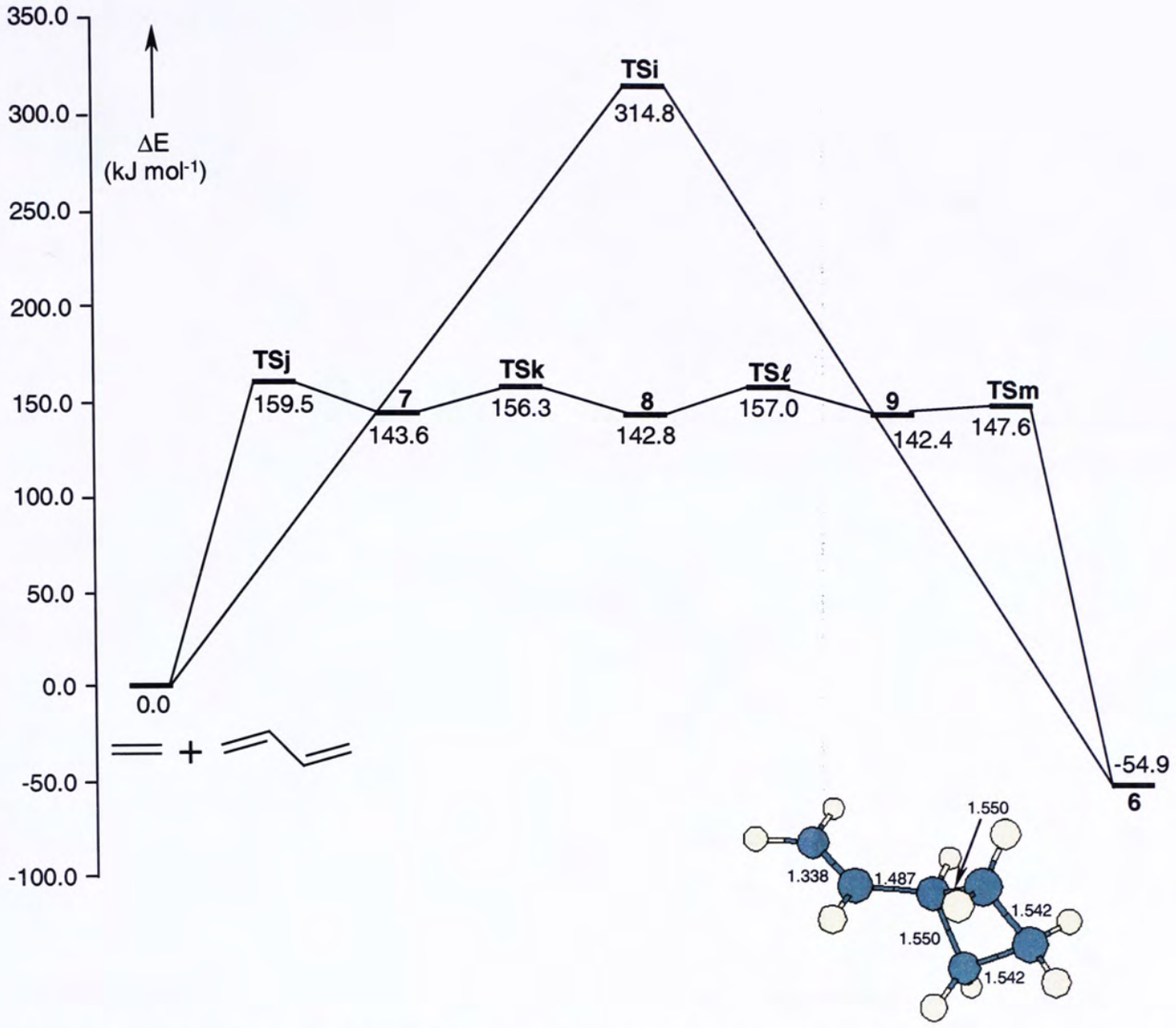

Figure 3. The G3 energy profiles showing two possible pathways for the [2+2] cycloaddition reaction between butadiene and ethylene.

Transition Structures

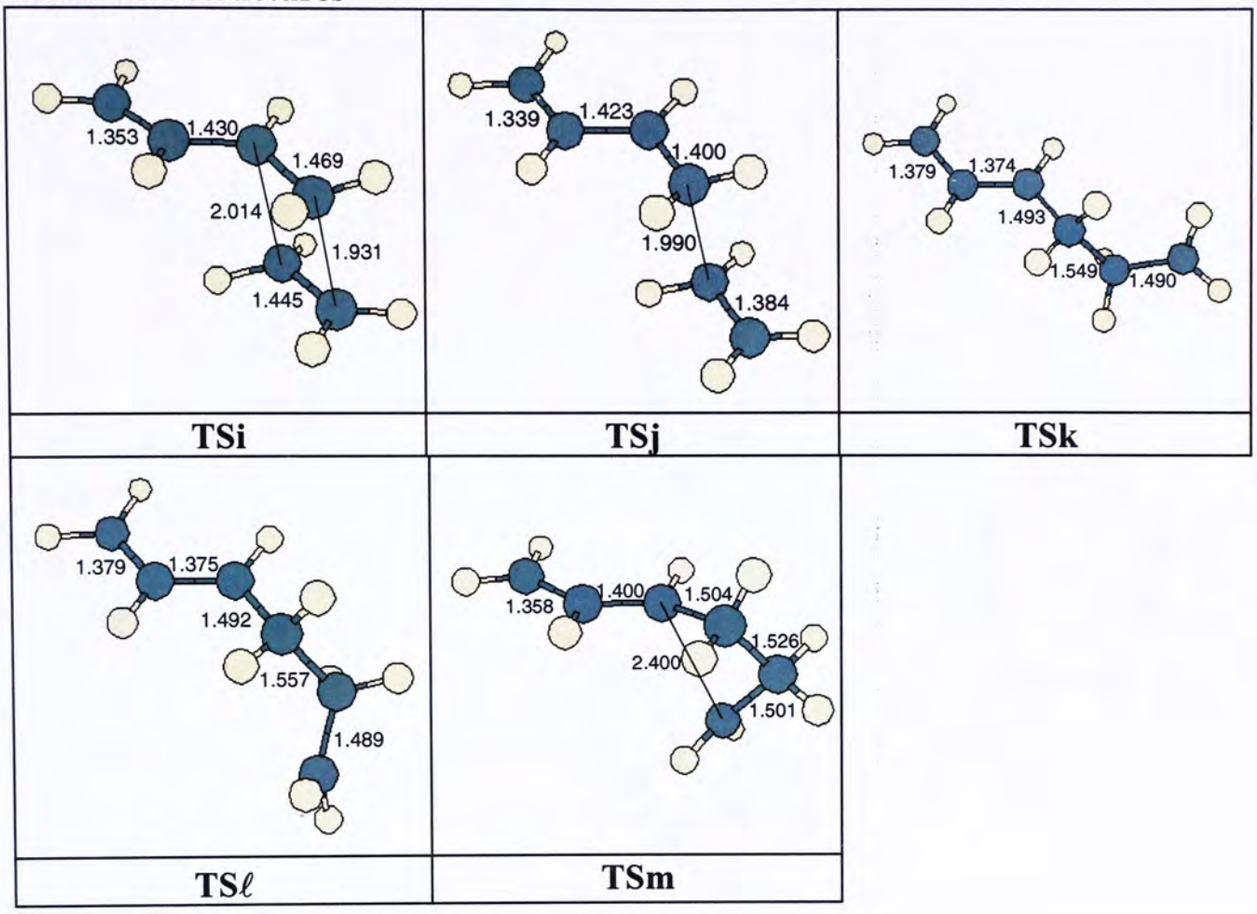

TSi	TSj	TSk

TSℓ	TSm

Intermediates

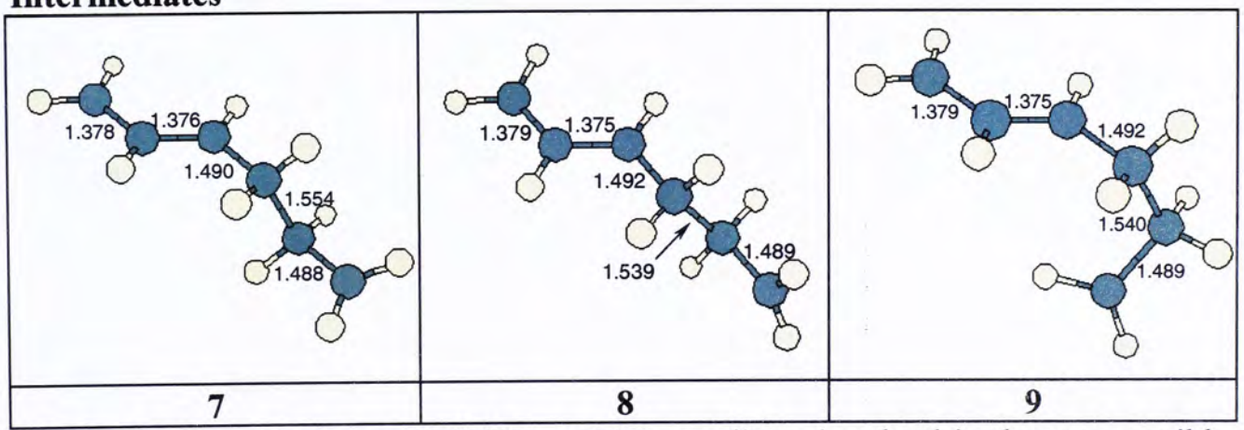

7	8	9

Figure 4. The structures of all TSs and intermediates involved in the two possible pathways for the [2+2] cycloaddition reaction between butadiene and ethylene.

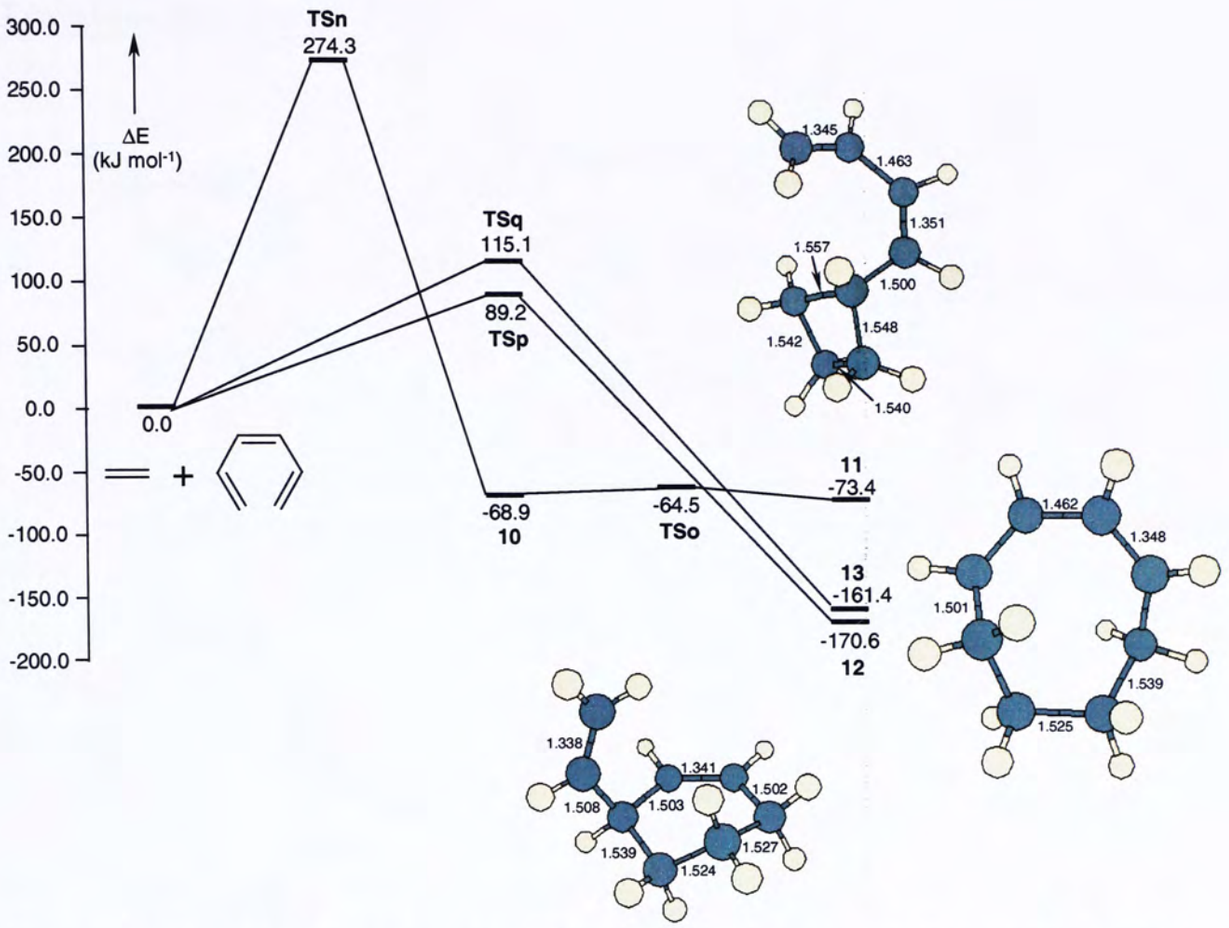

Figure 5. The G3(MP2) energy profiles showing three possible concerted pathways for the electrocyclic addition between hexatriene and ethylene.

Transition Structures

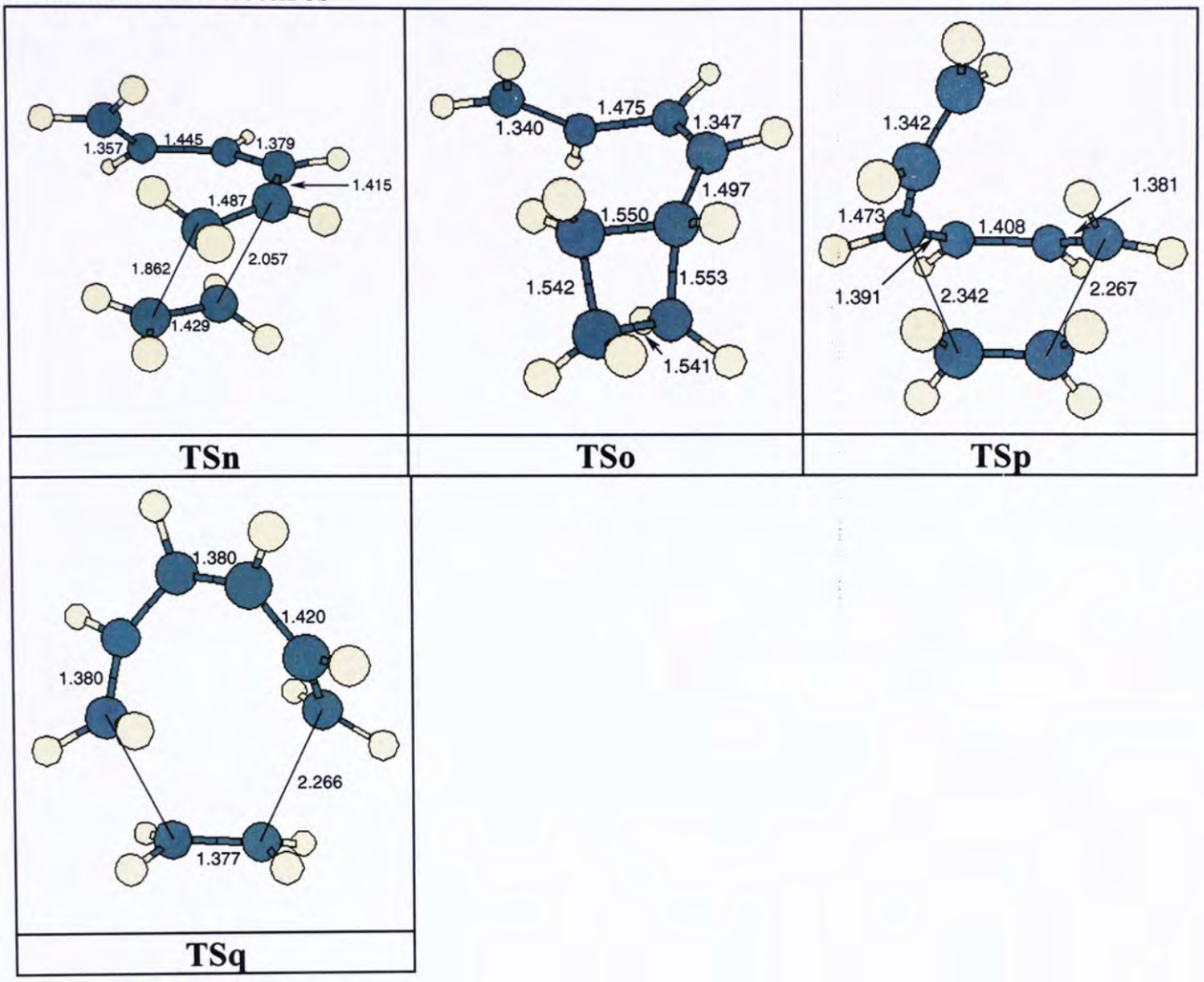

Intermediate

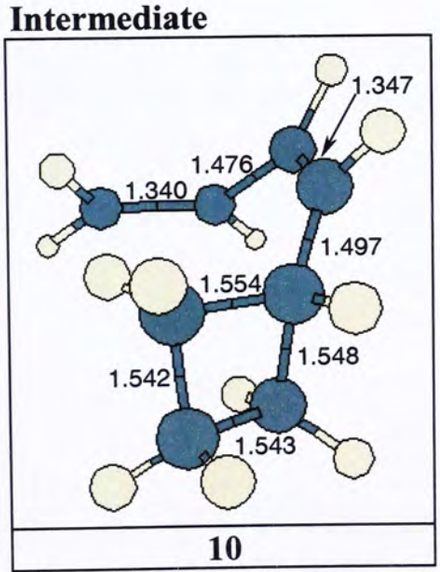

Figure 6. The structures of all TSs and intermediate involved in the three possible concerted pathways for the electrocyclic addition between hexatriene and ethylene.

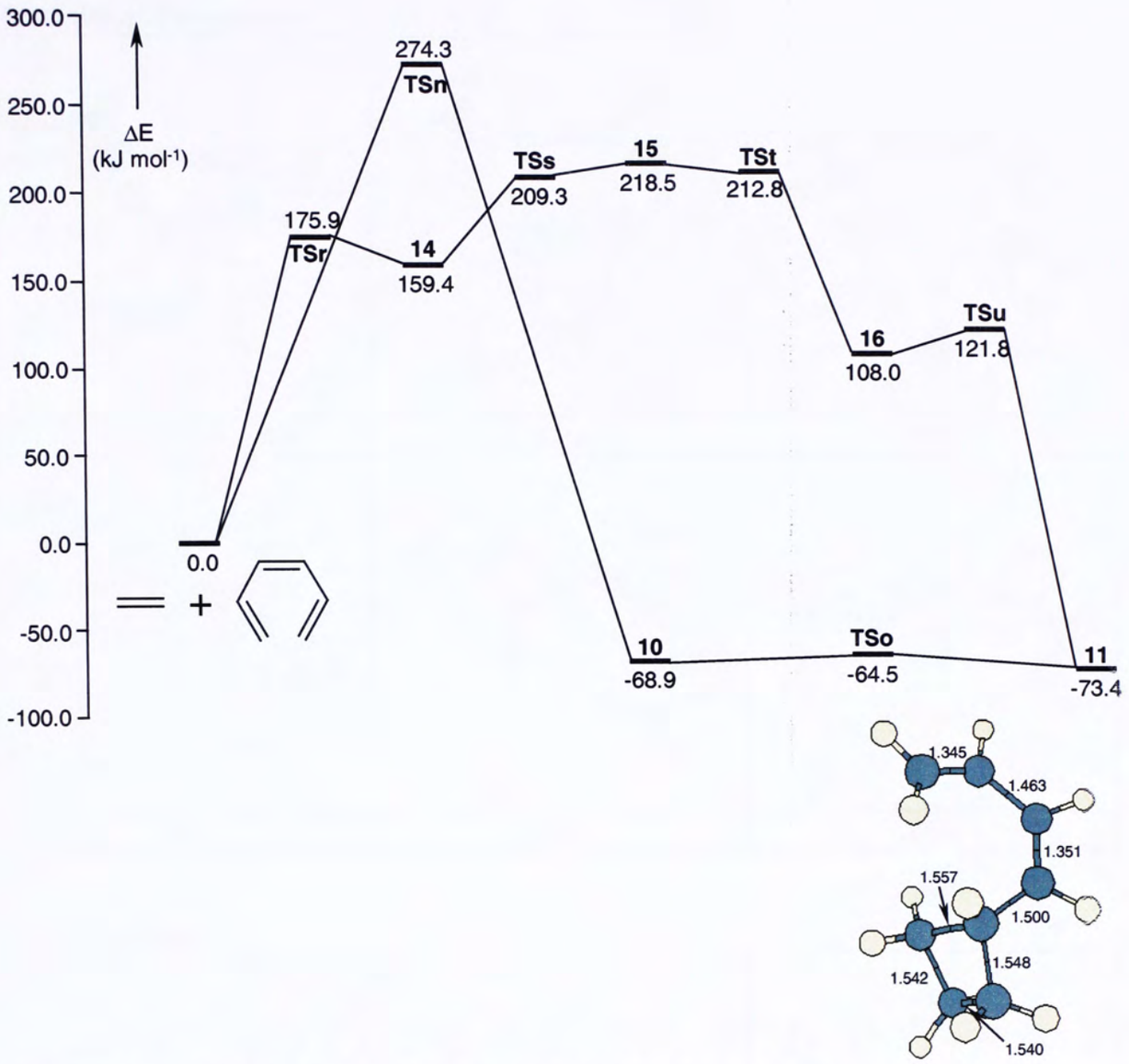

Figure 7. The G3(MP2) energy profiles showing the concerted and stepwise pathways for the [2+2] electrocyclic addition between hexatriene and ethylene.

Transition Structures

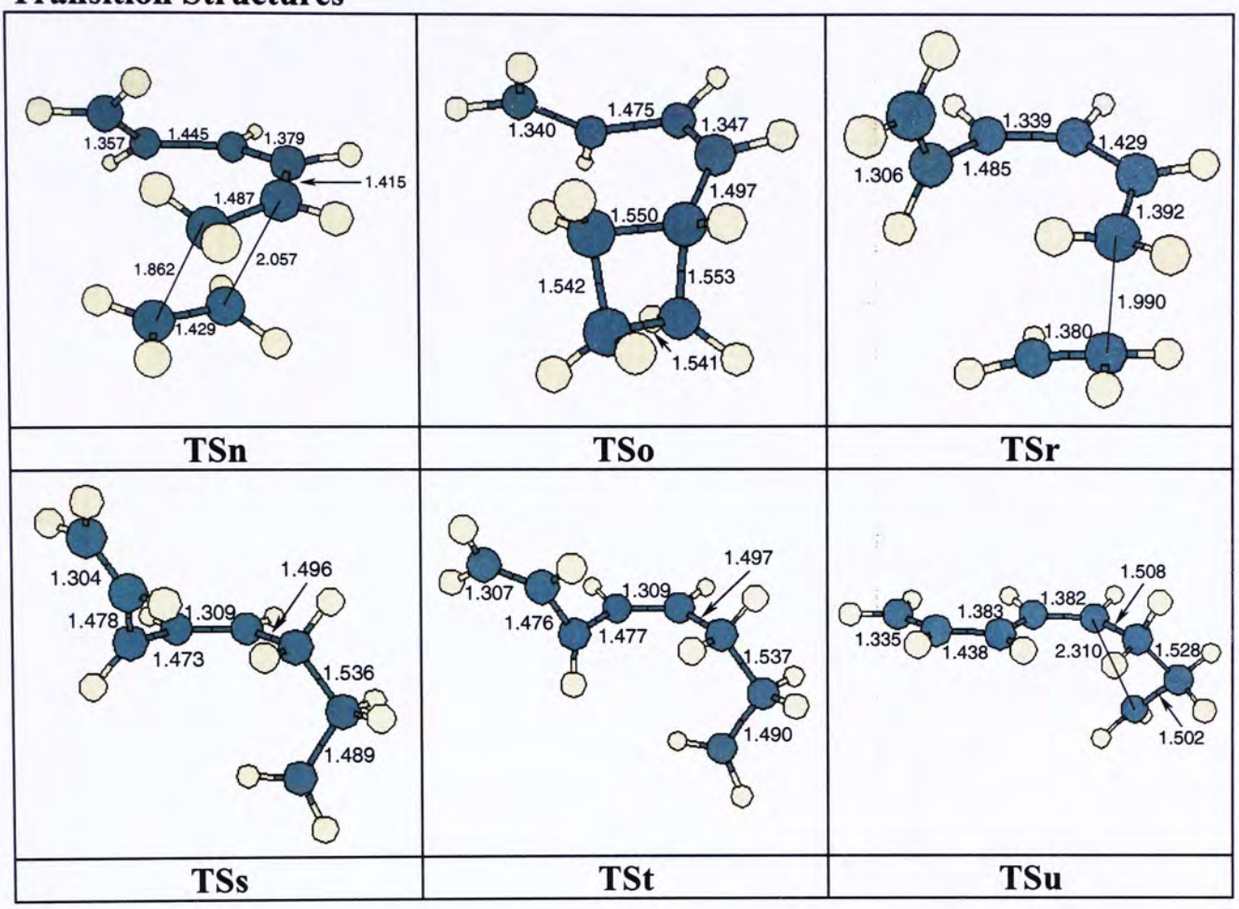

TSn	TSo	TSr
TSs	TSt	TSu

Intermediates

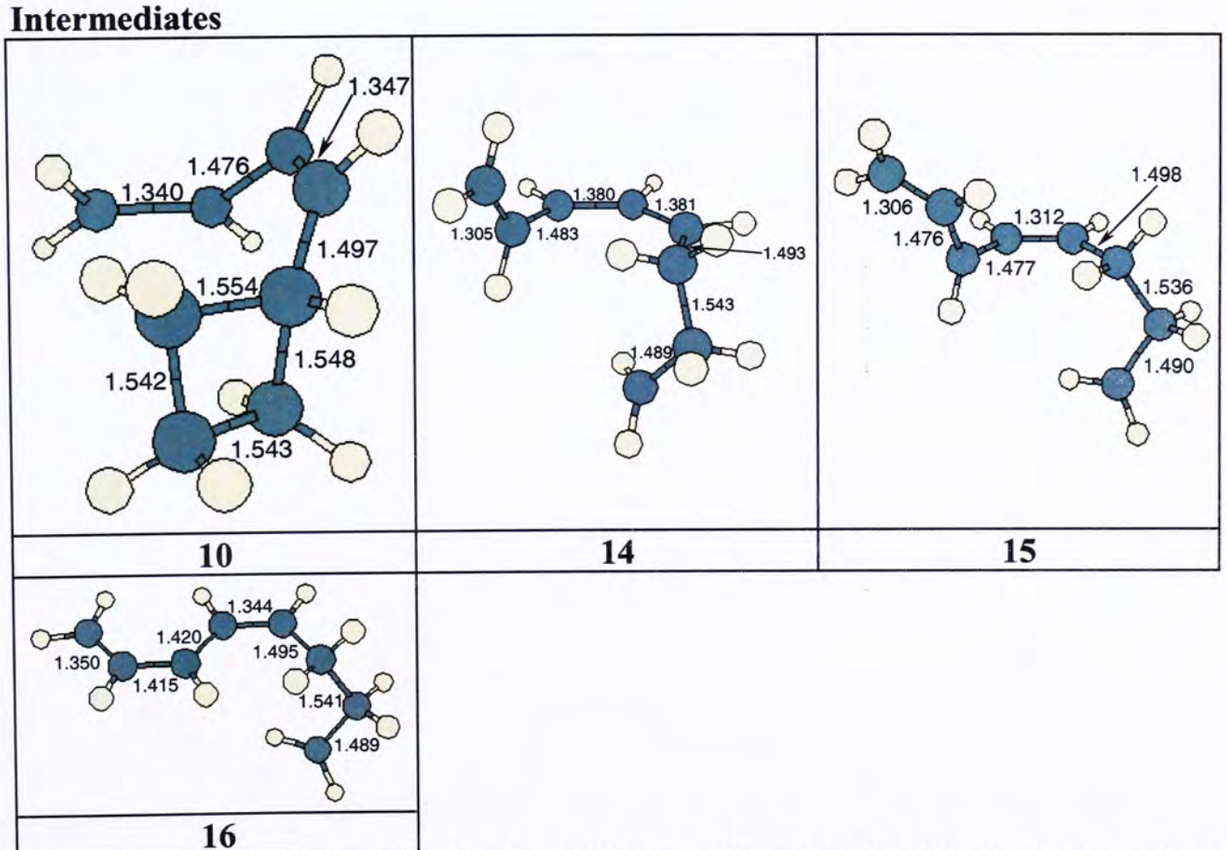

10	14	15
16		

Figure 8. The structures of all TSs and intermediates involved in the concerted and stepwise pathways for the [2+2] electrocyclic addition between hexatriene and ethylene.

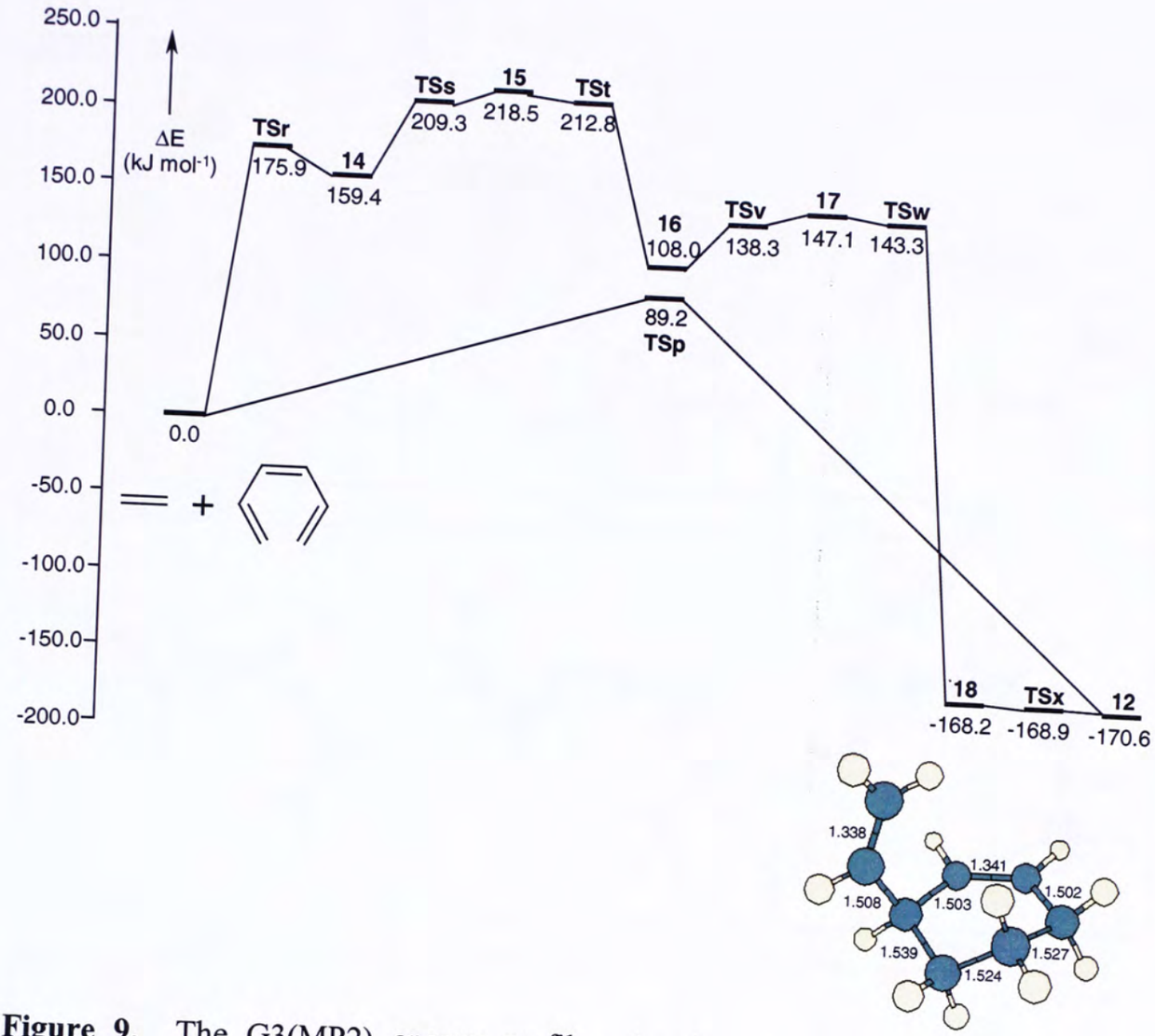

Figure 9. The G3(MP2) energy profiles showing the concerted and stepwise pathways for the [2+4] electrocyclic addition between hexatriene and ethylene.

Transition Structures

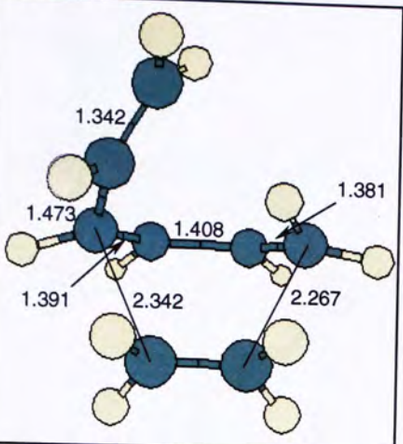

TSp

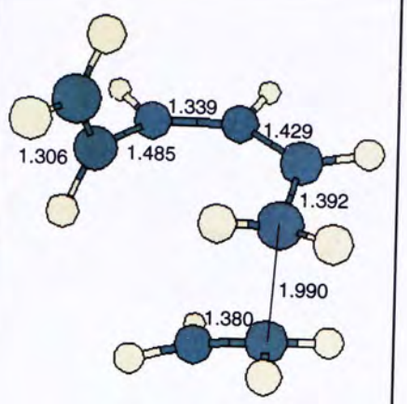

TSr

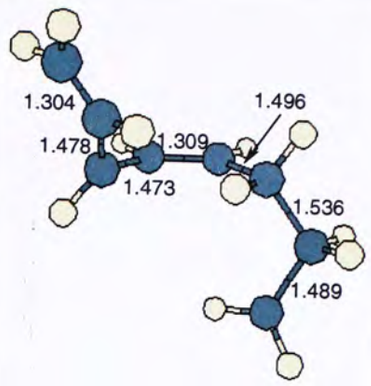

TSs

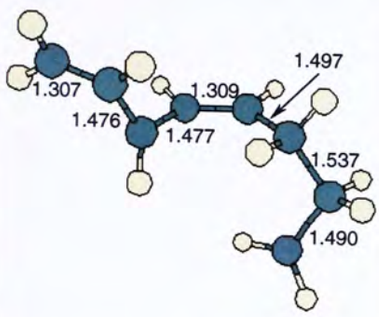

TSt

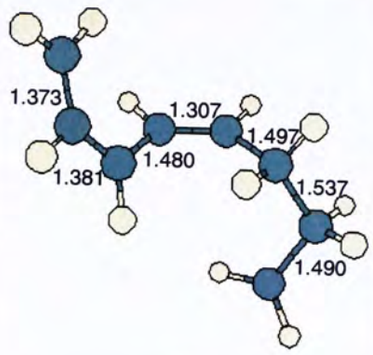

TSv

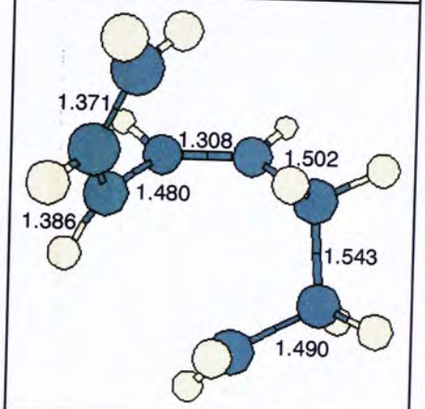

TSw

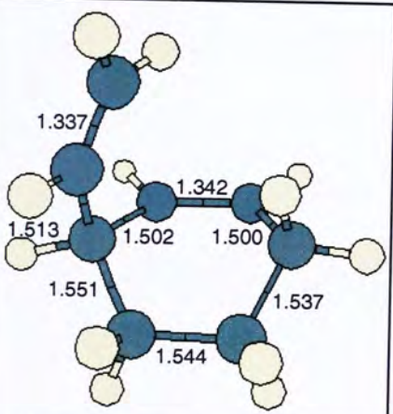

TSx

Intermediates

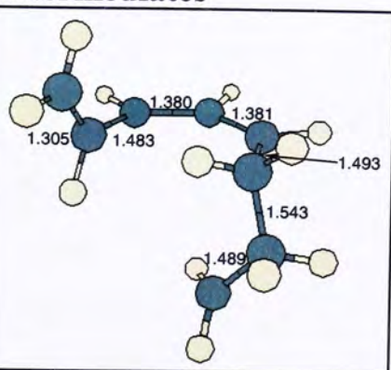

14

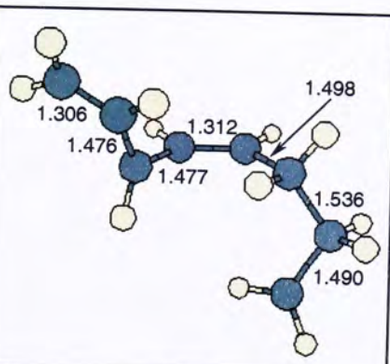

15

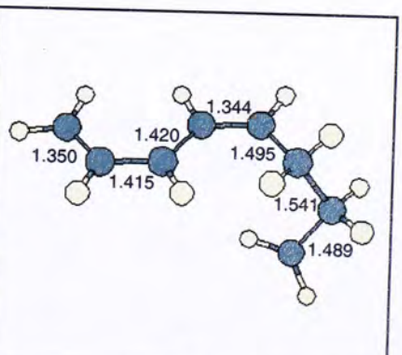

16

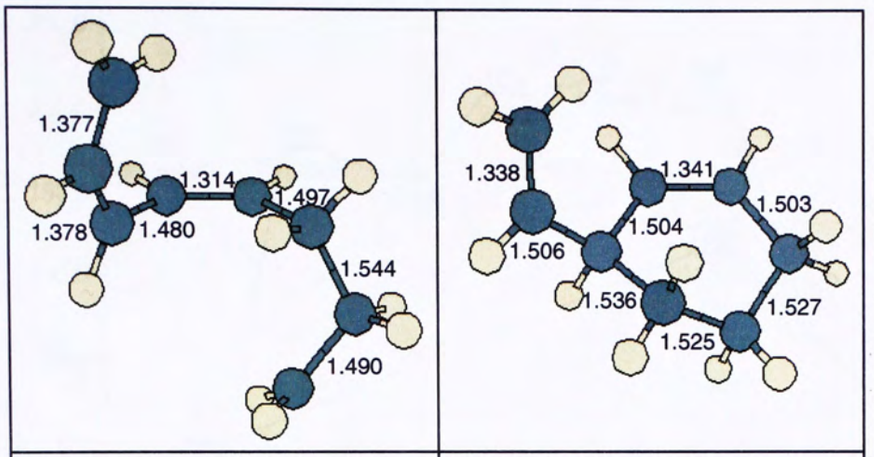

17	18

Figure 10. The structures of all TSs and intermediates involved in the concerted and stepwise pathways for the [2+4] electrocyclic addition between hexatriene and ethylene.

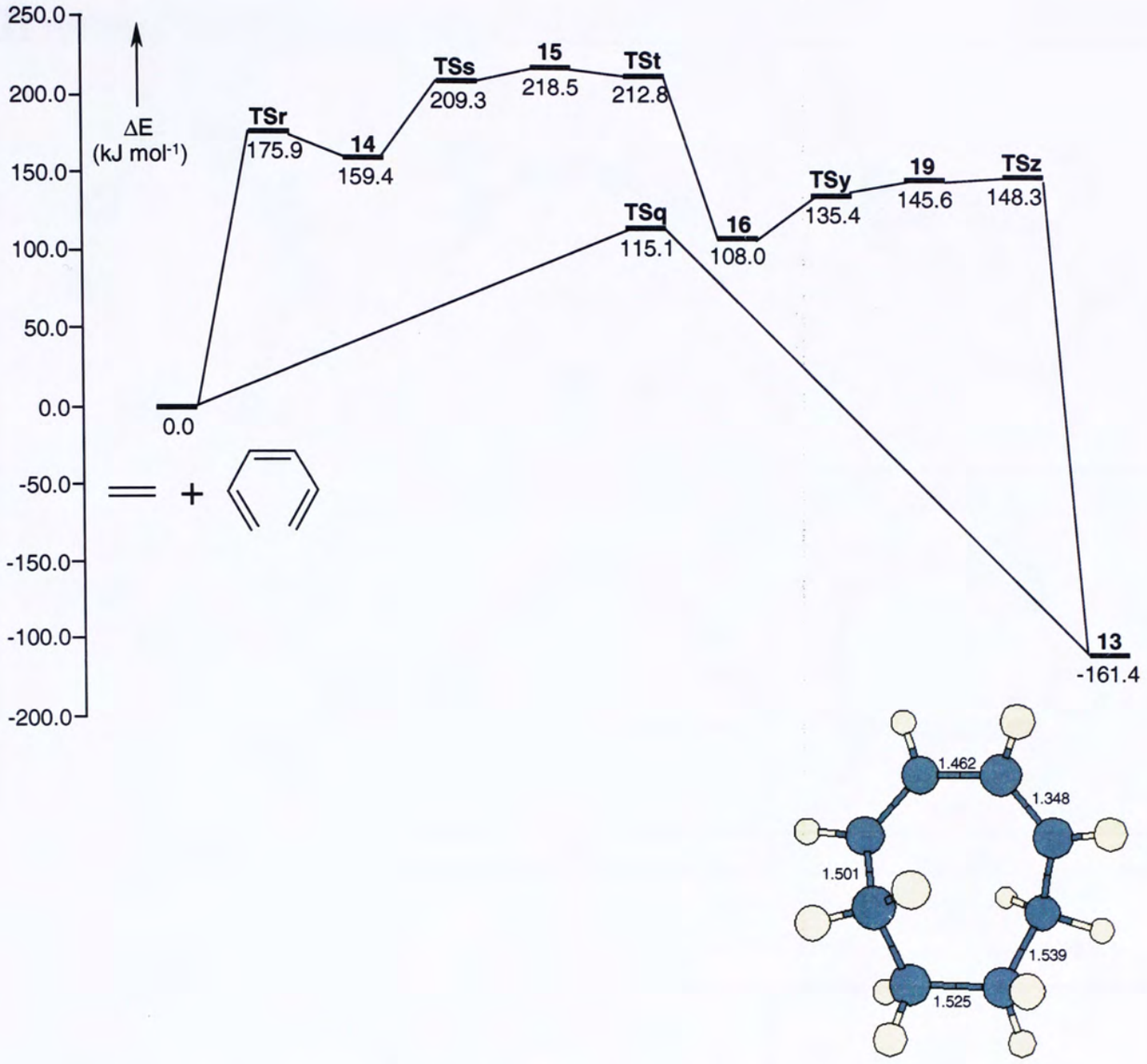

Figure 11. The G3(MP2) energy profiles showing the concerted and stepwise pathways for the [2+6] electrocyclic addition between hexatriene and ethylene.

Transition Structures

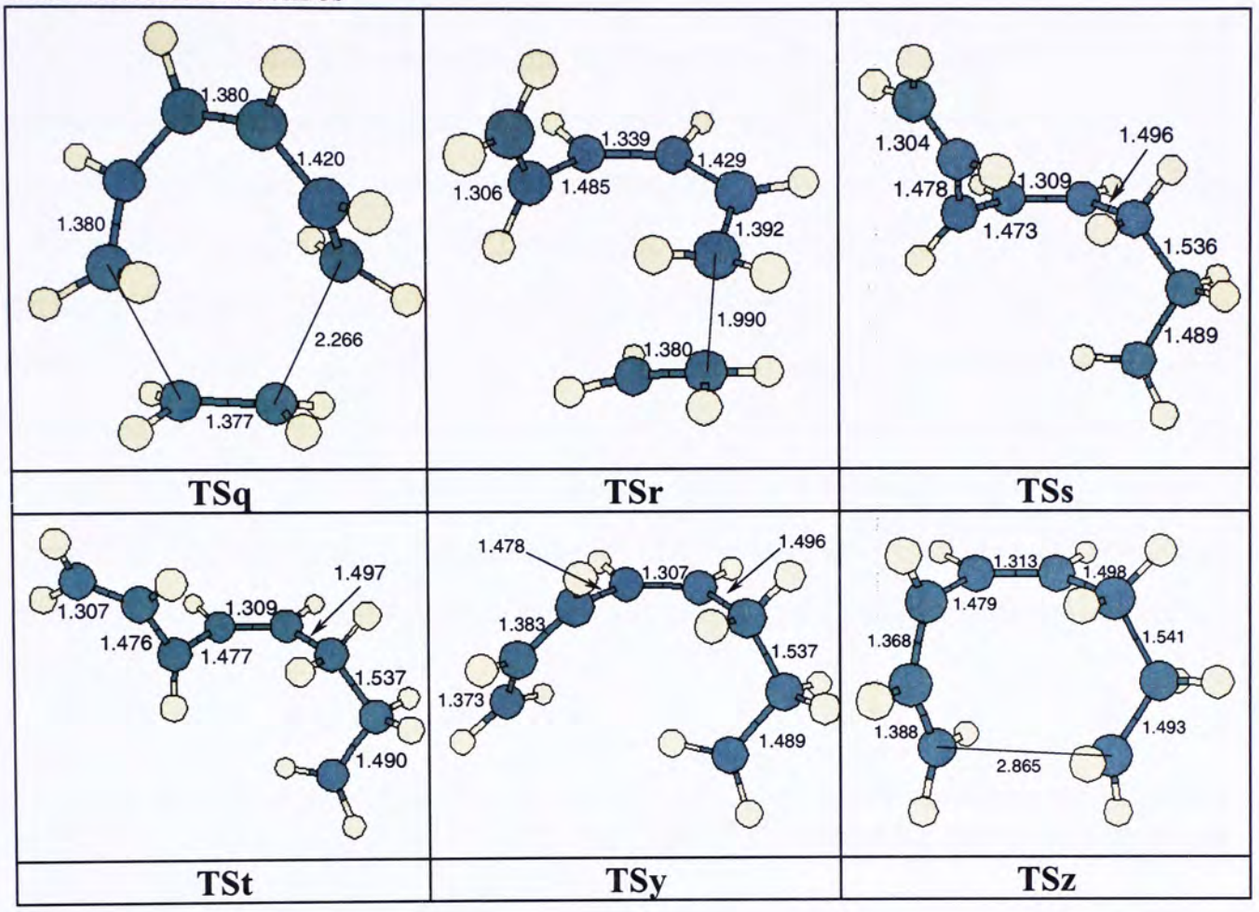

Intermediates

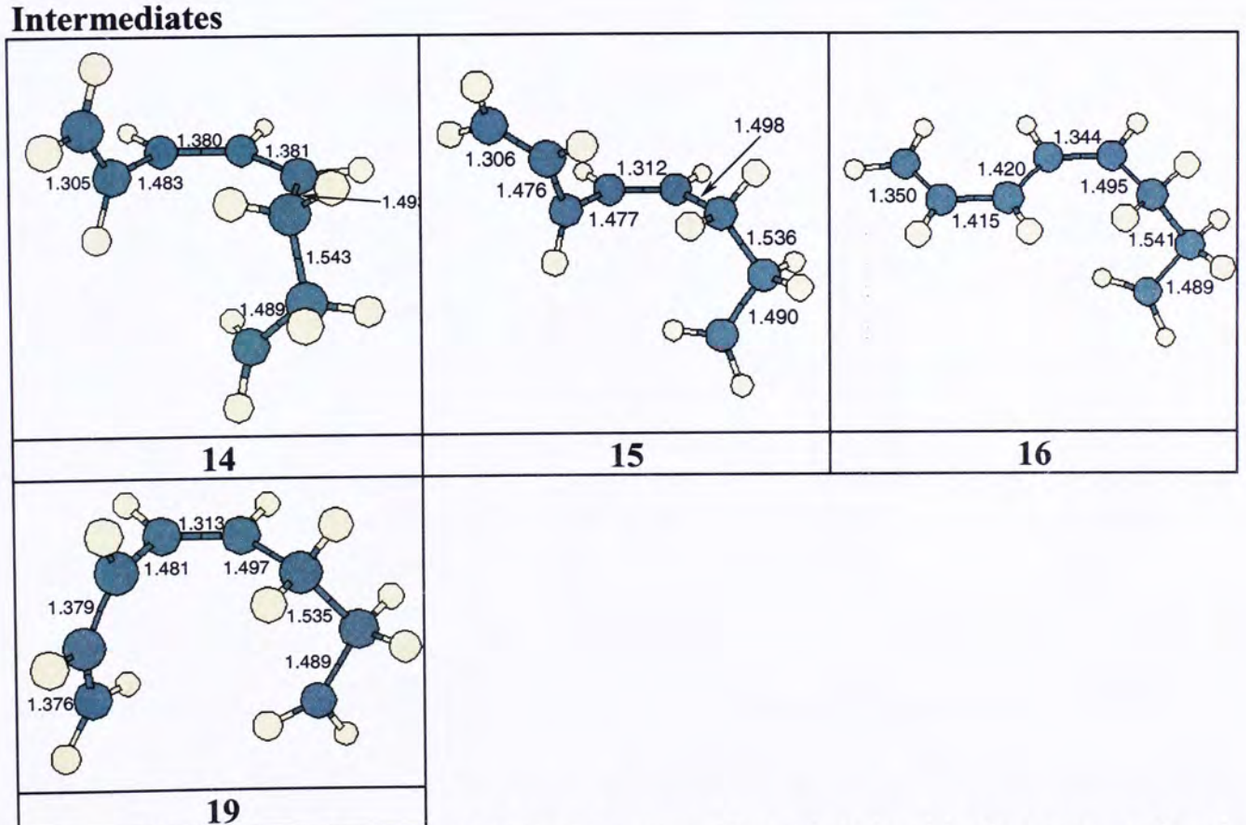

Figure 12. The structures of all TSs and intermediates involved in the concerted and stepwise pathways for the [2+6] electrocyclic addition between hexatriene and ethylene.

3.3.1 Reaction between ethylene and butadiene

Tables 1 and 2 summarize the total energies (E_0), enthalpies (H_{298}), relative energies, and relative enthalpies of all the species, including all the stable species and all the TSs, found in the Diels-Alder reaction between butadiene and ethylene calculated by the G3 and G3(MP2) methods, respectively. The G3 potential energy surfaces (PES) of this reaction are shown in Figure 1. [We have not shown the G3(MP2) profiles as they are very similar to the G3 ones.] There are two possible concerted pathways for this reaction. In the first one, *trans*-butadiene first "isomerizes" to *cis*-butadiene and then combines with ethylene to form **TSa** (with C_s symmetry). This TS then proceeds to yield the product cyclohexene (1) via **TSb** (also C_s). It is noted that **1** has C_2 symmetry and it has a *cis* arrangement around the C=C double bond.

Table 1: The total energies (E_0), enthalpies (H_{298}), relative energies, and relative enthalpies of the species involved in the Diels-Alder reaction between butadiene and ethylene calculated by the G3 method

Species	E_0 (Hartrees)	H_{298} (Hartrees)	Relative E_0 (kJ mol^{-1})	Relative H_{298} (kJ mol^{-1})
ethene	-78.50601	-78.50200	--	--
trans-butadiene	-155.84425	-155.83854	--	--
reactants	-234.35026	-234.34054	0.0	0.0
TSa	-234.31045	-234.30290	104.5	98.8
TSb	-234.40069	-234.39472	-132.4	-142.2
TSc	-234.28277	-234.27548	177.2	170.8
TSd	-234.30062	-234.29411	130.3	121.9
TSe	-234.28832	-234.27994	162.6	159.1
TSf	-234.29505	-234.28663	145.0	141.5
TSg	-234.29031	-234.28220	157.4	153.2
TSh	-234.29658	-234.28900	140.9	135.3
1	-234.40903	-234.40903	-154.3	-179.8
2	-234.32947	-234.32315	54.6	45.7
3	-234.29487	-234.28595	145.4	143.3
4	-234.29472	-234.28564	145.8	144.1
5	-234.29525	-234.28637	144.4	142.2

Table 2: The total energies (E_0), enthalpies (H_{298}), relative energies, and relative enthalpies of the species involved in the Diels-Alder reaction between butadiene and ethylene calculated by the G3(MP2) method

Species	E_0 (Hartrees)	H_{298} (Hartrees)	Relative E_0 (kJ mol^{-1})	Relative H_{298} (kJ mol^{-1})
ethene	-78.43336	-78.42935	--	--
trans-butadiene	-155.69756	-155.69184	--	--
reactants	-234.13092	-234.12119	0.0	0.0
TSa	-234.09354	-234.08599	98.1	92.4
TSb	-234.17989	-234.17392	-128.6	-138.4
TSc	-234.06506	-234.05777	172.9	166.5
TSd	-234.07874	-234.07223	137.0	128.5
TSe	-234.06631	-234.05793	169.6	166.1
TSf	-234.07300	-234.06458	152.1	148.6
TSg	-234.06828	-234.06018	164.5	160.2
TSh	-234.07448	-234.06690	148.2	142.5
1	-234.18819	-234.18169	-150.4	-158.8
2	-234.10983	-234.10351	55.4	46.4
3	-234.07281	-234.06390	152.6	150.4
4	-234.07270	-234.06360	152.9	151.2
5	-234.07318	-234.06430	151.6	149.4

The final steps (**TSa** → **TSb** → **1**) of this pathway deserves a fuller description. By carrying out an IRC calculation starting with **TSa** (C_s), energy will decrease until **TSb** (also C_s) is reached. Upon vibrational frequency calculation, it is found that **TSb** has one imaginary frequency at 28.0*i* cm^{-1} with A" symmetry. By carrying out an additional IRC calculation starting from **TSb**, i.e., by following the transition vector and by symmetry breaking, cyclohexene (**1**) with C_2 symmetry is obtained.

The second concerted pathway involves the addition of ethylene to *trans*-butadiene to form intermediate **2** (C_2) via **TSc** (C_2). It is noted that **2** is also a cyclohexene molecule except that there is a *trans* arrangement around the C=C double bond and hence it is about 200 kJ mol^{-1} less stable than **1**. The "isomerization" of **2** → **1** takes place via π-bond rotation transition state **TSd** (C_2). The G3 and G3(MP2) energy barriers of the first concerted pathway [reactants → **TSa** → **TSb** → **1**] are 104.5 and 98.1 kJ mol^{-1}, respectively. These results are in very good agreement with the experimental data, 105.0 kJ mol^{-1}.[10] [It is noted that, in the experimental study of this reaction, the investigation was carried out at 800 K. When the experimental result was "extrapolated" to 0 K, the barrier of 105.0 kJ mol^{-1}

was obtained. This "extrapolated" value is chosen for direct comparison between the calculated and experimental results, it does not mean the reaction would occur at 0 K.]

On the other hand, the G3 and G3(MP2) activation energies of the second concerted pathway [reactants → **TSc** → **2** → **TSd** → **1**] are 177.2 and 172.9 kJ mol^{-1}, respectively. The G3 and G3(MP2) π-rotation barriers between cyclohexenes **1** and **2** are 284.6 and 287.4 kJ mol^{-1} (with respect to **1**), respectively. These calculated barriers are in good accord with the experimental π-rotation energy in alkenes, ca. 272.0 kJ mol^{-1}.[18,19]

Our calculations show that the second concerted pathway lies 72.7 kJ mol^{-1} higher in energy than the first one. This means that the *cis*-conformer of butadiene presents a more favorable geometry for cycloaddition. This conformational preference is probably due to that the C1-C4 distance in the *trans*-conformer is about 0.65 Å longer than that in the *cis*-conformer. In other words, the *cis*-conformer has a more efficient overlap with ethylene than the *trans*-conformer.

In addition to the concerted pathways discussed so far, this [2+4] cycloaddition can also be achieved by a stepwise mechanism. In this pathway, also shown in Figure 1, the first step is the formation of an *anti* biradical intermediate **3** (C_1) via **TSe** (C_1). Then the newly attached C_2H_4 moiety undergoes a very facile rotation to form another biradical intermediate **4** (C_1) via **TSf** (C_1). Next, a rotation along the newly formed σ bond in **4** yields **5** (C_1) via **TSg** (C_1). Now **5** has the proper stereochemistry to undergo ring closure to form cyclohexene **1** via **TSh** (C_1) and **TSb**. The rate-determining step of this mechanism is the first process, the formation of **3** via **TSe**. The G3 and G3(MP2) activation energies are 162.6 and 169.6 kJ mol^{-1}, respectively. They are in fair agreement with the result (174.4 kJ mol^{-1}) of a previous calculation.[1]

Summarizing the results of this addition reaction, the Diels-Alder reaction between butadiene and ethylene should proceed via the concerted pathway: reactants → **TSa** → **TSb** → **1**. In other words, the remaining concerted pathway and the stepwise mechanism are merely of academic interest. Furthermore, the G3 and G3(MP2) models yield reliable quantitative energetic results for this reaction. Hence, it may be expected that these methods will also lead to dependable

quantitative results for other similar reactions for which no experimental data are available.

Other than the famous [2+4] Diels-Alder reaction, the [2+2] cycloaddition between butadiene and ethylene has also been investigated. Similar to the [2+4] reaction, both concerted and stepwise mechanisms are possible. Tables 3 and 4 show the E_0, H_{298}, relative energies, and relative enthalpies of all the species, including all the stable species and all the TSs, found in the [2+2] cycloaddition reaction between butadiene and ethylene calculated by the G3 and G3(MP2) methods, respectively. Figure 3 summarizes the G3 PESs of the concerted and stepwise pathways of this reaction. Once again, we have not shown the G3(MP2) profiles as they are very similar to the G3 ones.

Table 3: The total energies (E_0), enthalpies (H_{298}), relative energies, and relative enthalpies of the species involved in the [2+2] cycloaddition reaction between butadiene and ethylene calculated by the G3 method

Species	E_0 (Hartrees)	H_{298} (Hartrees)	Relative E_0 (kJ mol^{-1})	Relative H_{298} (kJ mol^{-1})
ethene	-78.50601	-78.50200	--	--
trans-butadiene	-155.84425	-155.83854	--	--
reactants	-234.35026	-234.34054	0.0	0.0
TSi	-234.23035	-234.22244	314.8	310.1
TSj	-234.28951	-234.28102	159.5	156.3
TSk	-234.29074	-234.28225	156.3	153.0
TSℓ	-234.29047	-234.28215	157.0	153.3
TSm	-234.29404	-234.28627	147.6	142.5
6	-234.37116	-234.36392	-54.9	-61.4
7	-234.29558	-234.28648	143.6	141.9
8	-234.29586	-234.28673	142.8	141.3
9	-234.29603	-234.28714	142.4	140.2

Table 4: The total energies (E_0), enthalpies (H_{298}), relative energies, and relative enthalpies of the species involved in the [2+2] cycloaddition reaction between butadiene and ethylene calculated by the G3(MP2) method

Species	E_0 (Hartrees)	H_{298} (Hartrees)	Relative E_0 (kJ mol^{-1})	Relative H_{298} (kJ mol^{-1})
ethene	-78.43336	-78.42935	--	--
trans-butadiene	-155.69756	-155.69184	--	--
reactants	-234.13092	-234.12119	0.0	0.0
TSi	-234.01160	-234.00368	313.3	308.5
TSj	-234.06735	-234.05887	166.9	163.6

TSk	-234.06854	-234.06006	163.8	160.5
TSℓ	-234.06825	-234.05993	164.5	160.8
TSm	-234.07176	-234.06399	155.3	150.2
6	-234.15016	-234.14293	-50.5	-57.1
7	-234.07336	-234.06427	151.1	149.4
8	-234.07367	-234.06454	150.3	148.7
9	-234.07384	-234.06495	149.9	147.7

In the concerted pathway, the ethylene directly attaches to the C1 and C2 atoms of *trans*-butadiene via **TSi** (C_1) to form vinylcyclobutane **6** (C_1). The G3 and G3(MP2) activation energy of this process is 314.8 and 313.3 kJ mol^{-1}, respectively. In the stepwise pathway, the first step is the formation of an *anti* biradical intermediate, **7** (C_1) via **TSj** (C_1). Next, the newly attached C_2H_4 moiety undergoes a very facile rotation via **TSk** (C_1) to form another biradical intermediate **8** (C_1). Then a rotation along the newly formed σ bond in **8** yields **9** (C_1) via **TSℓ** (C_1), without much energy cost. Now the conformation of **9** is suitable to undergo cyclization and form vinylcyclobutane **6** via **TSm** (C_1). The rate-determining step of this mechanism is the first process, the formation of **7** via **TSj**. The G3 and G3(MP2) activation energies are 159.5 and 166.9 kJ mol^{-1}, respectively. Obviously, the overall energy barrier of the stepwise pathway is much lower than the concerted one by 155.3 kJ mol^{-1}. Therefore, this reaction should proceed via the stepwise mechanism. On the other hand, the barrier for the [2+2] addition is still higher than that for the [2+4] addition, by about 55 kJ mol^{-1}.

Comparing the results of all the possible mechanisms of the two addition reactions between butadiene and ethylene, the [2+4] concerted pathway: reactants → **TSa** → **TSb** → **1** should be the most favorable.

3.3.2 Reaction between ethylene and hexatriene

As shown in the study of the previous reaction, both G3 and G3(MP2) methods are able to yield reliable results. Hence, for the present reaction, we elected to employ the less time consuming method, G3(MP2). When hexatriene reacts with ethylene, there are three possible processes: the [2+2], [2+4], and [2+6] cycloadditions. Table 5 lists the E_0, H_{298}, relative energies, and relative enthalpies of all the species involved in the cycloadditon between hexatriene and ethylene calculated by the G3(MP2) method.

Table 5: The total energies (E_0), enthalpies (H_{298}), relative energies, and relative enthalpies of the species involved in the electrocyclic addition between hexatriene and ethylene calculated by the G3(MP2) method

Species	E_0 (Hartrees)	H_{298} (Hartrees)	Relative E_0 (kJ mol^{-1})	Relative H_{298} (kJ mol^{-1})
ethene	-78.43336	-78.42935	--	--
hexatriene	-232.94855	-232.94062	--	--
reactants	-311.38191	-311.36997	0.0	0.0
TSn	-311.27744	-311.26754	274.3	268.9
TSo	-311.40649	-311.39762	-64.5	-72.6
TSp	-311.34793	-311.33814	89.2	83.6
TSq	-311.33807	-311.32846	115.1	109.0
TSr	-311.31491	-311.30452	175.9	171.8
TSs	-311.30219	-311.29153	209.3	205.9
TSt	-311.30087	-311.29027	212.8	209.3
TSu	-311.33551	-311.32563	121.8	116.4
TSv	-311.32925	-311.31919	138.3	133.3
TSw	-311.32733	-311.31741	143.3	138.0
TSx	-311.44623	-311.43814	-168.9	-179.0
TSy	-311.33035	-311.32025	135.4	130.5
TSz	-311.32544	-311.31589	148.3	142.0
10	-311.40817	-311.39877	-68.9	-75.6
11	-311.40988	-311.40044	-73.4	-80.0
12	-311.44690	-311.43823	-170.6	-179.2
13	-311.44339	-311.43503	-161.4	-170.8
14	-311.32120	-311.31039	159.4	156.4
15	-311.29868	-311.28731	218.5	217.0
16	-311.34076	-311.32985	108.0	105.3
17	-311.32587	-311.31487	147.1	144.7
18	-311.44598	-311.43723	-168.2	-176.6
19	-311.32645	-311.31561	145.6	142.7

(a) Comparison of the three concerted reaction pathways

The energy profiles for the concerted pathways of the three cycloadditions are summarized in Figure 5. The activation energies of the [2+2], [2+4], and [2+6] cycloadditions are 274.3, 89.2, and 115.1 kJ mol^{-1}, respectively. These results, which indicate that both the [2+4] and [2+6] pathways are much more probable than the [2+2] pathway, agree with the Woodward-Hoffmann rules. Also, among the two more probable processes, the overall energy barrier of [2+4] pathway is 25.9 kJ mol^{-1} lower.

If both the [2+4] and [2+6] concerted pathways are probable, in accordance with the Woodward-Hoffmann rules, why is the [2+4] pathway is energetically

favored? This is because the π-type atomic orbitals in **TSq** (the TS for the [2+6] process) are twisted, making the overlap between the reactants less effective. In addition, the C1-C4 distance in **TSp** (the TS for [2+4] process) is 2.99 Å, while that of C1-C6 in **TSq** is 3.33 Å. Hence **TSp** has a more favorable structural condition for cycloaddition. Furthermore, the strain energy of a six-membered ring is lower than that of an eight-membered ring, making **TSp** more stable.

(b) Comparison of the concerted and stepwise pathways

The reaction profiles of the concerted and stepwise pathways of the [2+2] cycloaddition are displayed in Figure 7 for direct comparison. As mentioned before, due to the geometric constraints, the formation of the TS, TSn, of this antarafacial pathway is difficult, leading to a very high energy barrier (274.3 kJ mol^{-1}). In the stepwise pathway, the terminal carbons of the two reactants first form a C–C σ bond, leading to the formation of intermediate **14** (C_1) via **TSr** (C_1). Then **14** undergoes rotation, at a fairly large energy cost, around the C3–C4 bond of the original hexatriene to yield **15** (C_1) via **TSs** (C_1). Next, **15** undergoes rotation, without much energy cost, around the same C–C bond to yield **16** (C_1) via **TSt** (C_1). Subsequently, **16** undergoes cyclization, without much energy expense, to yield product **11** (C_1) via **TSt** (C_1). The rate-determining step is the rotation of the C3–C4 bond of the original hexatriene. Rotations of this type disrupt the delocalization of π electrons and the unpaired electron, thus destabilizing the biradical. Therefore, the overall barrier is 218.5 kJ mol^{-1}. This barrier is significantly lower (by 55.8 kJ mol^{-1}) than that of the concerted pathway. This result agrees well with the Woodward-Hoffman prediction: The energy cost of the concerted pathway for this cycloaddition will be very high; thus it is more likely to take place via the stepwise mechanism.

Before proceeding to discussion the [2+4] process, it is noted that we did try to study the [2+2] addition between hexatriene and ethylene with the reaction taking place at the "middle" π bond of the triene. However, repeated attempts to locate the TS(s) were not successful.

The reaction profiles of the concerted and stepwise pathways of the [2+4] cycloaddition are shown in Figure 9. Similar to the stepwise pathway of the [2+2] cycloaddition, the first three steps produce **14** via **TSr**, next **15** via **TSs**, and then **16** via **TSt**. Then the C–C σ bond of C_2H_3 moiety undergoes a very facile upward

rotation to form **17** (C_1) via **TSv** (C_1). Subsequently, **17** undergoes cyclization, without much energy expense, to first form **18** (C_1) via **TSw** (C_1) and then yield product **12** (C_1) via **TSx** (C_1). The rate-determining step is again the rotation of the C3–C4 bond of the original hexatriene and the overall barrier is also 218.5 kJ mol^{-1}. This barrier is much higher than that for the concerted pathway, 129.3 kJ mol^{-1}. Thus the [2+4] cycloaddition will take place concertedly.

The PESs of the concerted and stepwise pathways of the [2+6] cycloaddition are displayed in Figure 11. Similar to the stepwise pathway of the [2+2] cycloaddition, the first three steps produce **14** via **TSr**, next **15** via **TSs**, and then **16** via **TSt**. Then the terminal C_2H_3 moiety of **16** undergoes a very facile downward rotation to form biradical intermediate **19** (C_1) via **TSy** (C_1). Finally, **19** undergoes cyclization, to form product **13** (C_2) via **TSz** (C_1). As the first few steps, i.e., **TSr** to **16**, of the stepwise [2+6] cycloaddition is identical to the [2+2] or [2+4] biradical mechanism, the rate-determining steps are thus identical, and the overall barrier is again 218.5 kJ mol^{-1}. This barrier is 103.4 kJ mol^{-1} higher than that for the concerted [2+6] pathway.

Summarizing the results of the various pathways of the three addition reactions between hexatriene and ethylene, it is found that the concerted [2+4] pathway has the lowest energy barrier, 89.2 kJ mol^{-1}. The one with the next lowest barrier is the concerted [2+6] pathway; this barrier is 115.1 kJ mol^{-1}.

3.3.3 Electrocyclic reaction of hexatriene

In addition to the three possible cycloaddition reactions between hexatriene and ethylene, we have also studied electrocyclic formation of cyclohexadiene, which is a competitive reaction for the Diels-Alder reaction. The G3(MP2) calculation was also employed in this reaction. Table 6 lists the E_0, H_{298}, relative energies, and relative enthalpies of all the species involved in the electrocylcic reaction of *cZc*-hexatriene. There are two possible mechanisms for the ring closing process. They are the conrotatory and disrotatory pathways. Repeated attempts were made to locate the TS of the conrotatory process. However, they were not successful. In other words, only the disrotatory pathway is found and it is shown in Figure 13. The structures of the intermediate and TSs of this pathway are displayed in Figure 14.

Table 6: The total energies (E_0), enthalpies (H_{298}), relative energies, and relative enthalpies of the species involved in the electrocyclic reaction of *cZc*-hexatriene calculated by the G3(MP2) method

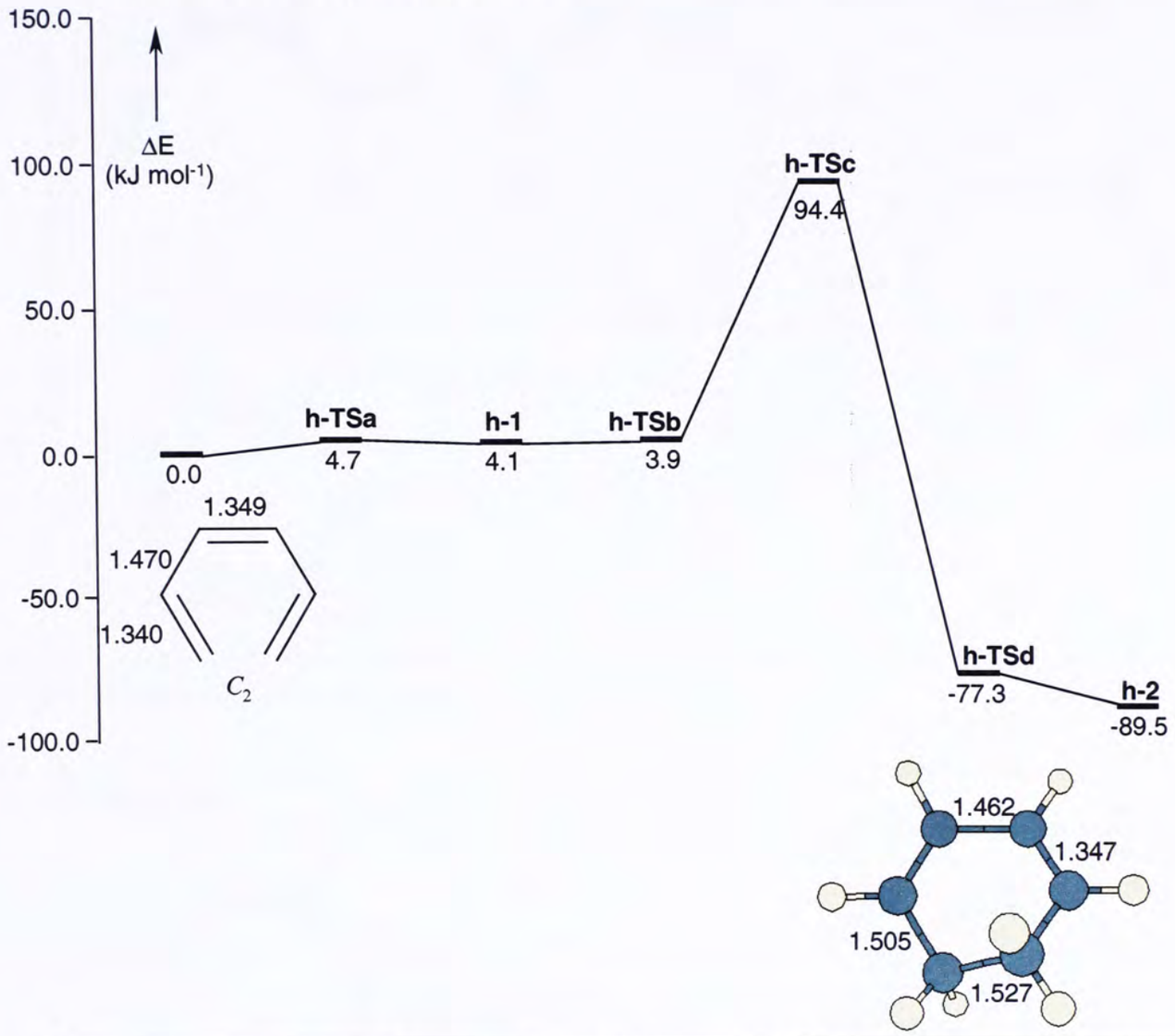

Species	E_0 (Hartrees)	H_{298} (Hartrees)	Relative E_0 (kJ mol^{-1})	Relative H_{298} (kJ mol^{-1})
***cZc*-hexatriene**	-232.94855	-232.94062	--	--
h-TSa	-232.94676	-232.93964	4.7	2.6
h-1	-232.94698	-232.93903	4.1	4.2
h-TSb	-232.94705	-232.93996	3.9	1.7
h-TSc	-232.91260	-232.90603	94.4	90.8
h-TSd	-232.97801	-232.97229	-77.3	-83.1
h-2	-232.98264	-232.97642	-89.5	-94.0

Figure 13. The G3(MP2) energy profile showing the disrotatory electrocyclic reaction of *cZc*-hexatriene studied in this work.

Transition Structures

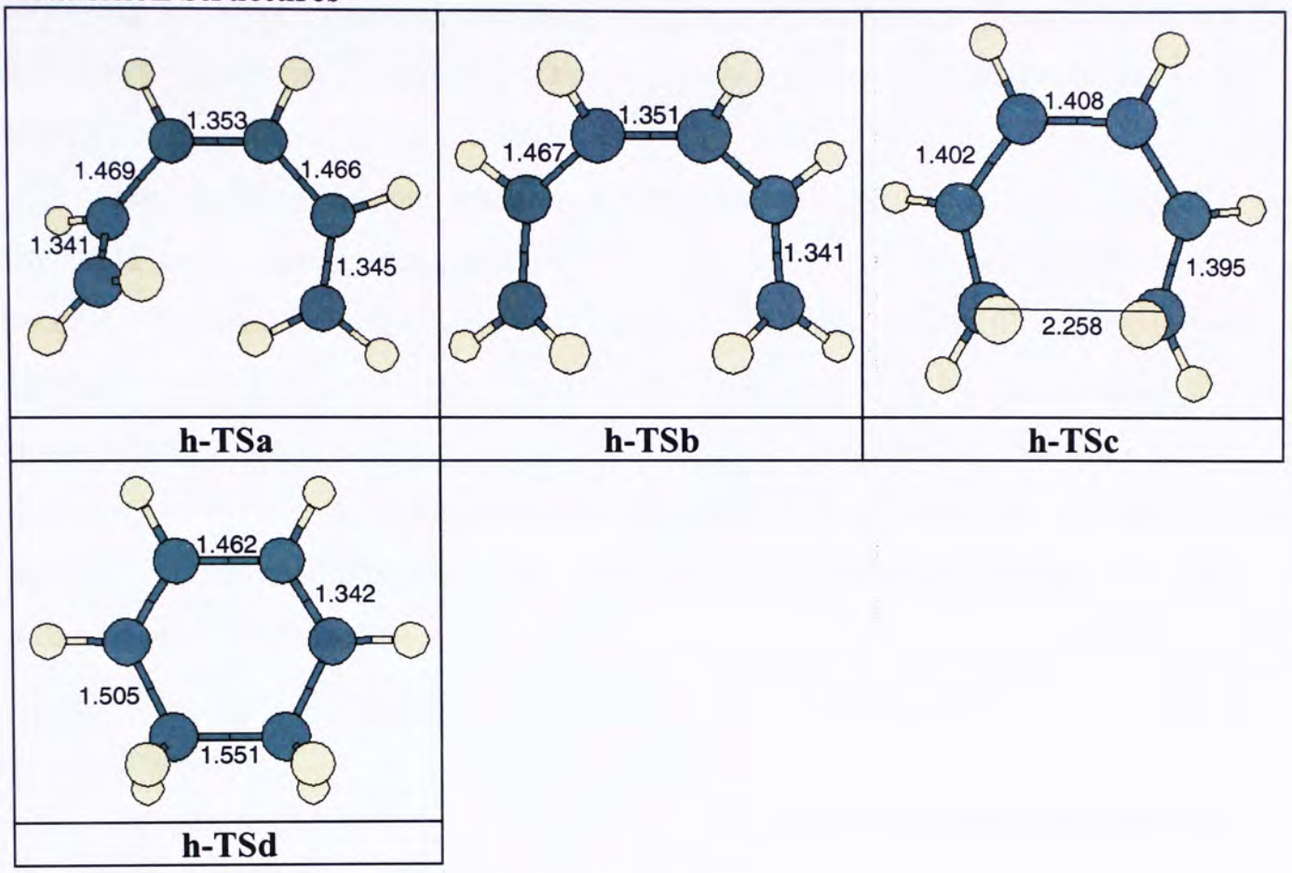

h-TSa | **h-TSb** | **h-TSc**

h-TSd

Intermediate

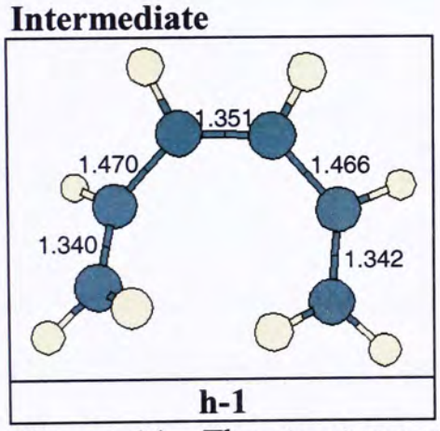

h-1

Figure 14. The structures of all TSs and intermediate involved in the disrotatory electrocyclic reaction of *cZc*-hexatriene.

In order to obtain a proper orientation for the disrotatory cyclization, *cZc*-hexatriene changes its geometry from C_2 symmetry to C_s through **h-TSa**. It is noted that *cZc*-hexatriene with C_s geometry (**h-TSb**) is not a stable species; it has one imaginary frequency at 45.2*i* cm^{-1} with A" symmetry. From **h-TSb** the cyclization process commences: it proceeds to form **h-TSd** via **h-TSc**. At **h-TSc**, the two terminal carbon atoms are 2.258 Å apart. Also, **h-TSd** is essentially cyclohexadiene. But it is a TS with C_{2v} symmetry; its imaginary frequency is at 191.4*i* cm^{-1} with A_2 symmetry. By carrying out an IRC calculation starting from **h-TSd**, i.e., by

following the aforementioned transition vector and by symmetry breaking, product **h-2** with C_2 symmetry is obtained. The overall energy barrier of this process is 94.4 kJ mol^{-1}.

Summarizing the four reactions involving hexatriene, the most energetically favorable mechanism is the concerted [2+4] pathway, forming product **12** in the process. The next favorable pathway, with a barrier about 5 kJ mol^{-1} higher, is the disrotatory electrocyclic reaction of hexatriene, yielding product **h-2**. In addition, the two products of these two processes, **12** and **h-2**, are of comparable stability. Since the error bar for the G3(MP2) method is at best ±10-15 kJ mol^{-1}, the two barriers obtained are essentially the same. As a result, it is likely that both of these processes will take place concurrently.

3.4 Conclusion

In this work, we have undertaken a study on the concerted and stepwise pathways of the [2+2] and [2+4] cycloadditions between ethylene and butadiene; the [2+2], [2+4] and [2+6] cycloadditions between ethylene and hexatriene, as well as the ring closing process of hexatriene. The butadiene reactions have been investigated using the G3 and G3(MP2) methods, while the remaining reactions have been studied employing only the G3(MP2) model.

For the reaction between ethylene and butadiene, it is found that the most favorable pathway is the concerted [2+4] addition with the mechanism: reactants → **TSa** → **TSb** → **1**. The calculated barriers are in excellent agreement with the experimental data.

Among the six possible mechanisms for the reaction between hexatriene and ethylene, it is found that the most energetically favorable pathway is the concerted [2+4] mechanism with a barrier of 89.2 kJ mol^{-1}, while the barrier of the [2+6] concerted pathway is 115.1 kJ mol^{-1}. On the other hand, the concerted [2+2] pathway has an exceedingly high energy barrier of 274.3 kJ mol^{-1}. These results are in accord with the Woodward-Hoffmann rules. On the other hand, all three stepwise pathways have the same rate-determining step with a barrier of 218.5 kJ mol^{-1}.

For the electrocyclic reaction of hexatriene, it is found that the disrotatory pathway is: hexatriene → **h-TSa** → **h-1** → **h-TSb** → **h-TSc** → **h-TSd** → **h-2**. The G3(MP2) barrier for this cyclization process is 94.4 kJ mol^{-1}.

After comparing the addition reactions with the elecrtocyclic reaction involving hexatriene, the barriers of the [2+4] cycloaddition process and the ring closing process differ by only about 5 kJ mol^{-1}, which is well within the error bar of the G3(MP2) methods, about ±10-15 kJ mol^{-1}. Hence it is likely both of these processes will take place concurrently.

3.5 References

1. Sakai, S. *J. Phys. Chem. A* **2000**, *104*, 922.
2. Goldstein, E.; Beno, B.; Houk, K. N. *J. Am. Chem. Soc.* **1996**, *118*, 6036.
3. Uchiyama, M.; Tomioka, T.; Amano, A. *J. Phys. Chem.* **1964**, *68*, 1878.
4. Bradley, A. Z.; Kociolek M. G.; Johnson, R. P. *J. Org. Chem.* **2000**, *65*, 7134.
5. Townshend, R. E.; Ramunni, G. *J. Am. Chem. Soc.* **1976**, *98*, 2190.
6. Dewar, M. J. S.; Pierini, A. B. *J. Am. Chem. Soc.* **1984**, *106*, 203.
7. Firestone, R. A. *Tetrahedron.* **1996**, *52*, 14459.
8. Li, Y.; Houk, K. N. *J. Am. Chem. Soc.* **1993**, *115*, 7478.
9. Carpenter, J. E.; Sosa, C. P. *J. Mol. Struct. (Theochem)* **1994**, *331*, 325.
10. Rowley, D.; Steiner, H. *Discuss. Faraday Soc.* **1951**, *10*, 198.
11. Curtiss, L. A.; Redfern, P. C. *J. Chem. Phys.* **1998**, *109*, 7764.
12. Curtiss, L. A.; Redfern, P. C. *J. Chem. Phys.* **1999**, *110*, 4703.
13. Cheng, M.-F.; Li, W.-K. *J. Phys. Chem. A* **2003**, 107, 5492.
14. Lau, J. K.-C.; Li, W.-K.; Qi, F.; Suits, A. G. *J. Phys. Chem. A* **2002**, *106*, 11025.
15. Frisch, M. J.; Trucks, G. W.; Schlegel, H. B.; Scuseria, G. E.; Robb, M. A.; Cheeseman, J. R.; Zakrzewski, V. G.; Montgomery, J. A.; Stratmann, R. E.; Burant, J. C.; Dapprich, S.; Millam, J. M.; Daniels, A. D.; Kudin, K. N.; Strain, M. C.; Farkas, O.; Tomasi, J.; Barone, V.; Cossi, M.; Cammi, R.; Mennucci, B.; Pomelli, C.; Adamo, C.; Clifford, S.; Ochterski, J.; Petersson, G. A.; Ayala, P. Y.; Cui, Q.; Morokuma, K.; Malick, D. K.; Rabuck, A. D.; Raghavachari, K.; Foresman, J. B.; Cioslowski, J.; Ortiz, J. V.; Stefanov, B. B.; Liu, G.; Liashenko, A.; Piskorz, P.; Komaromi, P. I.; Gomperts, R.; Martin, R. L.; Fox, D. J.; Keith, T.; Al-Laham, M. A.; Peng, C. Y.; Nanayakkara, A.; Gonzalez, C.; Challacombe, M.; Gill, P. M. W.; Johnson, B. G.; Chen, W.; Wong, M. W.; Andres, J. L.; Head-Gordon, M.; Replogle, E. S.; Pople, J. A.; Gaussian 98, Revision A.9, Gaussian, Inc., Pittsburgh PA, 1998.

16. Gonzalez, C.; Schlegel, H. B. *J. Chem. Phys.* **1989**, *90*, 2154.

17. Gonzalez, C.; Schlegel, H. B. *J. Chem. Phys.* **1990**, *94*, 5523.

18. Douglas, J. E.; Rabinovitch, B. S.; Looney, F. S. *J. Chem. Phys.* **1995**, *23*, 315.

19. Wallace, R. *Chem. Phys. Lett.* **1989**, *159*, 35.

Chapter 4

A G3(MP2) Study on the Electrocyclic Reactions of [12]annulene

Abstract

The pericyclic reactions of [12]annulene have not yet been investigated in depth by theoretical or experimental methods. Only Houk and his co-workers studied one of the electrocyclic reactions, the [2+2+2]-cycloreversion reaction of *cis*-tris-cyclobutenacyclohexane, by the DFT methods. In this paper, we consider some different electrocyclic processes: the possible $[_{\pi}4_a]$ cyclization reactions of [12]-27-annulene. At the MP2(Full)/6-31G(d) level, two conformers of [12]-27-annulene have been identified: **3** with D_2 symmetry and **6** with C_i symmetry, with the former being more stable by about 8 kJ mol^{-1}. Both **3** and **6** can undergo cyclization reactions to yield tricyclic products **5** and **8**. In all, four pathways are found for the four cyclization reactions. In addition, in all four pathways, the two cyclization steps do not take place concomitantly. All the intermediates and transition structures involved in these pathways, as well as all the steps linking them, are described in detail. According to the calculated G3(MP2) results, starting from **1**, the most stable conformer of [12]-27-annulene, the activation energies for the formation of products **5** and **8** will be the same.

4.1 Introduction

In organic chemistry, there are three main classes of reactions: ionic, radical and pericyclic reactions. Furthermore, pericyclic reactions can be further divided into four groups: cycloaddition, electrocyclic reaction, sigmatropic rearrangement and group transfer reaction.

In the past four decades or so, the electrocyclic reactions of some [n]annulenes (n = 8, 10, 14, 16, 18) have been investigated extensively by different chemists.[1-10] However, the pericyclic reactions of [12]annulene have not been studied to a large extent. Only Houk and his co-workers studied, by applying DFT methods, one of the pericyclic reactions of [12]annulene: the [2+2+2]-cycloreversion reaction of *cis*-tris-cyclobutenacyclohexane.[11] The calculated barrier of this [2+2+2]-cycloreversion reaction is 156.1 kJ mol^{-1}, and the reaction is exothermic. In

the present work, we will focus on the possible [$_{\pi}4_{a}$] cyclization reactions of [12]annulene, which have not been previously studied theoretically or experimentally.

In a previous work, we studied the electrocyclic reactions of [16]annulene at the theoretical level of MP2(Full)//B3LYP using the 6-31G(d) basis set.[12] Specifically, we investigated the two cyclization steps of [16]annulene, leading to a tricyclic product with two possible conformations. It turned out that the two cyclization steps do not take place concomitantly and the two possible products are formed by two distinct pathways. In addition, the intermediates of these two pathways may also be linked by additional routes. Hence, fairly rich chemistry is involved in the cyclization reactions of annulenes. This is the main impetus for us to extend our work to [12]annulene. Furthermore, since [12]annulene is a smaller system, the energetics results may be determined by a more reliable method.

Before discussing the electrocyclic reactions, let us first look at the various conformers of [12]annulene. It is noted [12]annulene was first synthesized by Oth and his partners in 1970.[13] That product is now known as [12]-21-annulene (for the nomenclature of [12]annulene, refer to the publication of Oth).[14] This annulene is proposed to be in dynamic equilibrium with [12]-5-annulene. In 2002, Schleyer and co-workers studied some of the conformers of [12]-annulene theoretically.[15] They found that the [12]-0-annulene (with D_2 symmetry) is the most stable conformer, even more stable than the putative [12]-21-annulene.

In the present paper, we report the potential energy profiles for the ring closing process of [12]-27-annulene. These profiles have been obtained using the theoretical model of G3(MP2),[16] which has been shown to give reliable results.[17,18] There are two conformers of [12]-27-annulene (**3** and **6**), both of which are likely to undergo cyclization. On the other hand, the most stable conformer of [12]-27-annulene is 1. Hence, in this study, we investigate the reaction sequence **1** → **3** or **6** → tricyclic products (to be called **5** and **8**).

4.2 Methods of Calculation

All calculations reported here have been carried out using the Gaussian 98 package of programs.[19] The method of calculation employed, G3(MP2), has been described in Chapter 1.

In addition, for each reaction studied, we have identified a number of transition structures (TSs). For each TS found, its "reactants" and "products" have been confirmed by intrinsic reaction coordinate (IRC) calculations.[20,21]

In this work, all the species along the concerted pathway are taken to be closed-shell entities. And the notation **1**, **2**, ..., etc. are used to label the stable species found. Furthermore, the identified TSs of the reactions are denoted as **TSa**, **TSb**, ..., etc. In the following discussion, all the energetic results refer to those obtained at 298 K.

4.3 Results and Discussion

The profiles of all the reactions studied are displayed in Figures 1-3. Also included in these figures are the structures (with selected parameters in Å and degrees) of the species involved in the reactions. Table 1 summarizes the total energies (E_0), enthalpies (H_{298}), relative energies, and relative enthalpies of all the species, including all the stable species and all the TSs, found in the electrocyclic reaction of [12]-27-annulene calculated by the G3(MP2) method.

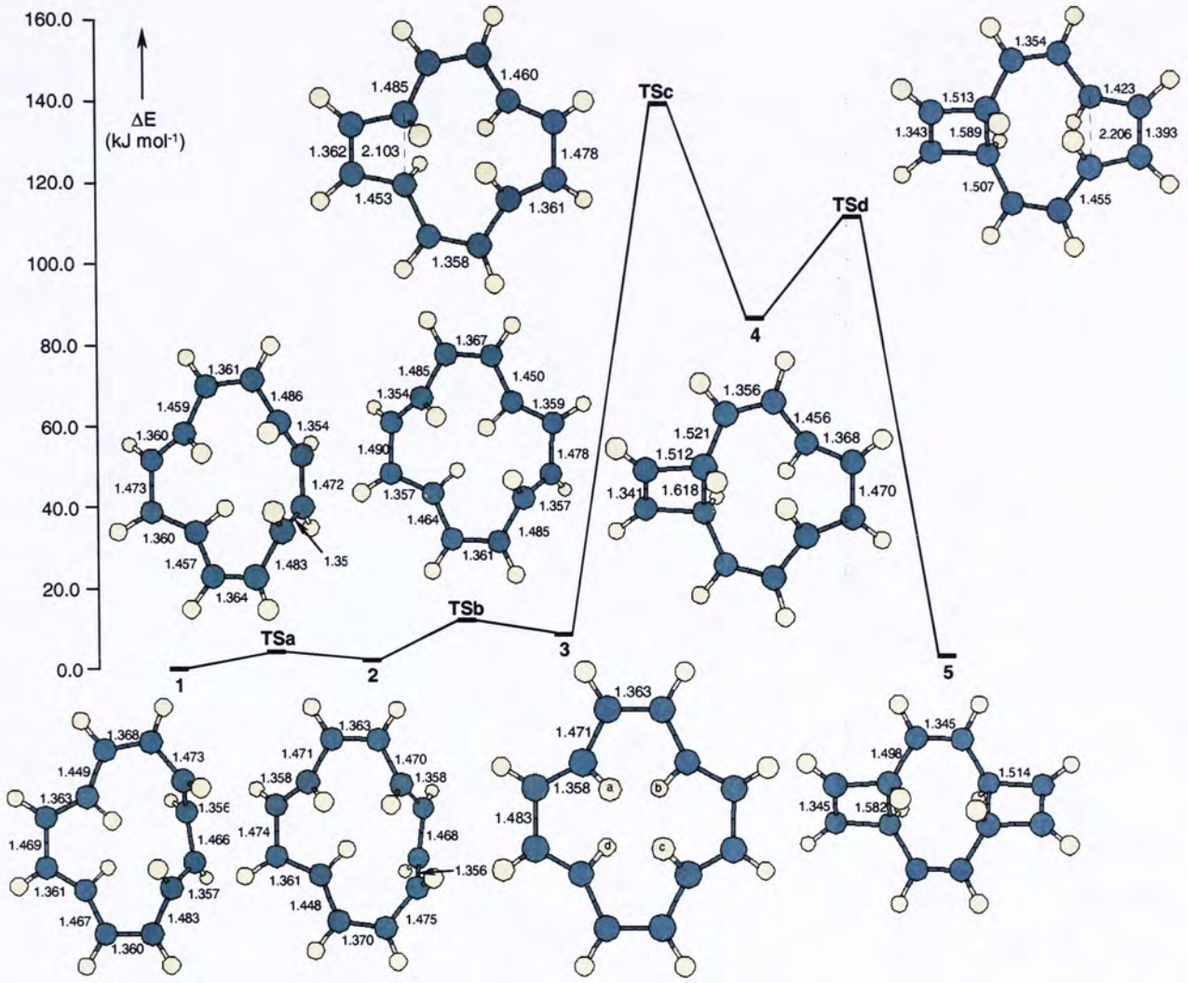

Figure 1. Energy profile of the pathway for the ring closing process (1): **1** → **5**, and the structures of the species involved in this pathway. All bond lengths are in Å.

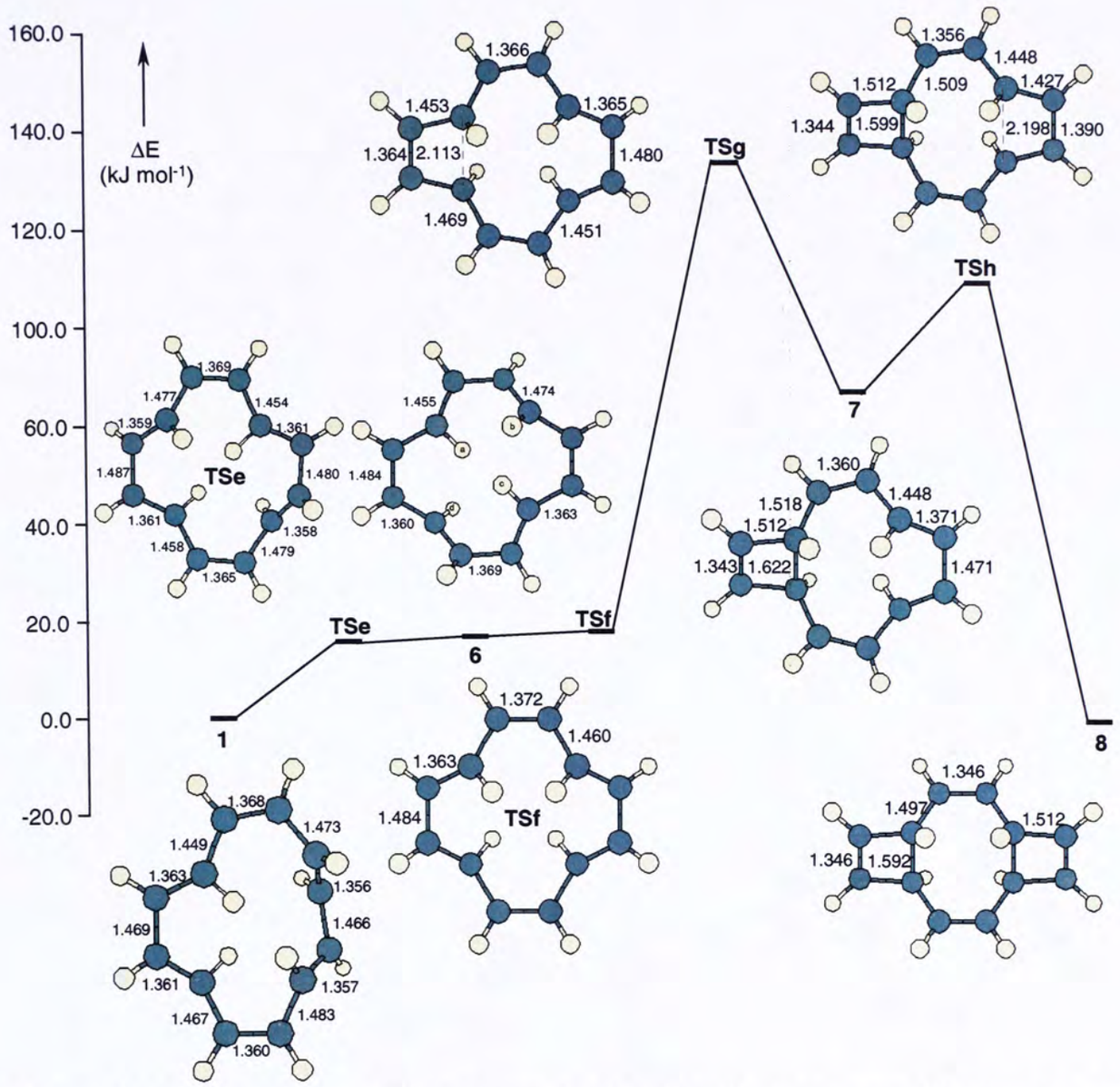

Figure 2. Energy profile of the pathway for the ring closing process (2): **1** → **8**, and the structures of the species involved in this pathway. All bond lengths are in Å.

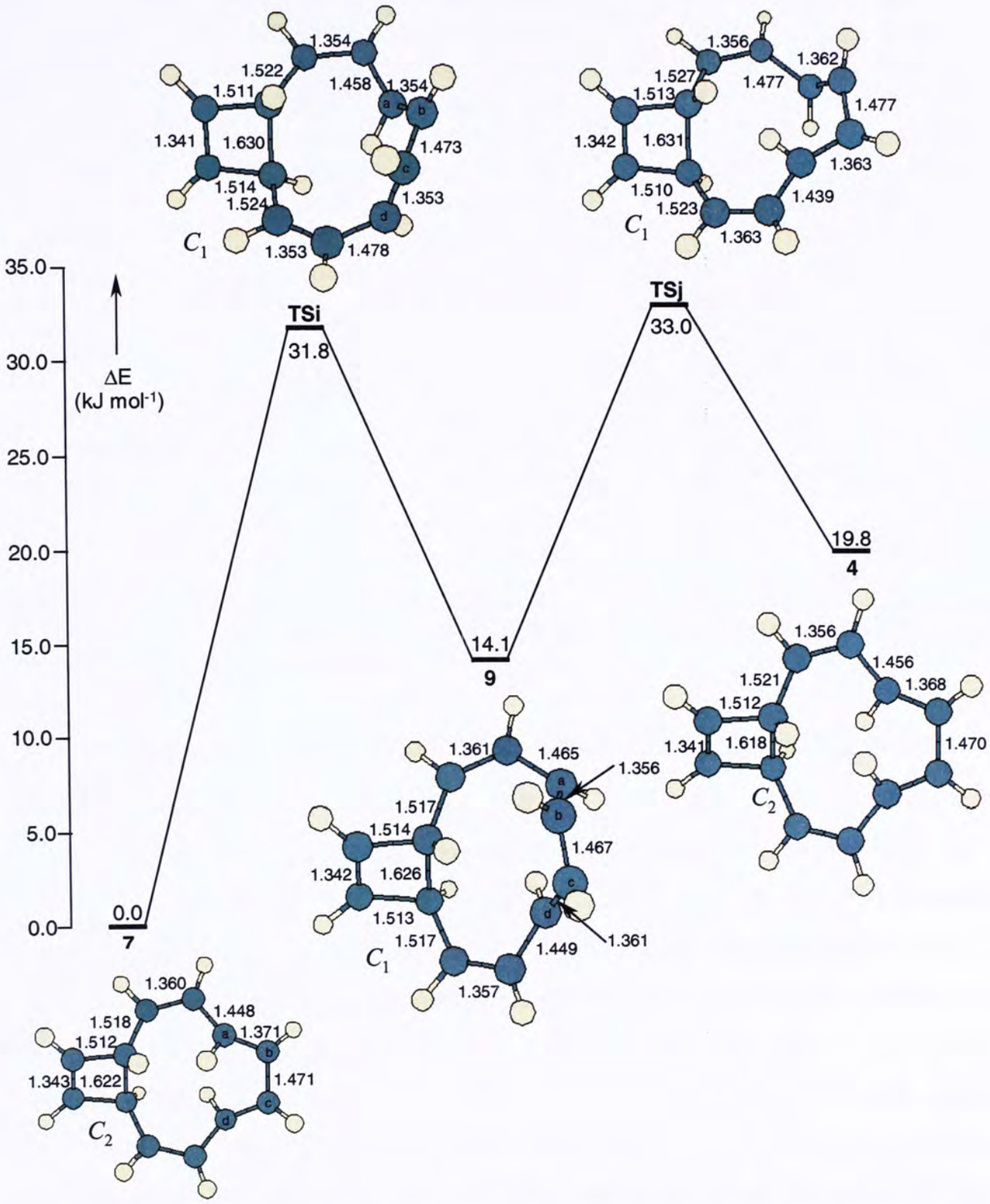

Figure 3. Energy profile of the pathway for the conversion of two intermediates found in processes (1) and (2), **7** → **4**, and the structures of the species involved in this conversion. All bond lengths are in Å.

Table 1: The G3(MP2) total energies (E_0), enthalpies (H_{298}), relative energies, and relative enthalpies of the species involved in this work

Species	Total Energies (E_0) (Hartrees)	Enthalpies (H_{298}) (Hartrees)	Relative Energies (kJ mol^{-1})	Relative Enthalpies (kJ mol^{-1})
1	-463.51068	-463.49890	0.0	0.0

2	-463.51007	-463.49818	1.6	1.9
3	-463.50748	-463.49569	8.4	8.4
4	-463.47705	-463.46579	88.3	86.9
5	-463.50836	-463.49774	6.1	3.0
6	-463.50443	-463.49255	16.4	16.7
7	-463.48456	-463.47333	68.6	67.1
8	-463.50995	-463.49927	1.9	-1.0
9	-463.47919	-463.46797	82.7	81.2
TSa	-463.50870	-463.49732	5.2	4.1
TSb	-463.50549	-463.49431	13.6	12.1
TSc	-463.45657	-463.44535	142.1	140.6
TSd	-463.46683	-463.45609	115.1	112.4
TSe	-463.50400	-463.49292	17.5	15.7
TSf	-463.50336	-463.49209	19.2	17.9
TSg	-463.46646	-463.45524	116.1	114.6
TSh	-463.47540	-463.46475	92.6	89.7
TSi	-463.47195	-463.46123	101.7	98.9
TSj	-463.47125	-463.46076	103.5	100.1
"TSk"[a]	-463.44507	-463.43441	172.3	169.3

[a] "**TSk**" has two imaginary vibrational frequencies at G3(MP2) level and hence is not a true TS. See text for details.

Ring Closing Process (1), 1 → 5. Annulene **1** (C_1 symmetry) is the most stable conformers of [12]-27-annulene. As shown in Figure 1, the σ bond (with length 1.466 Å) that connects the two *trans*-double bonds on the right side of **1** rotates and stable species **2** (C_1), is formed via **TSa** (C_1). Then the *cis*-butadienyl moiety on the right side of **2** flips upward to form intermediate **3** (D_2) via **TSb** (C_1). Next, the two conjugate *trans* double bonds of **3** undergo electrocyclic reaction via **TSc** (C_2) to form a bicyclic intermediate, **4** (C_2). Afterwards, the remaining two conjugate *trans* double bonds of **4** cyclize via **TSd** (C_2) to form a tricyclic stable species **5** (D_2). The enthalpies of **TSc** and **TSd** relative to **1** are 140.6 and 112.4 kJ mol^{-1}, respectively. Therefore, the overall activation energy of this two-step ring closing process is 140.6 kJ mol^{-1}. Additionally, an attempt was made to identify the TS for the one-step pathway of *3* → *5*, in which the two cyclizations take place concomitantly. However, that attempt was not successful.

Ring Closing Process (2), 1 → 8. Other than the cyclization processes mentioned above, annulene **1** can also undergo another reaction pathway to form another product, tricyclic compound **8**. The profile of this second process is summarized in Figure 2. In this pathway, the *cis*-butadienyl moiety of **1** flips upward to form conformer **6** via **TSe** (C_1). Afterwards, **6** proceeds to **TSf** (C_{2h}) by rotating

the relevant σ bonds. Then, the butadiene moiety on the left-hand side of **TSf** undergo electrocyclic reaction via **TSg** (C_2) to form a bicyclic intermediate, **7** (C_2). Next, the other butadiene moiety (on the right-hand side) of **7** cyclizes via **TSh** (C_2) to form a tricyclic stable species **8** (C_{2h}). The energies of **TSg** and **TSh** relative to **1** are 114.6 and 89.7 kJ mol^{-1}, respectively. Thus, the overall energy barrier of this two-step ring closing process is 114.6 kJ mol^{-1}.

The second part of this process, **6** → **TSf** → **TSg**, deserves a fuller description. By carrying out an IRC calculation starting with **TSg** (C_2), energy decreases until **TSf** (C_{2h}) is reached. Upon vibrational frequency calculation, it is found that **TSf** has one imaginary frequency at 149.1i cm^{-1} with B_g symmetry. By carrying out an additional IRC calculation starting from **TSf**, i.e., by following the aforementioned transition vector and by symmetry breaking, [12]-27-annulene (**6**) with C_i symmetry is obtained.

We also attempted to locate the concerted TS for this process, i.e., the TS for the one-step pathway **6** → TS → **8**. A trimerous stationary point, called "**TSk**" (displayed in Figure 4) having C_{2h} symmetry, apparently corresponding to this concerted step has been located. However, species "**TSk**" has two imaginary frequencies of very comparable magnitudes, 518i and 512i cm^{-1}. Hence "**TSk**" is not a true TS. The transition vector with the smaller negative force constant (ν = 512i cm^{-1}) is similar to that of **TSg**, which leads to the formation of one C–C bond (or one cyclization step). On the other hand, the remaining transition vector (ν = 518i cm^{-1}) of "**TSk**" corresponds to the concomitant formation of two C–C bonds (or two simultaneous cyclization steps). Repeated efforts to eliminate the imaginary vibrational frequency with ν = 512i cm^{-1} was not successful. In other words, we also failed to locate the one-step TS for **6** → **8**. It is of interest to note that "**TSk**" is about 54.7 kJ mol^{-1} less stable than **TSg**. Hence, if the one-step TS for **6** → **8** exists, it is probably to be less stable than **TSg**. In other words, reaction **6** → **8** is likely to be a two-step process.

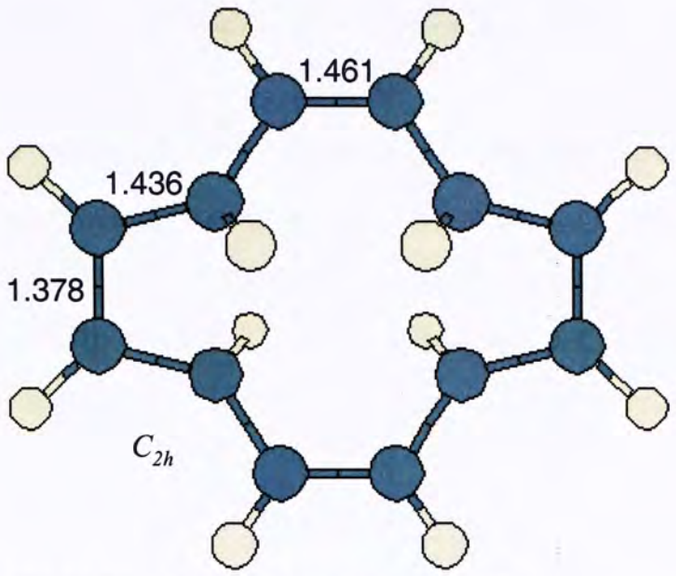

Figure 4. Structure of "**TSk**". All bond lengths are in Å.

Conversion between the two intermediates found in processes (1) and (2), 7 → 4. The intermediates in the ring closing processes (1) and (2) can be converted to each other in the manner described below. Here we choose the more stable intermediate, **7**, as the starting point. As shown in Figure 3, the *cis*-butadienyl moiety (on the right-hand side) of **7** flips upward to form species **9** (C_1) via **TSi** (C_1). This motion mainly involves carbons *a*, *b*, *c* (as labeled in Figure 3), the correspondingly attached hydrogens as well as the hydrogen attached to carbon *d*. Finally the same moiety of **9** flips downward to yield intermediate **4** via **TSj** (C_1). But this time the motion involves mainly four carbons *a*, *b*, *c*, *d* and the corresponding attached hydrogens. The overall activation energy of this conversion is 33.0 kJ mol^{-1}.

4.4 Summary

Summarizing the results described above, annulene **1** can undergo ring closing process (1) to form product **5:**

(a) **1 → TSa → 2 → TSb → 3→ TSc → 4 → TSd → 5** Barrier = 140.6 kJ mol^{-1}

However, **1** can also form product **5** by the following more involved mechanism:

(b) **1 → TSe → 6 → TSf → TSg → 7 → TSi → 9 → TSj → 4 → TSd → 5**

Barrier = 114.6 kJ mol^{-1}

Hence, for the cyclization reaction of **1 → 5**, mechanism (b) is preferred.

On the other hand, **1** can form product **8** via the following pathways:

(c) **1 → TSe → 6 → TSf → TSg → 7 → TSh → 8** Barrier = 114.6 kJ mol^{-1}

(d) **1** → **TSa** → **2** → **TSb** → **3**→ **TSc** → **4** → **TSj** → **9** → **TSi** → **7** → **TSh** → **8**

Barrier = 140.6 kJ mol^{-1}

Hence pathway (c) is preferred over pathway (d) for the reaction of **1** → **8**. Comparing the four ring closing processes, **1** will undergo ring closing processes (a) and (c), forming products **5** and **8**, respectively, and having the same reaction barrier. Upon comparing the enthalpies of the two tricyclic products, compound **8** is more energetically stable, so it should be the thermodynamically preferred product.

4.5 Conclusion

In this paper, we have studied the electrocyclic processes of $[_{\pi}4_a]$ cyclization reactions of [12]-27-annulene. Four pathways are found for the four cyclization reactions. In all four pathways, the two cyclization steps do not take place concomitantly. All the intermediates and transition structures involved in these pathways are described in detail. The G3(MP2) results indicate that, starting from the most stable species **1**, products **5** and **8** will be formed, with the latter being the thermodynamically preferred product.

Finally, it is worth pointing out that, in our previous work on the electrocyclic reactions of [16]annulene, two tricyclic products were also found, as in the case for [12]annulene.[12] Furthermore, the two cyclization steps of [16]annulene occur in a stepwise fashion, as also been found for [12]annulene. In other words, there is remarkable similarity between the electrocyclic reactions of [12]annulene and [16]annulene.

4.6 References

1. Conesa, C; Rzepa, H. S. *J. Chem. Soc. Perkin Trans. 2* **1998**, 2695.
2. Martin-Santamaria, S.; Lavan, B.; Rzepa, H. S. *J. Chem. Soc. Perkin Trans. 2* **2000**, 1415.
3. Sondheimer, F.; Gaoni, Y. *J. Am. Chem. Soc.* **1961**, *83*, 4883.
4. Schröder, G.; Martin, W.; Oth, J. F. M. *Angew. Chem., Int. Ed. Engl.* **1967**, *6*, 870.
5. Johnson, S. M.; Paul, I. C.; King, G. S. B. *J. Chem. Soc. B.* **1970**, 643.
6. Oth, J. F. M.; Gilles, J.-M. *Tetrahedron Lett.* **1968**, 6259.

7. Martin-Santamaria, S.; Lavan, B.; Rzepa, H. S. *J. Chem. Soc. Perkin Trans. 2* **2000**, 2372.
8. Karney, W. L.; Kastrup, C. J.; Oldfield, S. P.; Rzepa, H. S. *J. Chem. Soc. Perkin Trans. 2* **2002**, 388.
9. Kastrup, C. J.; Oldfield, S. P.; Rzepa, H. S. *Chem. Commun.* **2002**, 642.
10. Kennedy, R. D.; Lloyd, D.; McNab, H. *J. Chem. Soc. Perkin Trans. 1* **2002**, 1601.
11. Houk, K. N.; Sawicka ,D.; Li, Y. *J. Chem. Soc., Perkin Trans. 2*, **1999**, 2349.
12. Lee, H.-L.; Li, W.-K. *Org. Biomol. Chem.* **2003**, *1*, 2748.
13. Oth, J. F. M.; Röttele, H.; Schröder, G. *Tetrahedron Lett.*, **1970**, 61.
14. Oth, J. F. M.; Gillies, J.-M. *Tetrahedron Lett.*, **1968**, *60*, 6259.
15. Castro, C.; Isborn, C. M.; Karney, W. L.; Mauksch, M.; Schleyer, P. v. R. *Org. Lett.* **2002**, *4*, 3431.
16. Curtiss, L. A.; Redfern, P. C. *J. Chem. Phys.* **1999**, *110*, 4703.
17. Cheng, M.-F.; Li, W.-K. *J. Phys. Chem. A* **2003**, 107, 5492.
18. Lau, J. K.-C.; Li, W.-K.; Qi, F.; Suits, A. G. *J. Phys. Chem. A* **2002**, *106*, 11025.
19. Frisch, M. J.; Trucks, G. W.; Schlegel, H. B.; Scuseria, G. E.; Robb, M. A.; Cheeseman, J. R.; Zakrzewski, V. G.; Montgomery, J. A.; Stratmann, R. E.; Burant, J. C.; Dapprich, S.; Millam, J. M.; Daniels, A. D.; Kudin, K. N.; Strain, M. C.; Farkas, O.; Tomasi, J.; Barone, V.; Cossi, M.; Cammi, R.; Mennucci, B.; Pomelli, C.; Adamo, C.; Clifford, S.; Ochterski, J.; Petersson, G. A.; Ayala, P. Y.; Cui, Q.; Morokuma, K.; Malick, D. K.; Rabuck, A. D.; Raghavachari, K.; Foresman, J. B.; Cioslowski, J.; Ortiz, J. V.; Stefanov, B. B.; Liu, G.; Liashenko, A.; Piskorz, P.; Komaromi, P. I.; Gomperts, R.; Martin, R. L.; Fox, D. J.; Keith, T.; Al-Laham, M. A.; Peng, C. Y.; Nanayakkara, A.; Gonzalez, C.; Challacombe, M.; Gill, P. M. W.; Johnson, B. G.; Chen, W.; Wong, M. W.; Andres, J. L.; Head-Gordon, M.; Replogle, E. S.; Pople, J. A.; Gaussian 98, Revision A.9, Gaussian, Inc., Pittsburgh PA, 1998.
20. Gonzalez, C.; Schlegel, H. B. *J. Chem. Phys.* **1989**, *90*, 2154.
21. Gonzalez, C.; Schlegel, H. B. *J. Chem. Phys.* **1990**, *94*, 5523.

Chapter 5

A G3(MP2) Study on the Concerted Cycloaddition Reactions between Ethylene and Azines as well as Other Related Systems

Abstract

The concerted cycloaddition reactions between ethylene and azines as well as other related nitrogen-containing heterocyclic systems such as quinolene or other similar compounds have not been investigated experimentally or theoretically extensively. In this work, we study the concerted cycloaddition reactions between ethylene and eleven azines, as well as other related heterobicyclic aromatic systems, including quinolene, isoquinolene and 1,8-naphthyridine. For most of these reactions, there are two or more possible pathways. Upon obtaining the G3(MP2) barriers of all the possible pathways, it is found that three factors affect the activation energies of these processes. They are: (1) Whether a new C–N bond or C–C σ bond is formed? Our calculations indicate that the latter will lead to a smaller barrier. (2) The most favorable reaction site on the ring is the atom with the most positive charge. Often this is a carbon atom next to one or more nitrogen atoms on the ring(s). (3) In general, the pathway with the least disruption of the ring aromaticity is favored.

5.1 Introduction

Pericyclic reaction is one of the major classes of organic reactions. Chemists believe that the selectivity of these reactions depends on the HOMO-LUMO interaction as well as the HOMO and LUMO coefficients of the reactant(s).[1] In this work, we are concerned with the addition of ethylene to azines, quinolenes and related nitrogen-containing heterocyclic aromatic systems. For most of these reactions, there are two or more possible reaction pathways and it is not immediately obvious which of the pathways should have the lowest barrier.

For the reactions involving azines, usually two kinds of [2+4] cycloadditions are available, i.e., 1,4- and 2,5-addditions. Why is one pathway more favorable than the other cannot be explained by simply considering the HOMO-LUMO interaction of the reactants. In the present work, we report the calculated results on the

aforementioned Diels-Alder reactions. In addition, we suggest some factors that may affect the regioseletivty and reactivity of these reactions.

Previously[2] we applied ab initio and DFT methods to study the Diels-Alder reactivity and the aromaticity of four linear acenes, namely, naphthalene, anthracene, tetracene and pentacene. In total eight addition pathways between ethylene and four acenes were studied and it was found that all of the reactions are concerted and exothermic reactions. It was also found that the most reactive sites on the acenes are the center ring's meso-carbons. Furthermore, reactivity decreases along the series pentacene > tetracene > anthracene > naphthalene. These results are in good accord with the available experimental kinetics data. Hence it is clear that Diels-Alder reactions may be fruitfully studied by high-level computational methods.

5.2 Methods of Calculation

All calculations reported here have been carried out using the Gaussian 98 package of programs.[3] The method of calculation employed was G3(MP2).[4] This method has been described in Chapter1 previously.

In addition, for each reaction pathway studied, we identified a transition structure (TS). For each TS found, its "reactants" and "products" were confirmed by intrinsic reaction coordinate (IRC) calculations. [5,6]

In this work, all the species along the concerted pathway are taken to be closed-shell entities. The labels **1**, **2**, **3**, **4a**, **4b** (with **4a** and **4b** being isomers), ..., etc. refer to the reactants, while the products found are denoted by **2-PT-1**, **3-PT-1** (product of pathway **3-1**, the first addition reaction of reactant **3**), **3-PT-2** (product of pathway **3-2**, the second addition reaction of reactant **3**),..., etc. Furthermore, the TSs of the concerted reaction pathways are denoted as **2-TS-1**, **3-TS-1** (TS of pathway **3-1**), **3-TS-2** (TS of pathway **3-2**), ..., etc. [Refer to Figures. 1 and 2 for the identity of all the pathways, their reactants, TSs and products.] In the following discussion, all the energetic results refer to those obtained at 298 K.

5.3 Results and Discussion

5.3.1 Addition of ethylene to azines

All possible reaction pathways are schematically displayed in Figure 1. In the TSs shown in Figure 1, the C···C and/or C···N distances for the bonds about to be formed are also given. Table 1 lists the calculated total energies and total enthalpies

of all stationary points for Diels-Alder reactions between azines and ethylene. The energy barriers of these addition reactions are summarized in Table 2. In order to rationalize some of the computational results, it is convenient to make use of the Mulliken atomic charges on some atoms of the reactants. The Mulliken charges of all the atoms of all the reactants involved in the azine reaction pathways are tabulated in Table 3.

Table 1: The G3(MP2) total energies (E_0) and enthalpies (H_{298}) of all the species involved in the Diels-Alder reaction pathways between ethylene (1) and azines (2-7)

Species	Point Group	E_0 (Hartrees)	H_{298} (Hartrees)
Reactant			
1	D_{2h}	-78.43336	-78.42935
2	D_{6h}	-231.82845	-231.82281
3	C_{2v}	-247.86623	-247.86084
4a	C_{2v}	-263.87262	-263.86727
4b	C_{2v}	-263.90768	-263.90244
4c	D_{2h}	-263.90088	-263.89563
5a	C_{2v}	-279.88577	-279.88046
5b	C_s	-279.91068	-279.90545
5c	D_{3h}	-279.95270	-279.94757
6a	C_{2v}	-295.89496	-295.88958
6b	D_{2h}	-295.91528	-295.91004
6c	C_{2v}	-295.92661	-295.92138
7	C_{2v}	-311.90582	-311.90027
Transition State			
2-TS-1	C_{2v}	-310.20612	-310.19851
3-TS-1	C_s	-326.23019	-326.22284
3-TS-2	C_1	-326.25366	-326.24621
4a-TS-1	C_1	-342.25223	-342.24492
4a-TS-2	C_s	-342.26794	-342.26053
4b-TS-1	C_1	-342.28287	-342.27569
4b-TS-2	C_s	-342.30322	-342.29592
4c-TS-1	C_{2v}	-342.24963	-342.24238
4c-TS-2	C_2	-342.30026	-342.29301
5a-TS-1	C_s	-358.27551	-358.26826
5a-TS-2	C_1	-358.27933	-358.27205
5b-TS-1	C_1	-358.27808	-358.27093
5b-TS-2	C_1	-358.30295	-358.29578
5b-TS-3	C_1	-358.31616	-358.30886
5c-TS-1	C_s	-358.33688	-358.32987
6a-TS-1	C_s	-374.27979	-374.27260
6a-TS-2	C_1	-374.30090	-374.29363
6b-TS-1	C_2	-374.30399	-374.29691
6b-TS-2	C_{2v}	-374.33112	-374.32379

6c-TS-1	C_s	-374.31009	-374.30303
6c-TS-2	C_1	-374.32794	-374.32081
7-TS-1	C_1	-390.31012	-390.30294
7-TS-2	C_s	-390.32367	-390.31639
Product			
2-PT-1	C_{2v}	-310.25208	-310.24512
3-PT-1	C_s	-326.27103	-326.26420
3-PT-2	C_1	-326.30173	-326.29495
4a-PT-1	C_1	-342.29800	-342.29128
4a-PT-2	C_s	-342.32071	-342.31393
4b-PT-1	C_1	-342.32379	-342.31713
4b-PT-2	C_s	-342.35165	-342.34505
4c-PT-1	C_{2v}	-342.28836	-342.28165
4c-PT-2	C_2	-342.35028	-342.34370
5a-PT-1	C_s	-358.32510	-358.31845
5a-PT-2	C_1	-358.43067	-358.42131
5b-PT-1	C_1	-358.31836	-358.31172
5b-PT-2	C_1	-358.34973	-358.34318
5b-PT-3	C_1	-358.36935	-358.36278
5c-PT-1	C_s	-358.37662	-358.37011
6a-PT-1	C_s	-374.46939	-374.46019
6a-PT-2	C_1	-374.35129	-374.34446
6b-PT-1	C_2	-374.34711	-374.34057
6b-PT-2	C_{2v}	-374.38593	-374.37941
6c-PT-1	C_s	-374.34833	-374.34174
6c-PT-2	C_1	-374.47629	-374.46710
7-PT-1	C_1	-390.48017	-390.47104
7-PT-2	C_s	-390.37491	-390.36820

Table 2: The G3(MP2) barriers for the Diels-Alder reaction pathways between ethylene (1) and azines (2-7) at 298 K

Reaction	Barrier (kJ mol^{-1})
2-1	140.9
3-1	176.8
3-2	115.5
4a-1	135.7
4a-2	94.8
4b-1	147.3
4b-2	94.2
4c-1	216.9
4c-2	83.9
5a-1	99.1
5a-2	109.1
5b-1	167.7
5b-2	102.4
5b-3	68.1
5c-1	123.5
6a-1	121.6

6a-2	66.4
6b-1	111.5
6b-2	41.0
6c-1	125.2
6c-2	78.6
7-1	70.0
7-2	34.7

Table 3: The Mulliken charge on the C atoms or N atoms of ethylene (1) and azines (2-7) calculated at the MP2(Full)/6-31G(d) level

Species	Charge at position					
	1	2	3	4	5	6
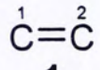 **1**	-0.354	-0.354	--	--	--	--
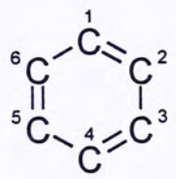 **2**	-0.200	-0.200	-0.200	-0.200	-0.200	-0.200
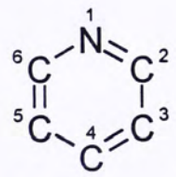 **3**	-0.521	0.065	-0.255	-0.144	-0.255	0.065
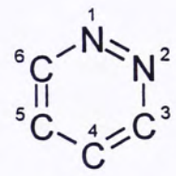 **4a**	-0.278	-0.278	0.024	-0.201	-0.201	0.024
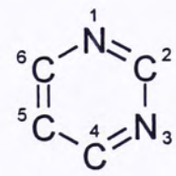 **4b**	-0.519	0.261	-0.519	0.097	-0.297	0.097
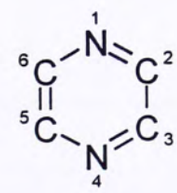 **4c**	-0.463	0.014	0.014	-0.463	0.014	0.014

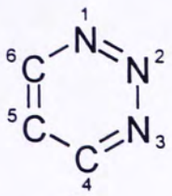 **5a**	-0.315	0.003	-0.315	0.080	-0.259	0.080
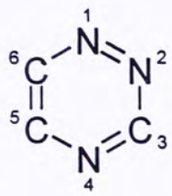 **5b**	-0.288	-0.226	-0.025	0.064	-0.479	0.241
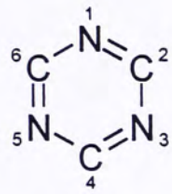 **5c**	-0.515	0.281	-0.515	0.281	-0.515	0.281
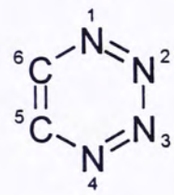 **6a**	-0.260	-0.032	-0.032	-0.260	0.034	0.034
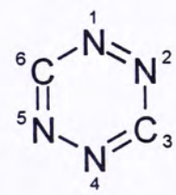 **6b**	-0.233	-0.233	0.211	-0.233	-0.233	0.211
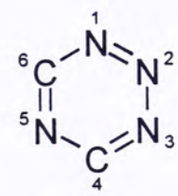 **6c**	-0.314	0.045	-0.314	0.276	-0.478	0.276
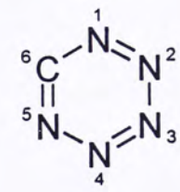 **7**	-0.267	0.027	-0.070	0.027	-0.267	0.278

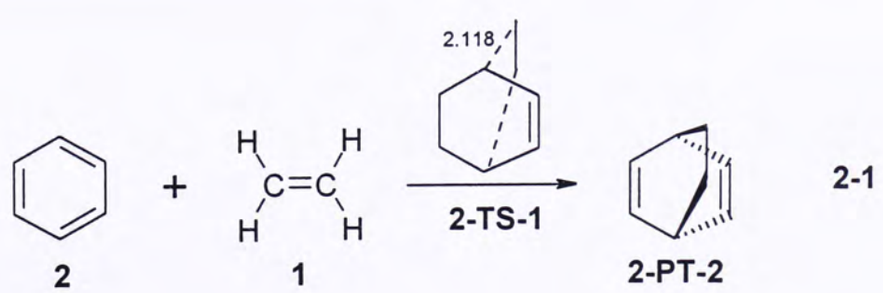

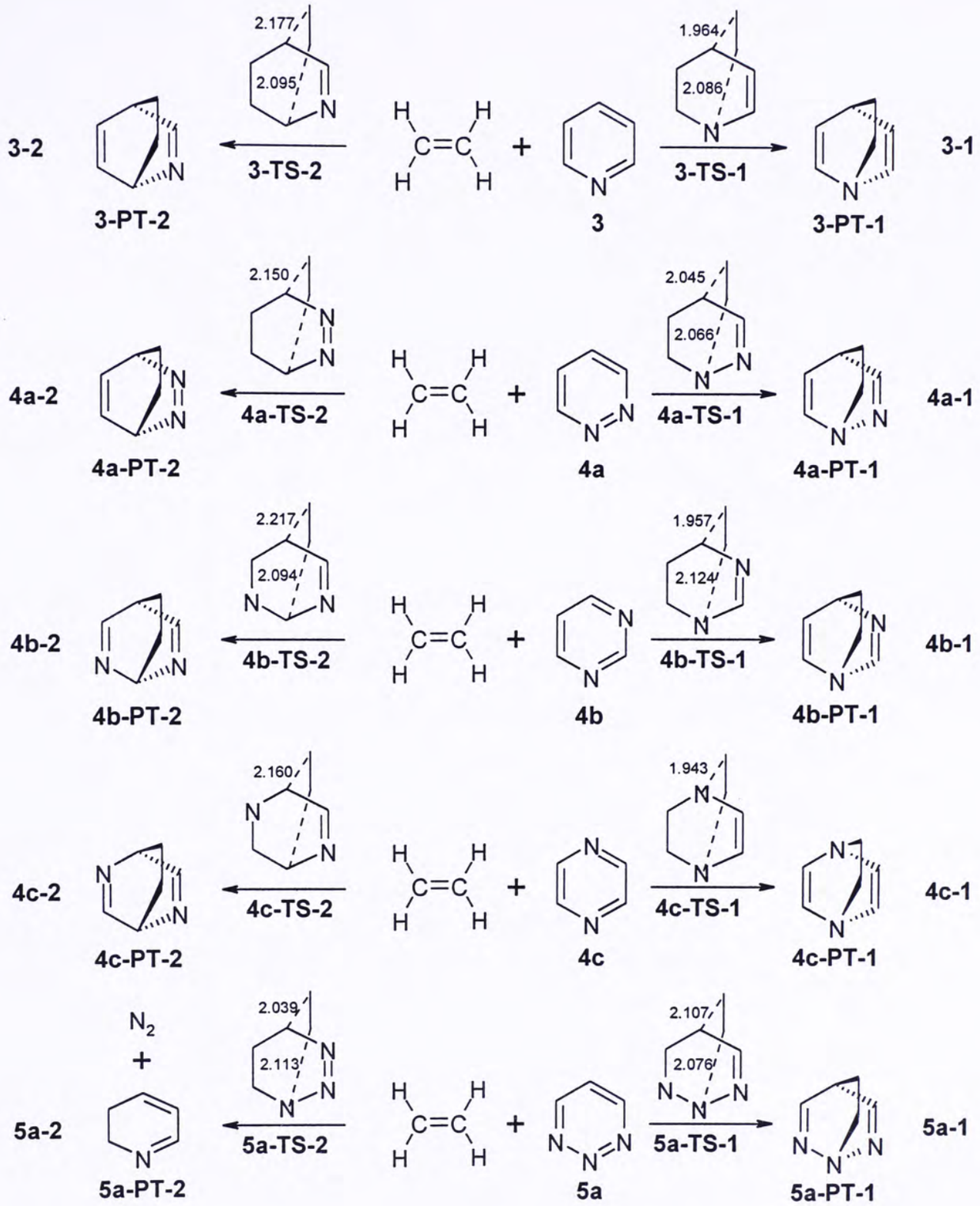
3-2
2.177
2.095
3-TS-2
3-PT-2
1.964
2.086
3-TS-1
3
3-PT-1
3-1
4a-2
2.150
4a-TS-2
4a-PT-2
2.045
2.066
4a-TS-1
4a
4a-PT-1
4a-1
4b-2
2.217
2.094
4b-TS-2
4b-PT-2
1.957
2.124
4b-TS-1
4b
4b-PT-1
4b-1
4c-2
2.160
4c-TS-2
4c-PT-2
1.943
4c-TS-1
4c
4c-PT-1
4c-1
N2
+
5a-2
2.039
2.113
5a-TS-2
5a-PT-2
2.107
2.076
5a-TS-1
5a
5a-PT-1
5a-1

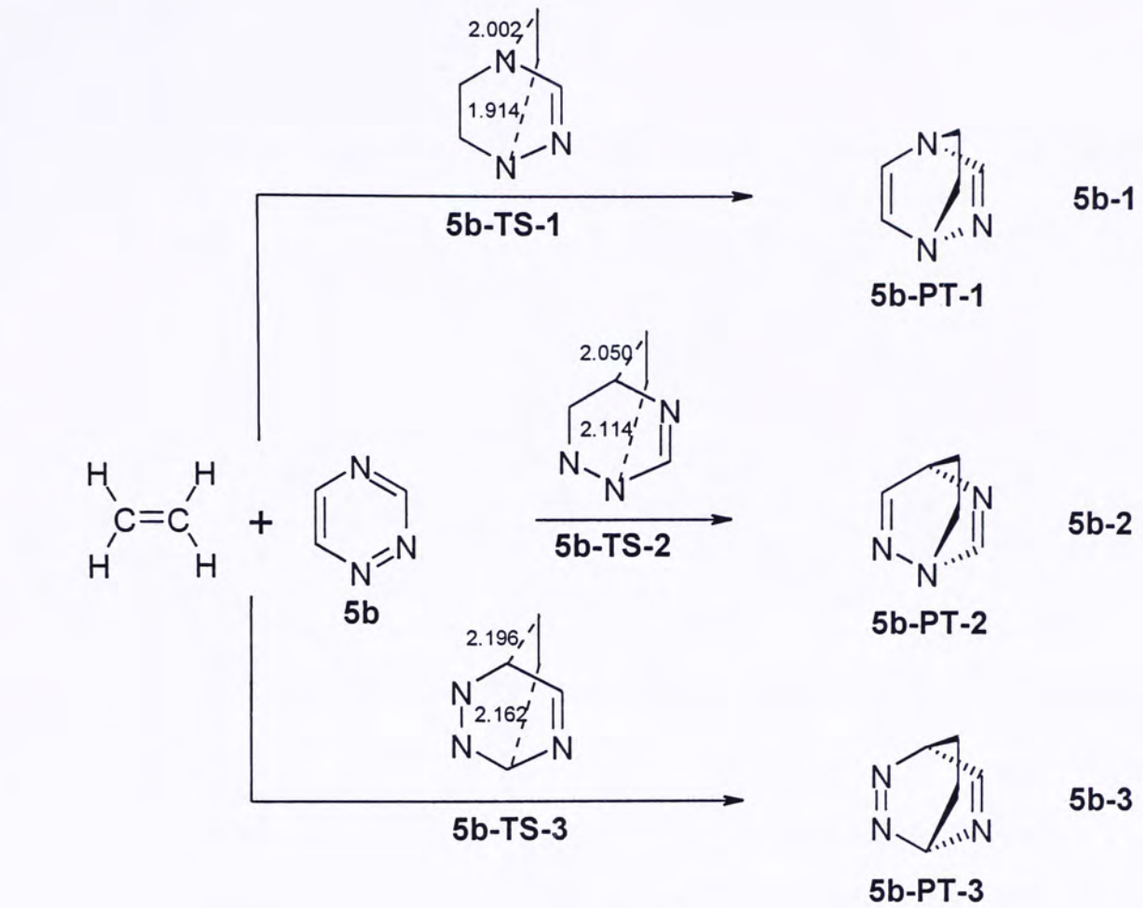
2.002
1.914
5b-TS-1
5b-PT-1
5b-1
2.050
2.114
5b-TS-2
5b-PT-2
5b-2
5b
2.196
2.162
5b-TS-3
5b-PT-3
5b-3

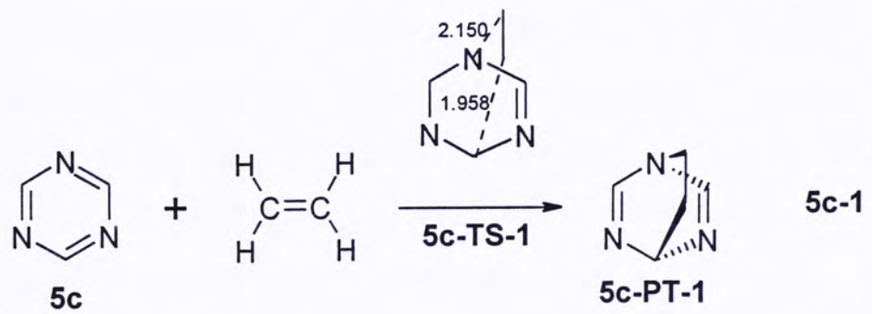
2.150
1.958
5c-TS-1
5c-PT-1
5c-1
5c

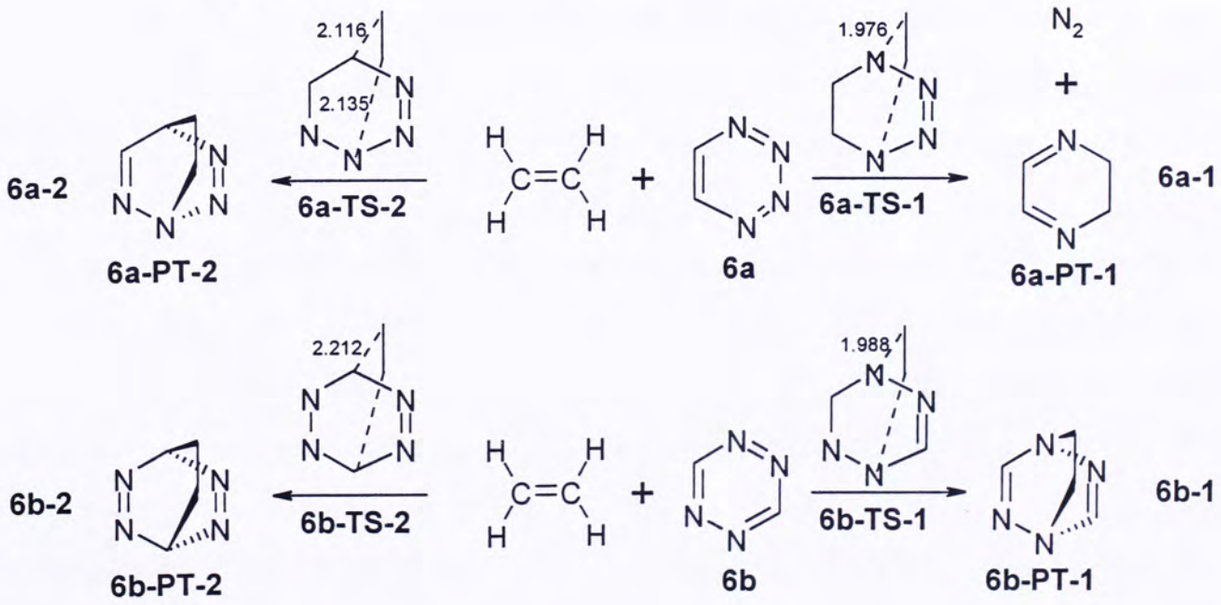
2.116
2.135
1.976
N2
6a-2
6a-TS-2
6a-TS-1
6a-1
6a-PT-2
6a
6a-PT-1
2.212
1.988
6b-2
6b-TS-2
6b-TS-1
6b-1
6b-PT-2
6b
6b-PT-1

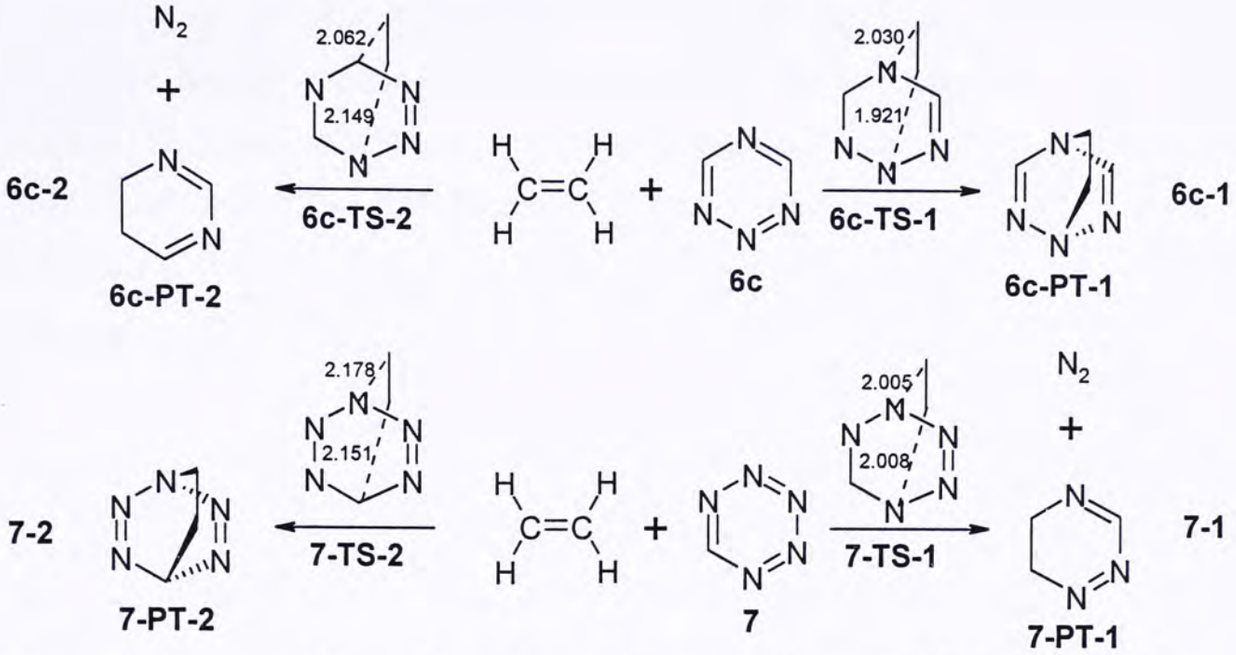

Figure 1. The possible reaction pathways between azines and ethylene studied in this work.

Examining these results, the following points may be noted:

(1) Using reaction **2-1** (between benzene and ethylene and with a barrier of 140.9 kJ mol^{-1}) as a reference, we now compare the barriers of reaction pathways **3-1** and **3-2**, which have pyridine and ethylene as their reactants. It is seen that pathway **3-1**, the 1,4-addition, has a larger barrier, 176.8 kJ mol^{-1}, while pathway **3-2**, the 2,5-addition, has a smaller barrier, 115.5 kJ mol^{-1}. One reason for this trend is that it is known that the overlap between the 2*p* orbitals for a C–C σ bond is more efficient than that for a C–N σ bond. At the same time, the resonance integral of C–C σ bond is also larger than that of a C–N σ bond.[1] Secondly, examining the Mulliken charges listed in Table 3, it is seen that the carbon atoms in ethylene have a charge of -0.354. For pyridine, the charge on N1 and C4 are -0.521 and -0.144, respectively, and those for C2 and C5 are 0.065 and -0.255, respectively. Based on these charges, it is clear the 1,4-addition is less favored than the 2,5-addition. Furthermore, based on the results of these two pathways, it may be *generally* concluded that the carbon atom next to a nitrogen atom is a favorable reaction site for the ethylene addition. Lastly, comparing the C···C and C···N distances found in **3-TS-1** and **3-TS-2** given in Figure 1, it is seen that the 2,5-addition (with a smaller barrier) has an earlier TS than the 1,4-addition (with a larger barrier). Such a trend is also found in the Diels-Alder reactions between ethylene and acenes.[2]

(2) For the reactions between ethylene and isomers of $C_4H_4N_2$, including pyridazine (**4a**), pyrimidine (**4b**) and pyrazine (**4c**), i.e., reaction pathways **4a-1**, **4a-2**, **4b-1**, **4b-2**, **4c-1** and **4c-2**, it is found that these processes follow essentially the same trend discussed above. For example, for the reactions involving **4a** or **4b**, the 2,5-addition (with two new C–C σ bonds formed) is energetically favored over the 1,4-addition (with one new C–C σ bond one new C–N σ bond formed). For those involving **4c**, again the 2,5-addition (with two new C–C σ bonds formed) is favored over the 1,4-addition (with two new C–N σ bonds formed).

(3) The remaining reactions listed in Figure 1 follow the same trend: The reaction involving the formation of new C–C σ bonds is favored over the reaction involving the formation of new C–N σ bonds.

(4) For the reactions between ethylene and 1,2,3-triazine (**5a**), there are two reaction routes, both involving the formation of one new C–C σ bond and one new C–N σ bond. Our G3(MP2) results indicate that the 2,5-addition is slightly favored (by 10 kJ mol^{-1}) over the 1,4-addition. This result may be rationalized in the following way. Previously it has been established that the formation of a new C–N σ bond is more difficult that the formation of a new C–C σ bond. In reaction pathway **5a-1** (the 2,5-addition between ethylene and **5a**), the atoms that form the new C–N bond have opposite Mulliken charges (-0.354 for C of ethylene and 0.003 for N2 of **5a**). On the other hand, in reaction **5a-2** (the 1,4-addition between the same two reactants), the two atoms that form the new C–N σ bond bear charges of the same sign (-0.354 for C of ethylene and -0.315 for N1 of **5a**). Based on these charges, it is now obvious that the 2,5-addition is favored.

(5) As indicated in Figure 1, reactions **5a-2**, **6a-1**, **6c-2** and **7-1** are not strictly addition reactions. For these reactions, starting from the TSs located, IRC calculations do not yield bridged ring products. Instead, they lead to mixture consisting of N_2 and a monocyclic product. For example, for reaction **5a-2**, the monocyclic product is 2,3-dihydro-pyridine. Such a finding is not unprecedented. In their study of the addition reaction between acetylene and 1,2,4,5-tetrazine (**6b**), Cioslowski and co-workers obtained the products of N_2 and pyridazine (**4a**).[7]

5.3.2 Addition of ethylene to quinolene, isoquinolene and 1,8-naphthyridine

Attention is now turned to the addition of ethylene to quinolene (**9**), isoquinolene (**10**) and 1,8-naphthyridine (**11**). This time the reference reaction is the Diels-Alder reaction between ethylene and naphthalene (**8**). All possible reaction pathways involving the additions of ethylene to **8** to **11** are schematically shown in Figure 2. Once again, in the TSs shown in Figure 2, the C···C and/or C···N distances for the bonds about to be formed are also given. Table 4 lists the calculated total energies and total enthalpies of all stationary points for these reactions. The activation energies of the reaction pathways are summarized in Table 5. The Mulliken atomic charges on each atom of **8** to **11** are summarized in Table 6.

Table 4: The G3(MP2) total energies (E_0) and enthalpies (H_{298}) of all the species involved in the Diels-Alder reaction pathways between ethylene (1) and naphthalene (8), quinolene (9), isoquinolene (10) or 1,8-naphthyridine (11)

Species	Point Group	E_0 (Hartrees)	H_{298} (Hartrees)
Reactant			
1	D_{2h}	-78.43336	-78.42935
8	D_{2h}	-385.21411	-385.20522
9	C_s	-401.25284	-401.24463
10	C_s	-401.25131	-401.24303
11	C_{2v}	-417.28964	-417.28175
Transition State			
8-TS-1	C_s	-463.60138	-463.59082
8-TS-2	C_1	-463.58002	-463.56978
9-TS-1	C_1	-479.62827	-479.61821
9-TS-2	C_1	-479.62970	-479.61966
9-TS-3	C_1	-479.62729	-479.61705
9-TS-4	C_1	-479.64166	-479.63139
9-TS-5	C_1	-479.61905	-479.60899
9-TS-6	C_1	-479.62180	-479.61174
10-TS-1	C_1	-479.62817	-479.61810
10-TS-2	C_1	-479.60135	-479.59130
10-TS-3	C_1	-479.64755	-479.63712
10-TS-4	C_1	-479.63977	-479.62949
10-TS-5	C_1	-479.61865	-479.60859
10-TS-6	C_1	-479.61862	-479.60854
11-TS-1	C_1	-495.66687	-495.65700
11-TS-2	C_1	-495.66577	-495.65579
11-TS-3	C_1	-495.66818	-495.65832
Product			
8-PT-1	C_s	-463.65659	-463.64683
8-PT-2	C_1	-463.61243	-463.60254
9-PT-1	C_1	-479.66272	-479.65301
9-PT-2	C_1	-479.66345	-479.65379
9-PT-3	C_1	-479.67624	-479.66664
9-PT-4	C_1	-479.69678	-479.68729
9-PT-5	C_1	-479.65176	-479.64209
9-PT-6	C_1	-479.62180	-479.61174
10-PT-1	C_1	-479.66220	-479.65250
10-PT-2	C_1	-479.63065	-479.62089
10-PT-3	C_1	-479.70483	-479.69527
10-PT-4	C_1	-479.69501	-479.68553
10-PT-5	C_1	-479.65109	-479.64142
10-PT-6	C_1	-479.65143	-479.64170
11-PT-1	C_1	-495.70114	-495.69166
11-PT-2	C_1	-495.71542	-495.70609
11-PT-3	C_1	-495.70404	-495.69457

Table 5: The G3(MP2) barriers for the Diels-Alder reaction pathways between ethylene (1) and naphthalene (8), quinolene (9), isoquinolene (10) or 1,8-naphthyridine (11) at 298 K

Reaction	Barrier (kJ mol^{-1})
8-1	114.9
8-2	170.1
9-1	146.4
9-2	142.6
9-3	149.5
9-4	111.8
9-5	170.6
9-6	163.4
10-1	142.5
10-2	212.9
10-3	92.6
10-4	112.6
10-5	167.5
10-6	167.6
11-1	142.0
11-2	145.2
11-3	138.6

Table 6: The Mulliken charge on the C atoms or N atoms of naphthalene (8), quinolene (9), isoquinolene (10) and 1,8-naphthyridine (11) calculated at the MP2(Full)/6-31G(d) level

Charge at Position	Species			
	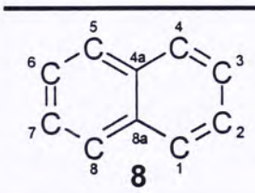 **8**	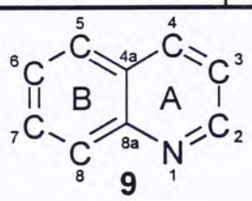 **9**	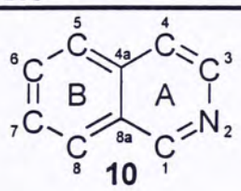 **10**	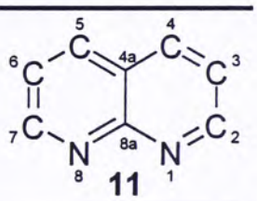 **11**
1	-0.203	-0.578	0.081	-0.539
2	-0.209	0.072	-0.535	0.077
3	-0.209	-0.272	0.049	-0.274
4	-0.203	-0.136	-0.258	-0.133
4a	0.006	-0.013	0.060	-0.055
5	-0.203	-0.203	-0.210	-0.133
6	-0.209	-0.211	-0.192	-0.274
7	-0.209	-0.204	-0.218	0.077
8	-0.203	-0.195	-0.189	-0.539
8a	0.006	0.252	-0.061	0.491

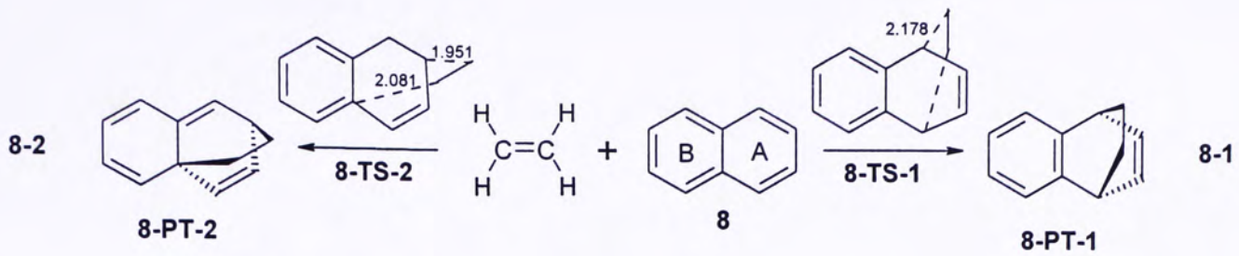
8-2
8-PT-2
8-TS-2
1.951
2.081
+
8
8-TS-1
2.178
8-PT-1
8-1

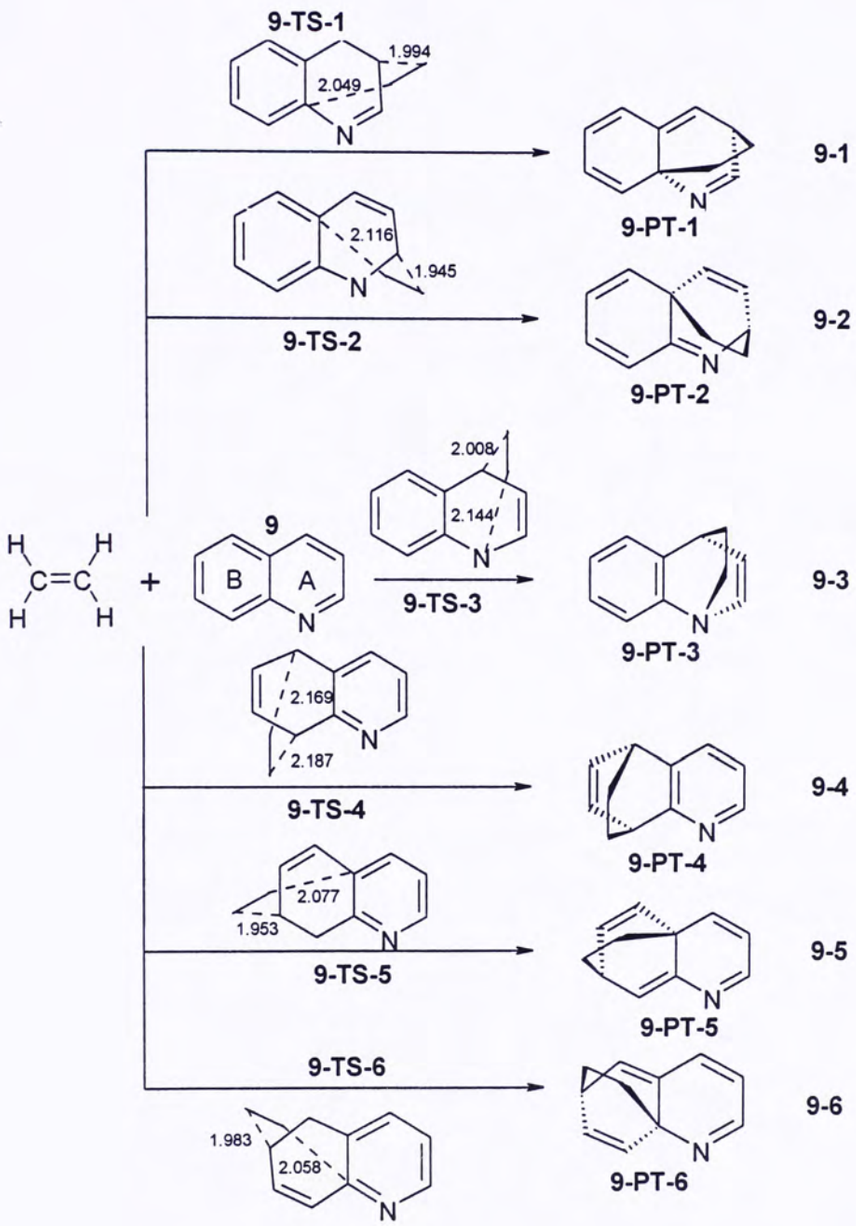
9-TS-1
1.994
2.049
9-1
9-PT-1
2.116
1.945
9-TS-2
9-2
9-PT-2
9
2.008
2.144
9-TS-3
9-3
9-PT-3
2.169
2.187
9-TS-4
9-4
9-PT-4
2.077
1.953
9-TS-5
9-5
9-PT-5
9-TS-6
9-6
9-PT-6
1.983
2.058

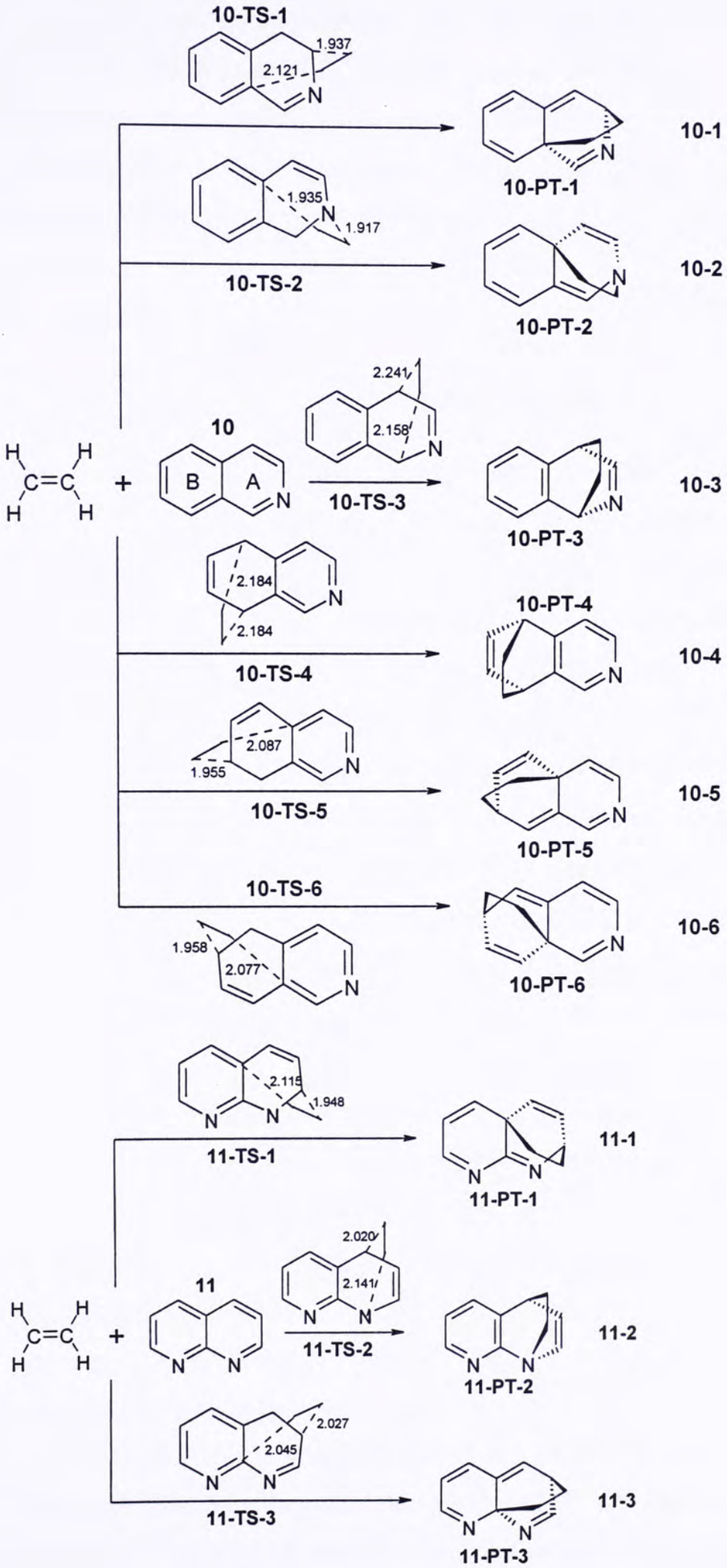

Figure 2. The possible reaction pathways between ethylene and naphthalene, quinolene, isoquinolene and 1,8-naphthyridine studied in this work.

Upon examining the results, the following points are noted:

(1) There are two possible routes for the addition reaction between naphthalene and ethylene, they are reaction pathways **8-1** and **8-2**, with barriers 114.9 and 170.1 kJ mol^{-1}, respectively. These results agree with our expectation, as **8-1** disrupts the aromticity of only ring A, where formation of new bonds takes place, while the aromaticity of ring B is retained. On the other hand, reaction **8-2** disrupts the aromtcitiy of both rings A and B. Therefore the activation energy barrier of reaction **8-1** is lower than that of reaction **8-2**. The difference between the barriers is fairly substantial, about 55 kJ mol^{-1}. This reaction is now taken as the reference reaction for the following processes.

(2) We now study the reaction between ethylene and quinolene (**9**), which has six following possible pathways: **9-1** to **9-6**. Upon comparing the barriers of these six pathways, it is seen that reaction **9-4**, the 5,8-addition, has the smallest barrier, 111.8 kJ mol^{-1}. This barrier is similar to that of reaction pathway **8-1**. Among the six pathways, only 1,4- (pathway **9-3**) and 5,8-additions do not disrupt the aromaticity of both rings A and B. Furthermore, 1,4-addition involves the formation of a new C–N σ bond which has already been established previously to be less favored in the Diels-Alder reaction when compared with the formation of a new C–C σ bond. As a result, the 5,8-addition reaction is preferred.

(3) For the reaction between ethylene and isoquinolene (**10**), there are again six possible pathways: **10-1** to **10-6**. Among the six possibilities, it is found that reaction pathway **10-3** (the 1,4-addition) is preferred, having a barrier of 92.6 kJ mol^{-1}. Indeed, the next favored reaction pathway, **10-4** (the 5,8-addition), has a barrier that is about 20 kJ mol^{-1} larger. Again, among the six possible pathways, only these two do not disrupt the aromaticity of both rings A and B. Additionally, for isoquinolene, the charge on C1 and C4 are 0.081 and -0.258, respectively, and those for C5 and C8 are -0.210 and -0.189, respectively. Based on these charges, it is clear the 1,4-addition is favored over the 5,8-addition. In other words, the carbon atom next to the nitrogen atom is generally the favored reaction site.

(4) For the addition reaction of ethylene to 1,8-naphthyridine (**11**), there are now only three possible pathways: **11-1** to **11-3**. The barriers of these pathways are very close to each other, being 142.0, 145.2 and 138.6 kJ mol^{-1}, respectively. At first it is surprising to see that the activation energy of the 1,4-addition (pathway **11-2**),

with the aromaticity of only one ring disrupted, is the highest among the three. However, upon examining the Mulliken charges on the atoms of 1,8-naphthyridine, it is seen that N1 and C4 have charges -0.539 and -0.133, respectively, those on C2 and C4a are -0.077 and 0.055, respectively, while those on C3 and C8a are -0.274 and 0.491, respectively. Among these charges, C8a has the highest positive charge, making it the most favorable reaction site. Thus the 3,8a-addition pathway is the most favored kinetically. Still, since the error bar for the G3(MP2) method is at best ±10 kJ mol^{-1}, the three barriers obtained are essentially the same. In passing, it is noted that, among the three products formed, **11-PT-2** is the most stable, by at least 30 kJ mol^{-1}. Thus pathway **11-2** is the most favored thermodynamically.

5.4 Conclusion

In this work, we have studied the concerted cycloaddition reactions between ethylene and azines as well as other related heterocyclic aromatic systems. It is found that three factors affect the activation energy of these reactions. They are: (1) Whether a new C–N bond or C–C σ bond is formed? Our calculations indicate that the latter is preferred. (2) The most favorable reaction site on the ring is the atom with the most positive Mulliken charge. (3) In general, the pathway with the least disruption of the ring aromaticity is favored.

5.5 References

1. Fleming, I. Frontier Orbitals and Organic Chemical Reactions, Wiley, London, 1976.
2. Frisch, M. J.; Trucks, G. W.; Schlegel, H. B.; Scuseria, G. E.; Robb, M. A.; Cheeseman, J. R.; Zakrzewski, V. G.; Montgomery, J. A.; Stratmann, R. E.; Burant, J. C.; Dapprich, S.; Millam, J. M.; Daniels, A. D.; Kudin, K. N.; Strain, M. C.; Farkas, O.; Tomasi, J.; Barone, V.; Cossi, M.; Cammi, R.; Mennucci, B.; Pomelli, C.; Adamo, C.; Clifford, S.; Ochterski, J.; Petersson, G. A.; Ayala, P. Y.; Cui, Q.; Morokuma, K.; Malick, D. K.; Rabuck, A. D.; Raghavachari, K.; Foresman, J. B.; Cioslowski, J.; Ortiz, J. V.; Stefanov, B. B.; Liu, G.; Liashenko, A.; Piskorz, P.; Komaromi, P. I.; Gomperts, R.; Martin, R. L.; Fox, D. J.; Keith, T.; Al-Laham, M. A.; Peng, C. Y.; Nanayakkara, A.; Gonzalez, C.; Challacombe, M.; Gill, P. M. W.; Johnson, B. G.; Chen, W.; Wong, M. W.;

Andres, J. L.; Head-Gordon, M.; Replogle, E. S.; Pople, J. A.; Gaussian 98, Revision A.9, Gaussian, Inc., Pittsburgh PA, 1998.

3. Curtiss, L. A.; Redfern, P. C. *J. Chem. Phys.* **1999**, *110*, 4703.
4. Gonzalez, C.; Schlegel, H. B. *J. Chem. Phys.* **1989**, *90*, 2154.
5. Gonzalez, C.; Schlegel, H. B. *J. Chem. Phys.* **1990**, *94*, 5523
6. Cheng, M.-F.; Li, W.-K. *Chem. Phys. Lett.* **2003**, *368*, 630.
7. Cioslowski, J.; Sauer, J.; Hetzenegger, J.; Karcher, T.; Hierstetter, T. *J. Am. Chem. Soc.* **1993**, *115*, 1353.

Chapter 6
Conclusion

Since conclusions have been made for each project in the respective chapter, we will not specifically comment on the chemical systems studied in this thesis. On the other hand we wish to mention that Gaussian-3 (G3) model and its variant, G3(MP2), have been employed to study the structures and energetics of several interesting systems. They include: the cycloaddition reaction between ethylene and butadiene, that between ethylene and hexatriene, as well as the electrocyclic reaction of hexatriene. Comparing with the experimental estimate, excellent agreements between the G3 results and experimental values are observed in the case where experimental estimate is available. In addition, we have used G3(MP2) model to study the electrocyclic reactions of [12]annulene. Furthermore, the same method has been used to study the concerted cycloaddition reactions between ethylene and azines as well as other related heterocyclic aromatic systems. Some interesting results and trends have been obtained for the studied reactions and systems. These results are reported and discussed in the respective chapters.

Appendix A

Energetic and Bonding Investigation of Phosphabenzene and Arsabenzene: A Gaussian-3 Study

Abstract

The structures and the heats of formation (ΔH_f) at 0 K and 298 K have been determined for phosphabenzene (PC_5H_5) and arsabenzene (AsC_5H_5), applying the Gaussian-3 (G3) model and its variant G3(MP2) and following the atomization scheme. After comparing the calculated results with available experimental data, it is found that the calculated structural parameters agree well with the experimental ones. According to the previous calculations, the calculated ΔH_f values for phosphabenzene and arsabenzene should be reliable: the error bar for the G3 model is roughly ±10 kJ mol^{-1}. In addition, the aromaticity of the topic compounds has been studied using the GIAO method. It is found that phosphabenzene and arsabenzene are comparably aromatic and both of them are more aromatic than pyridine. These results, as well as those found in the literature, are discussed in detail.

A.1 Introduction

Benzene and pyridine are familiar to all chemists in chemistry. Their properties and the properties of their derivatives have been studied thoroughly by both experiment and theory. However, the properties of the congeners of pyridine, phosphabenzene (PC_5H_5) and arsabenzene (AsC_5H_5), have not been well studied, though they were synthesized more than thirty years ago.[1] In this work, the structures, the heats of formation (ΔH_f) and aromaticity of the topic compounds are studied.

A.2 Methods of Calculation

All calculations reported here have been carried out using the Gaussian 98 package of programs.[2] The method of calculation employed were G3 and G3(MP2).[3,4] These methods have been described in Chapter 1.

In addition, Nucleus-Independent Chemical Shifts (NICS) calculations were carried out in order to study the aromaticity of the two compounds. The NICS – defined as a negative value of the absolute shielding – was computed at the ring centers at the HF/6-31+G(d) level of theory using the GIAO method,[5] based on the structure optimized at MP2(Full)/6-31G(d) level. The aromatic rings are those rings with negative NICS values: the more negative the index, the more aromatic the system. It is known that NICS values are not very sensitive to the basis set and the use of 6-31+G(d) is recommended. [5]

A.3 Results and Discussion

Table 1 lists the total energies at 0 K (E_0) and enthalpies at 298 K (H_{298}) for phosphabenzene and arsabenzene calculated at the G3 and G3(MP2) level. To convert these results into ΔH_f values the atomization scheme is applied. The G3 and G3(MP2) heats of formations at 0 K and 298 K for the two compounds are shown in Table 2. Furthermore, the structural parameters of the topic compounds, optimized at MP2(Full)/6-31G(d) level, are summarized in Table 3. The available experimental structural data are also included for ready comparison. The molecular structures and labeling of the atoms for the topic compounds are displayed in Figure 1. In addition, the NICS values of PC_5H_5 and AsC_5H_5 are compared with that of pyridine (also optimized at MP2(Full)/6-31G(d) level) and these results are summarized in Table 4.

Table 1: Total energies (in hartrees) at 0 K (E_0) and enthalpies at 298 K (H_{298}) for the phosphabenzene and arsabenzene calculated at the G3 and G3(MP2) levels

Compound	E_0		H_{298}	
	G3	G3(MP2)	G3	G3(MP2)
Phosphabenzene	-534.57914	-534.10486	-534.57324	-534.09895
Arsabenzene	-2428.67598	-2427.75732	-2428.66985	-2427.75120

Table 2: Heats of formation (kJ mol^{-1}) at 0 K (ΔH_{f0}) and 298 K (ΔH_{f298}) for phosphabenzene and arsabenzene calculated with the G3 and G3(MP2) models

Compound	E_0		H_{298}	
	G3	G3(MP2)	G3	G3(MP2)
Phosphabenzene	175.5	167.1	161.2	152.8
Arsabenzene	274.1	251.2	260.7	237.7

Table 3: Structural parameters (in Å and degrees) optimized at the MP2(Full)/6-31G(d) level for phosphabenzene and arsabenzene

Parameter	Calculated	Experimental
Phosphabenzene[a]		
PC^1	1.739	1.733±0.003
C^1C^2	1.393	1.413±0.010
C^2C^3	1.396	1.384±0.012
C^1PC^1	100.0	101.1±0.3
PC^1C^2	125.6	124.4±0.7
$C^1C^2C^3$	123.1	123.7±0.8
$C^2C^3C^2$	122.6	122.5
Arsabenzene[b]		
AsC^1	1.847	1.847±0.002
C^1C^2	1.390	1.388±0.009
C^2C^3	1.397	1.396±0.010
C^1AsC^1	97.3	97.0±0.33
AsC^1C^2	125.0	125.3±0.69
$C^1C^2C^3$	124.4	123.9±1.3
$C^2C^3C^2$	123.9	124.5±1.1

[a] Experimental data of this compound are taken from Ref. 6.
[b] Experimental data of this compound are taken from Ref. 7.

Table 4: Calculated NICS values of pyridine, phosphabenzene and arsabenzene based on structures optimized at the MP2(Full)/6-31G(d) level

Compound	NICS value
Pyridine	-8.2
Phosphabenzene	-9.5
Arsabenzene	-9.4

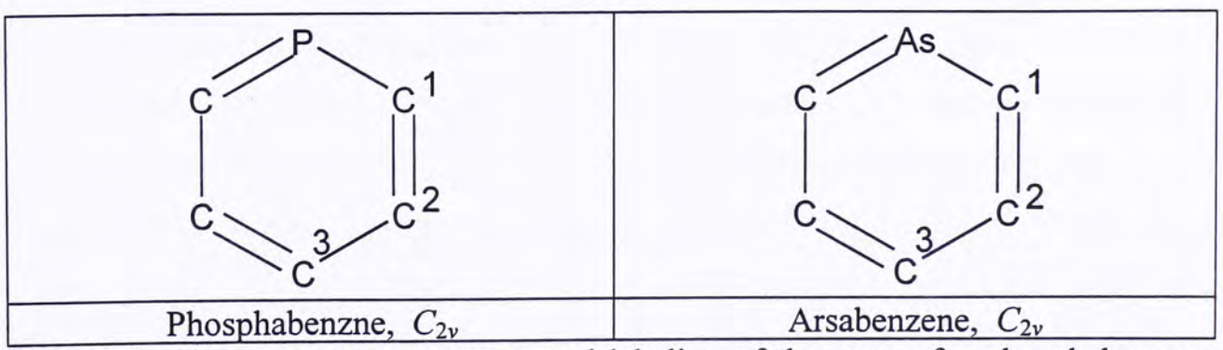

Phosphabenzne, C_{2v} | Arsabenzene, C_{2v}

Figure 1. The molecular structures and labeling of the atoms for phosphabenzene and arsabenzene.

Examining Table 2, it is seen that no experimental heats of formation are found in the literature. Nevertheless, according to our previous studies, the G3 and G3(MP2) models yield accurate results for aromatic systems,[8,9] so the energetic data obtained in this work should be reliable.

Upon comparing the calculated structural parameters with the available experimental data, it is found that the agreement is excellent. The only relatively large deviations are those for the C^1C^2 bond length (0.02 Å) and the C^2C^3 bond length (0.012 Å). It is noted that the uncertainty of the measurements on PC_5H_5 by Wong and Bartell[6] is quite large. In addition, our calculated C^1C^2 and C^2C^3 bond lengths are within error limits of the experimental data. Moreover, the experimental C^1C^2 and C^2C^3 bond lengths (1.413 and 1.384 Å, respectively) show fairly obvious bond alternation, while the calculated bond lengths (1.393 and 1.396 Å) do not. Since, experimentally, both pyridine (1.394 and 1.392 Å) and arsabenzene (1.388 and 1.396 Å) do not exhibit significant bond alternation (a similar trend is also obtained in calculations). Thus the bond lengths C^1C^2 and C^2C^3 of phosphabenzene should be similar, as the G3 and G3(MP2) results indicate.

Attention is now turned to the aromaticity of pyridine, as well as to its phosphorus and arsenic congeners. The NICS values of pyridine, phosphabenzene and arsabenzene are -8.2, -9.5 and -9.4 ppm, respectively. The results indicate that the aromaticity of phosphabenzene and arsabenzene are similar and, surprisingly, phosphabenzene and arsabenzene are more aromatic than pyridine. From the NBO analysis,[10] the nitrogen atom electrons of pyridine has a larger π electron population than the heteroatoms of phosphabenzene and arsabenzene. Hence, there is better π electron delocalization in phosphabenzene and arsabenzene than in pyridine.

The aromaticity of pyridine and phosphabenzene have also been determined by Bachrach using DFT method in 2002.[11] His results show that the aromaticity of pyridine and that of phosphabenzene are similar, i.e., -6.3 and -6.4 ppm, respectively. His calculated results are different from those of this work. The disagreement is due to the difference in geometry of the phosphabenzene. In Bachrach's calculation, carried out at the B3LYP/aug-cc-pVDZ level, the bond lengths PC^1, C^1C^2 and C^2C^3 are 1.7519, 1.3952 and 1.4000 Å, respectively. Compared to the experimental data of Wong and Bartell,[6] these results are not as good as ours. Specifically, Bachrach's PC^1 bond is too long, which leads to less effective overlap between the corresponding *p* orbitals. Hence, the magnitude of the ring current becomes smaller. Our optimized geometries are in excellent agreement with the experiment. Therefore, the aromaticity of the compounds obtained in this work should be more reliable.

A.4 Conclusion

The structures and the heats of formation of phosphabenzene and arsabenzene have been determined using the G3 and G3(MP2) models. Upon comparing the results, it is found that the optimized geometrical parameters in this work are in excellent agreement with the experimental ones. While there are no experimental energetic data for phosphabenzene and arsabenzene, the G3 and G3(MP2) results reported here should be reliable estimates. In addition, the aromaticity of the topic compounds has been studied using the GIAO method. It is found that phosphabenzene and arsabenzene are comparably aromatic and both of them are more aromatic than pyridine. These results, as well as those found in the literature, are discussed in detail.

A.5 References

1. Ashe III, A. J. *J. Am. Chem. Soc.* **1971**, *93*, 3293.
2. Frisch, M. J.; Trucks, G. W.; Schlegel, H. B.; Scuseria, G. E.; Robb, M. A.; Cheeseman, J. R.; Zakrzewski, V. G.; Montgomery, J. A.; Stratmann, R. E.; Burant, J. C.; Dapprich, S.; Millam, J. M.; Daniels, A. D.; Kudin, K. N.; Strain, M. C.; Farkas, O.; Tomasi, J.; Barone, V.; Cossi, M.; Cammi, R.; Mennucci, B.; Pomelli, C.; Adamo, C.; Clifford, S.; Ochterski, J.; Petersson, G. A.; Ayala, P. Y.; Cui, Q.; Morokuma, K.; Malick, D. K.; Rabuck, A. D.; Raghavachari, K.; Foresman, J. B.; Cioslowski, J.; Ortiz, J. V.; Stefanov, B. B.; Liu, G.; Liashenko, A.; Piskorz, P.; Komaromi, P. I.; Gomperts, R.; Martin, R. L.; Fox, D. J.; Keith, T.; Al-Laham, M. A.; Peng, C. Y.; Nanayakkara, A.; Gonzalez, C.; Challacombe, M.; Gill, P. M. W.; Johnson, B. G.; Chen, W.; Wong, M. W.; Andres, J. L.; Head-Gordon, M.; Replogle, E. S.; Pople, J. A.; Gaussian 98, Revision A.9, Gaussian, Inc., Pittsburgh PA, 1998.
3. Curtiss, L. A.; Redfern, P. C. *J. Chem. Phys.* **1998**, *109*, 7764.
4. Curtiss, L. A.; Redfern, P. C. *J. Chem. Phys.* **1999**, *110*, 4703.
5. Schleyer, P. v. R. *J. Am. Chem. Soc.* **1996**, *118*, 6317.
6. Wong, T. C. Bartell, L. S. *J. Chem. Phys.* **1974**, *61*, 2840.
7. Wong, T. C. Bartell, L. S. *J. Mol. Struct. (Theochem)* **1978**, *44*, 169.
8. Cheng, M.-F.; Ho, H.-O.; Lam, C.-S.; Li, W.-K. *J. Serb. Chem. Soc.* **2002**, *67*, 257.
9. Cheng, M.-F.; Li, W.-K. *J. Phys. Chem. A* **2003**, *107*, 5492.

10. Reed, A. E.; Curtiss, L. A.; Weinhold, F. *Chem. Rev.* **1988**, *88*, 899.
11. Bachrach, S. M. *J. Organomet. Chem.* **2002**, *643-644*, 39.

Appendix B

Energetics and Bonding Study of Hexamethylenetetramine (HMT) and Fourteen Related Cage Molecules: A G3(MP2) Investigation

Abstract

The G3(MP2) method of theory has been applied to hexamethylenetetramine (HMT) and fourteen related cage systems. The agreement between calculated and available experimental molecular dimensions as well as the heats of formation (ΔH_f) at 0 K and 298 K ranges from satisfactory to excellent.

B.1 Introduction

Hexamethylenetetramine (HMT) is a white, crystalline, water-soluble powder, used as a vulcanization accelerator, an absorbent in gas masks, in the manufacture of the explosive RDX and synthetic resins, and in medicine as a diuretic and urinary antiseptic. It was discovered by Butlerow[1,2] over a century ago, and it was the first organic compound to have its molecular structure and crystal structure elucidated by X-ray analysis. A large number of its salts, molecular adducts and coordination complexes have been reported in literature. Relevant information of HMT, the physical and chemical properties, as well as its industrial and physiological uses are available in book form.[3-5]

The experimental dimensions of four derivatives of HMT, namely $[(CH_2)_6N_4H]^+$,[6] $(CH_2)_6N_4O$,[7] $(CH2)_6N_4BH_3$[8] and $[(CH_2)_6N_4CH_3]^+$ [9,10] have been determined by X-ray crystallography. In these four cases, quaternization of one N atom markedly differentiates the H_2C–N single bonds in the heterocyclic cage system into three types. Moving away from the formally positive quaternary N atom, the three types of bonds vary in the order long : short : normal with respect to the standard value of 1.476(2) Å in crystalline HMT.[11]

In this work, a structural and energetics G3(MP2) study has been carried for the following cage species: HMT (**a**), $[(CH_2)_6N_4H]^+$ (**b**), $[(CH_2)_6N_3(CH)]$ (**c**), $[(CH_2)_6N_3BH]^-$ (**d**), $(CH_2)_6N_4O$ (**e**), $(CH2)_6N_4BH_3$ (**f**), $(CH2)_6N_3BNH_3$ (**g**), $[(CH_2)_6N_4CH_3]^+$ (**h**), $[(CH_2)_6N_3CNH_3]^+$ (**i**), $[(CH_2)_6N_3PH]^+$ (**j**), $(CH_2)6N_3PO$ (**k**), $(CH2)_6N_3PBH_3$ (**ℓ**), $(CH2)_6N_3BPH_3$ (**m**), $[(CH_2)_6N_3PCH_3]^+$ (**n**), and

$[(CH_2)_6N_3CPH_3]^+$ (**o**). Among these 15 species, there are several isoelectronic pairs as well as some other pairs which bear interesting inverse relationships to each other. Where possible, the calculated results will be compared with experimental data.

B.2 Methods of Calculation

All calculations reported here have been carried out using the Gaussian 98 package of programs.[12] The method of calculation employed was G3(MP2).[13] This method has been described in Chapter 1.

B.3 Results and Discussion

Figure 1 shows the optimized structures (bond lengths in Å and angles in degrees) of HMT and fourteen other caged systems. These structures have been optimized at the MP2(Full)/6-31G(d) level. Where available, the experimental structural parameters are given in parentheses. Table 1 summarizes the total G3(MP2) energies at 0 K (E_0) and total enthalpies at 298 K (H_{298}) as well as the heats of formation (ΔH_f) at 0 K and 298 K.

(a)

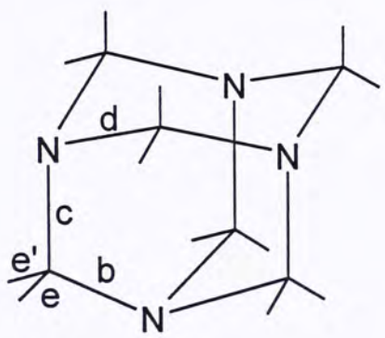

T_d symmetry
b = c = d = 1.470 [1.476], e = 1.096 [1.088]
bc = 113.0 [113.6], cd = 107.6 [107.2]
ee' = 108.5 [106]

(b)

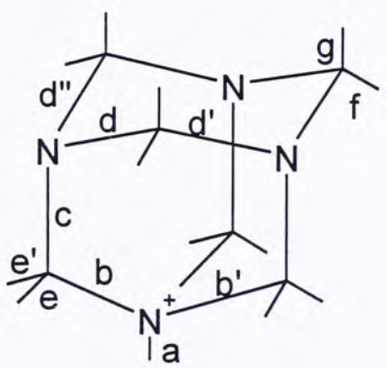

C_{3v} symmetry
a = 1.031, b = 1.540 [1.512], c = 1.428 [1.458],
d = 1.471 [1.465], e = 1.094, f = 1.094, g = 1.092
ab = 110.7, bb' = 108.1 [109.7],
bc = 109.2 [108.5], cd = 109.7 [108.8],
dd' = 111.1 [112.7], dd" = 108.9 [108.4],
ee' = 110.1, fg = 108.6

(c)

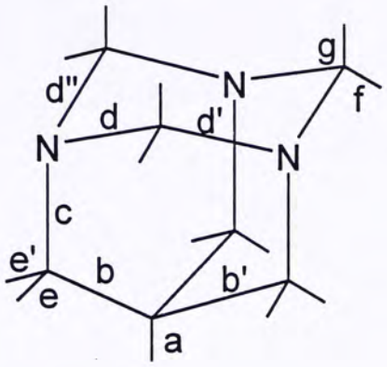

C_{3v} symmetry
a = 1.099, b = 1.534, c = 1.473, d = 1.468
e = 1.098, f = 1.096, g = 1.096
ab = 110.9, bb' = 108.0,bc = 110.4,
cd = 108.5, dd' = 113.8, ee' = 107.5
fg = 108.5

(d)

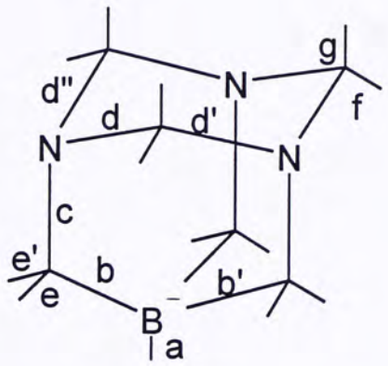

C_{3v} symmetry
a = 1.236, b =1.635, c = 1.503, d = 1.465,
e = 1.104, f = 1.098, g = 1.102
ab = 113.1, bb' = 105.6, bc = 110.5,
cd = 108.7, dd' = 116.2, dd" = 106.7,
ee' = 105.8, fg = 108.3

(e)

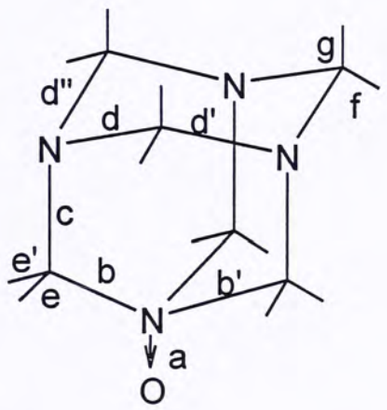

C_{3v} symmetry
a = 1.347 [1.363], b = 1.508 [1.514],
c = 1.450 [1.445], d = 1.470 [1.474],
e = 1.093, f = 1.095, g = 1.095
ab = 111.4 [111.4], bb' = 107.4 [107.4],
bc = 111.7 [111.4], cd = 108.5 [109.5],
dd' = 109.3 [111.6], dd" = 108.1 [107.2],
ee' = 109.3, fg = 108.8

(f)

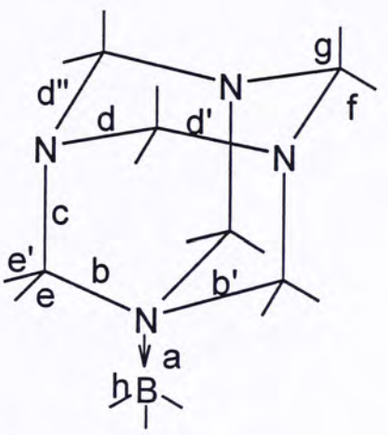

C_{3v} symmetry
a = 1.623 [1.661], b = 1.501 [1.527],
c = 1.451 [1.475], d = 1.469 [1.475],
e = 1.094 [1.03], f = 1.095 [1.04]],
g = 1.095 [1.02], h = 1.213 [1.08]
ab = 111.4 [111.5], ah = 105.3 [117],
bb' = 107.5 [107.4], bc = 111.8 [111.4],
cd = 108.5 [108.2], dd' = 112.3 [112.7],
dd" = 108.1 [108.5], ee' = 109.0 [110],
fg = 108.7 [109]

(g)

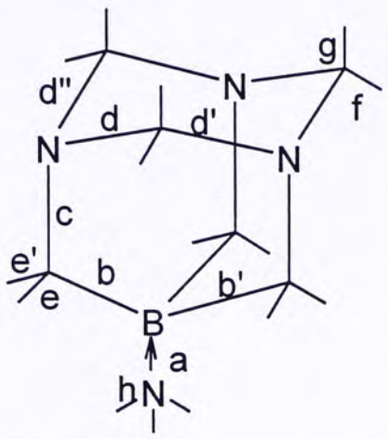

C_{3v} symmetry
a = 1.637, b = 1.612, c = 1.492, d = 1.468,
e = 1.103, f = 1.097, g = 1.098, h = 1.023
ab = 110.2, ah = 111.3, bb' = 108.8,
bc = 107.1, cd = 109.1, dd' = 115.5,
dd" = 107.3, ee' = 106.2, fg = 108.3

(h)

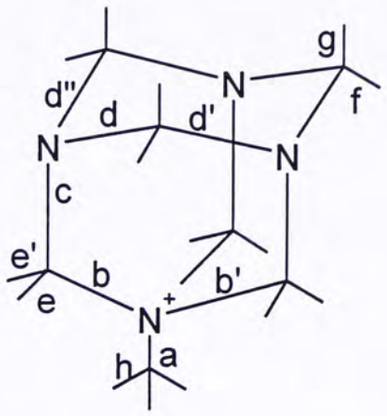

C_{3v} symmetry
a = 1.480 [1.47], b = 1.539 [1.53],
c = 1.428 [1.45], d = 1.470 [1.45],
e = 1.095, f = 1.094, g = 1.092, h = 1.092
ab = 111.7 [111], ah = 109.1, bb' = 107.1 [107],
bc = 110.5 [110], cd = 109.6 [109],
dd' = 111 [112], dd" = 108.9 [109], ee' = 109.9,
fg = 108.7

(i)

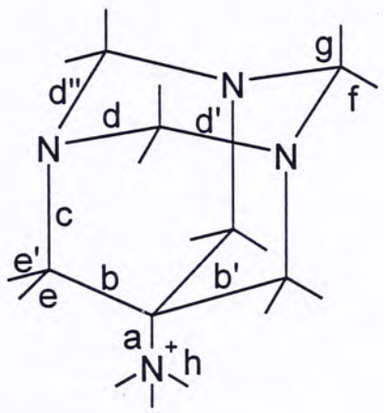

C_{3v} symmetry
a = 1.513, b = 1.535, c = 1.460, d = 1.470,
e = 1.110, f = 1.095, g = 1.093, h = 1.031
ab = 109.8, ah = 111.5, bb' = 109.1,
bc = 108.6,cd = 109.0, dd' = 112.8,
dd" = 108.3, ee' = 108.1, fg = 108.4

(j)

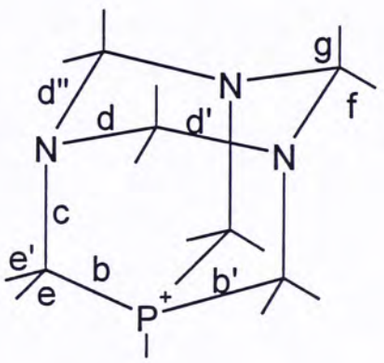

C_{3v} symmetry
a = 1.407, b = 1.846, c = 1.459, d = 1.470,
e = 1.095, f = 1.095, g = 1.093
ab = 116.1, bb' = 102.2, bc = 106.7, cd = 112.3,
dd' = 113.6, dd" = 108.9, ee' = 108.5, fg =108.4

(**k**)

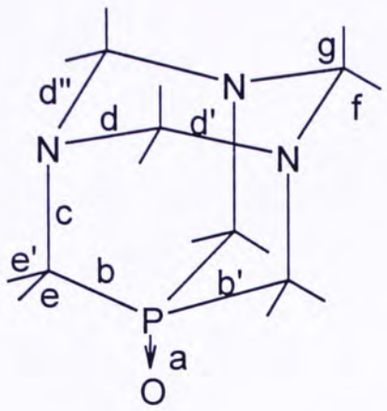

C_{3v} symmetry
a = 1.507, b = 1.835, c = 1.476,
d =1.467,e = 1.097, f = 1.095,
g = 1.096ab = 118.4, bb' = 99.3,
bc = 111.1, cd = 111.0, dd' = 114.9,
dd" = 108.1, ee' = 107.2, fg = 108.4

(ℓ)

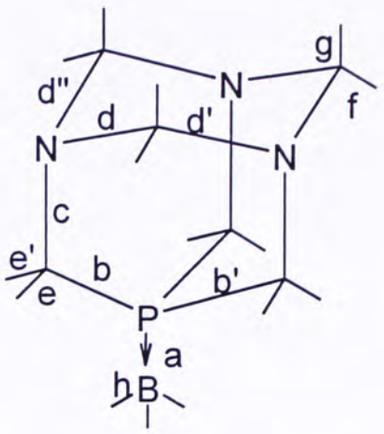

C_{3v} symmetry
a = 1.916, b = 1.846 , c = 1.469, d = 1.468,
e = 1.096, f = 1.096, g = 1.096, h = 1.211
ab = 119.0, ah = 104.9, bb' = 98.5, bc = 111.7,
cd = 111.1, dd' = 114.9, dd" = 108.1,
ee' = 107.3, fg = 108.5

(**m**)

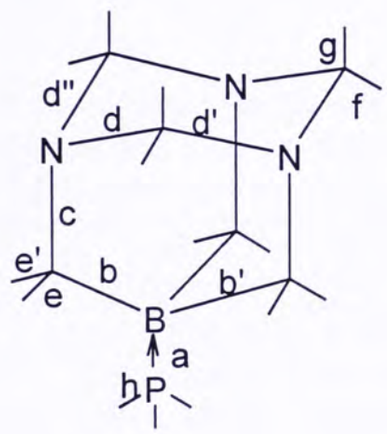

C_{3v} symmetry
a = 1.944, b = 1.622, c = 1.489, d = 1.467,
e = 1.101, f = 1.097, g = 1.097, h = 1.407
ab = 110.2, ah = 117.4, bb' = 108.8,
bc = 106.6, cd = 109.4, dd' = 115.3,
dd" = 107.4 ee' = 106.6, fg = 108.5

(**n**)

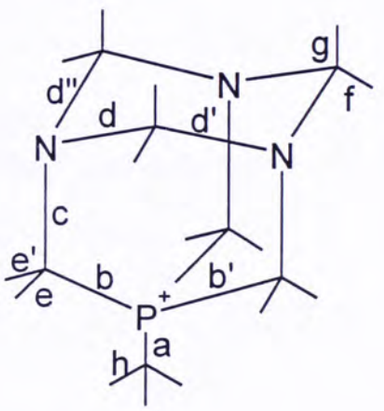

C_{3v} symmetry
a = 1.806, b = 1.839, c = 1.462, d = 1.470,
e = 1.096, f = 1.095, g = 1.094, h = 1.094,
ab = 116.4, ah = 109.9, bb' = 101.7,
bc = 107.6,cd = 112.0, dd' = 113.9,
dd" = 108.8, ee' = 108.1, fg = 108.3

(**o**)

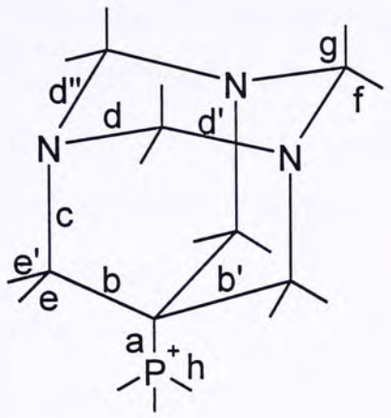

C_{3v} symmetry
a = 1.797, b = 1.558, c = 1.456, d = 1.469,
e = 1.098, f = 1.095, g = 1.094, h = 1.400,
ab = 110.8, ah = 112.4, bb' = 108.1, bc = 109.1,
cd = 109.3, dd' = 112.6, dd" = 108.3,
ee' = 108.3, fg = 108.5

Figure 1. The optimized structures (bond lengths in Å and bond angles in degrees) of HMT and 14 other closely related caged systems. Where available, experimental data are given in parentheses.

Table 1. Total energies (in hartrees) at 0 K (E_0), enthalpies at 298 K (H_{298}), heats of formation (ΔH_f) at 0 K and 298 K for HMT and fourteen related cage systems calculated with the G3(MP2) method

Compound	E_0 (Hartrees)	H_{298} (Hartrees)	ΔH_{f0} (kJ mol^{-1})	ΔH_{f298} (kJ mol^{-1})	Experiment (kJ mol^{-1})
a	-454.09018	-454.08284	258.6	206.2	199.0[a]
b	-454.44873	-454.44114	850.8	794.8	
c	-438.05754	-438.04993	186.3	134.0	
d	-424.85355	-424.84528	89.8	38.8	
e	-529.12421	-529.11599	389.2	335.3	
f	-480.68294	-480.67361	203.6	142.7	
g	-480.70211	-480.69183	153.2	94.8	
h	-493.69074	-493.68166	815.2	754.0	
i	-493.68432	-493.67501	832.1	711.5	
j	-740.68707	-740.67832	861.4	807.3	
k	-815.53228	-815.52287	-45.9	-97.8	
ℓ	-766.92604	-766.91499	201.6	144.1	
m	-766.90914	-766.89781	246.0	189.2	
n	-779.94832	-779.93765	775.2	717.1	
o	-779.90183	-779.89162	897.3	838.0	

[a] Experimental ΔH_{f298} of HMT (**a**) is taken from Ref. 8.

Upon examining Figure 1, the following points are noted. The optimized structure of **a**, HMT, is in good accord with the experimental data. However, for the other systems where experimental data are available, the agreement is less satisfactory. For **b**, the protonated HMT at one of the nitrogens, CH_2–N bond b is lengthened and bond c is shortened, whereas bond d is normal, with respect to the standard value of 1.476 Å in crystalline HMT (1.470 Å, calculated). Both the lengthening and shortening effects on bonds b and c are overestimated. The calculated result suggests that protonation has very little effect on the CNC angles, where N is the protonated nitrogen atom.

For $(CH_2)_6N_4O$ (**e**), HMT oxide, all the calculated parameters are in good agreement with the experimental values, except the N–O bond. The interaction of N–O bond is overestimated. As a result, the calculated N–O bond length (1.347 Å) is shorter than the experimental one (1.363 Å). Again, the formation of the N–O bond has little effect on the CNC angles, where N now is the nitrogen atom that forms the N–O bond.

For $(CH2)_6N_4BH_3$ (**f**), HMT→BH_3, the agreement between calculation and experiment is not as good as those for HMT (**a**), protonated HMT (**b**) and HMT oxide (**e**). Once again, the effect of the formation of the dative covalent B–N bond is overestimated. The calculated bond length is 1.623 Å, while the experimental value is 1.661 Å. In addition, the calculated bond angle NBH is 105.3°, which is significantly smaller than the experimental value of 117°. Moreover, except the CH_2–N bond d, all the calculated CH_2–N bond lengths are about 0.02 Å off. On the other hand, for the unknown compound $(CH2)_6N_3BNH_3$ (**g**), which is an isomer of **f**, the calculated N–B dative covalent bond of **g** is slightly longer than that of **f**. This result differs from that of the previous MNDO calculation,[14] which suggests that the N–B bond of **f** should be longer than that of **g**, but the present ab initio calculations give the opposite result.

When HMT forms an adduct with other atom or molecule, bond b is lengthened from the standard CH_2–N bond length of 1.476 Å to about 1.5 Å. In addition, bond c is shortened in most cases, from 1.476 Å to about 1.45 Å, and bond d is essentially unchanged. The lengthening of bond b in **b** facilitates the acid-catalyzed fragmentation of HMT.[6]

For cages **d** and **g**, the bond B–C distances are 1.635 and 1.612 Å, respectively. This is much longer than the B–C bond, 1.564 Å, found in the adamantane-like molecule $(MeB)_6(CH)_4$,[15] which has trigonal planar sp^2 hybridization for each B atom. On the other hand, the unknown compound **c** is isoelectronic to HMT. The bond distances of bonds c and d of compound **c** are relatively unchanged, even though one of the nitrogen atoms is replaced by CH group.

Compound **h**, considered as an adduct of HMT and H_3C^+, the optimized structure is in fairly good accord with the experimental data, except the calculated bond c is 0.022 Å too short and bond d is 0.02 Å too long. On the other hand, unknown compound **i** is isoelectronic to **h**. The calculated bond a of **i** is longer than that of **h** by 0.033 Å. An interesting finding is that bond b of **i**, a C–C bond, is almost as long as bond b of **h**, a C–N bond. This calculation also shows that bond c of **i** is longer than that of **h** by 0.032 Å, while bond d of these two compounds are the same.

Unknown compounds **j**, **k**, **ℓ**, **m**, **n** and **o** are the congeners of **b**, **e**, **f**, **g**, **h** and **i**, respectively. Comparing the bond c and d of these compounds and their corresponding congener, bond c of these unknown compounds are longer than that of their corresponding congeners by about 0.02 to 0.03 Å while bond d remain unchanged in most cases, except compounds **m** and **o**. For compound **m** and its congener **g**, bond b of **m** is longer than that of **g** by 0.01 Å, bond c and d of these two compounds are about the same. For compound **o** and its congener **i**, bond b of **o** is longer than that of **i** by 0.023 Å. Once again, bond c and d of this pair congeners are about the same. Unknown compounds **ℓ** and **m** are isoelectronic, the P–B bond of **ℓ** is shorter than that of **m** by 0.028 Å, bond c of **ℓ** is shorter than that of **m** by 0.02 Å, while their bond d are about the same. Unknown compounds **n** and **o** are also isoelectronic. The P–C bond of **n** is shorter than that of **n** by 0.009 Å, while their bond c and d are about the same.

The heats of formation of HMT and fourteen related cage systems have been calculated using the G3(MP2) models. Unfortunately, only the experimental heat of formation of HMT at 298 K is available for comparison. For this particularly compound, the G3(MP2) value, 206.2 kJ mol^{-1}, is in very good agreement with the experimental result, 199.0 kJ mol^{-1}. Indeed, the deviation is well within the

uncertainty of the G3(MP2) method, 10-15 kJ mol^{-1}. Hence the calculated heats of formation for the 14 cage systems related to HMT should be reliable estimates.

B.4 Conclusion

We have applied the high-level ab initio method of G3(MP2) to HMT and fourteen related cage systems. The agreement between calculated and available experimental molecular dimensions for five of these 15 species ranges from satisfactory to excellent. In addition, there is excellent agreement between the calculated and experimental heat of formation at 298 K for HMT. Hence the calculated heats of formation for the other 14 cage species should be accurate estimates.

B.5 References

1. Butlerow, A. *Justus Liebigs Ann.Chem.* **1859**, *111*, 250.
2. Butlerow, A. *Justus Liebigs Ann.Chem.* **1860**, *115*, 322.
3. Walker, J. Formaldehyde, Reinhold, New York, 3rd Ed. 1964.
4. Dickinson, R. G.; Raymond, A. L. *J. Am. Chem. Soc.* **1923**, *45*, 22.
5. Gonnell, H. W.; Mark, Z. *Phys. Chem.* **1923**, *107*, 191.
6. Mak, T. C. W.; Li, W. K.; Yip, W. H. *Acta Crystallogr.* **1983**, *C39*, 134.
7. Mak, T. C. W.; Ladd, M. F. C.; Povey, D. C. *J. Chem. Soc. Perkin Trans. 2.* **1979**, 593.
8. Hanic, F.; Šubtrová, V. *Acta Crystallogr. Sect. B* **1969**, *25*, 405.
9. Hon, P. K.; Mak. T. C. W.; Trotter, J. *Inorg. Chem.* **1979**, *18*, 2916.
10. Hon, P. K.; Mak. T. C. W.; Trotter, J. *Z. Kristallogr.* **1982**, *158*, 213.
11. Becka, L. N.; Cruickshank, D. W. J. *Proc. R. Soc. London, Ser. A.I* ***1963,*** 273, 435.
12. Frisch, M. J.; Trucks, G. W.; Schlegel, H. B.; Scuseria, G. E.; Robb, M. A.; Cheeseman, J. R.; Zakrzewski, V. G.; Montgomery, J. A.; Stratmann, R. E.; Burant, J. C.; Dapprich, S.; Millam, J. M.; Daniels, A. D.; Kudin, K. N.; Strain, M. C.; Farkas, O.; Tomasi, J.; Barone, V.; Cossi, M.; Cammi, R.; Mennucci, B.; Pomelli, C.; Adamo, C.; Clifford, S.; Ochterski, J.; Petersson, G. A.; Ayala, P. Y.; Cui, Q.; Morokuma, K.; Malick, D. K.; Rabuck, A. D.; Raghavachari, K.; Foresman, J. B.; Cioslowski, J.; Ortiz, J. V.; Stefanov, B. B.; Liu, G.; Liashenko, A.; Piskorz, P.; Komaromi, P. I.; Gomperts, R.; Martin, R. L.; Fox, D. J.; Keith,

T.; Al-Laham, M. A.; Peng, C. Y.; Nanayakkara, A.; Gonzalez, C.; Challacombe, M.; Gill, P. M. W.; Johnson, B. G.; Chen, W.; Wong, M. W.; Andres, J. L.; Head-Gordon, M.; Replogle, E. S.; Pople, J. A.; Gaussian 98, Revision A.9, Gaussian, Inc., Pittsburgh PA, 1998.

13. Curtiss, L. A.; Redfern, P. C. *J. Chem. Phys.* **1999**, *110*, 4703.
14. Ip, W.-K.; Li, W.-K.; Mak, T.C.W. *J. Mol. Struct. (THEOCHEM)* **1982**, *90*, 177.
15. Payment, I.; Shearer, H. M. M. *J. Chem. Soc.* **1977**, *Dalton Trans.* 136.

Appendix C

The Gaussian-3 Theoretical Models

The mathematical details of the Gaussian-3 (G3) methodologies as well as the variant of the G3 method, G3(MP2), are presented below.

C.1 The G3 Theory

The G3 energy is the approximation of the energy calculated at the ab initio QCISD(T)/G3large level. It involves geometry optimization at the MP2(Full)/6-31G(d) level. Also, vibrational frequency calculations at the MP2(Full)/6-31G(d) level for the zero-point vibrational energy (ZPVE), thermal corrections, and a semi-empirical higher-level correction (HLC) are required. Based on the optimized geometry, several single-point energy calculations are performed, and the G3 energy is given as follows.

The G3 energy:

$$E(G3) = E_{base} + \Delta E(QCI) + \Delta E(+) + \Delta E(2df) + \Delta E(G3large) + \Delta E(SO) + 0.9661 \times ZPVE_{MP2} + HLC_{G3}, \quad (1)$$

where E_{base} = E[MP4SDTQ/6-31G(d)],

$\Delta E(QCI)$ = E[QCISD(T)/6-31G(d) – MP4SDTQ/6-31G(d)],

$\Delta E(+)$ = E[MP4SDTQ/6-31+G(d) – MP4SDTQ/6-31G(d)],

$\Delta E(2df)$ = E[MP4SDTQ/6-31G(2df,p) – MP4SDTQ/6-31G(d)],

$\Delta E(G3large)$ = E[MP2(full)/G3large – MP2/6-31G(2df,p) – MP2/6-31+G(d) + MP2/6-31G(d)],

$ZPVE_{MP2}$ = ZPVE at MP2(Full)/6-31G(d),

$HLC_{G3} = -6.386\times10^{-3}n_\beta - 2.977\times10^{-3}(n_\alpha - n_\beta)$ and $-6.219\times10^{-3}n_\beta - 1.185\times10^{-3}(n_\alpha - n_\beta)$, for molecular and atomic species, respectively. Here $n_\alpha \geq n_\beta$ and n_α and n_β are the numbers of α and β valence electrons, respectively.

$\Delta E(SO)$ is spin-orbit correction for atomic species, and is taken from experiment or accurate theoretical calculations in the case where no experimental data are available.

C.2 The G3(MP2) Theory

In the G3(MP2) procedure, the basis-set-extension corrections is obtained at MP2 level, instead of the MP4 level in G3, thus eliminating the MP4 calculations: The G3(MP2) energy:

$$E(G3(MP2)) = E[QCISD(T)/6\text{-}31G(d)] + \Delta E_{MP2} + \Delta E(SO) + 0.9661 \times ZPVE_{MP2} + HLC_{G3(MP2)}, \quad (2)$$

where $\Delta E_{MP2} = E[MP2/G3MP2large - MP2/6\text{-}31G(d)]$,

$HLC_{G3(MP2)} = -9.729\times10^{-3} n_\beta - 4.471\times10^{-3}(n_\alpha - n_\beta)$ and

$-9.345\times10^{-3} n_\beta - 2.021\times10^{-3}(n_\alpha - n_\beta)$ for molecular and atomic species, respectively.

Appendix D
Calculation of Enthalpy at 298 K, H_{298}

The theoretical energies obtained with the Gaussian-n methods refer to isolated molecules at 0 K with stationary nuclei, while thermochemical measurements are carried out with vibrating molecules at finite temperature, usually 298 K. Hence, comparison of theoretical results with experimental data normally requires zero-point vibrational energy and thermal corrections. From statistical mechanics, and assuming ideal gas behavior, the difference between the enthalpy at finite temperature (H_T) and the energy at 0 K (E_0) is given by

$$H_T - E_0 = E_T^{trans} + E_T^{rot} + E_T^{vib} + RT$$

where $E_T^{trans} = \frac{3}{2}RT$,

$E_T^{rot} = \frac{3}{2}RT$ (for a non-linear molecule)

$E_T^{rot} = RT$ (for a linear molecule) or 0 (for an atom)

$E_T^{vib} = E_T^{vib} - E_0^{vib}$

$= \sum_i^{3n-6} \frac{h\nu_i}{\exp(h\nu_i / kT) - 1}$, where ν_i's are scaled harmonic frequencies.

(for a non-linear molecule)

$= \sum_i^{3n-5} \frac{h\nu_i}{\exp(h\nu_i / kT) - 1}$, where ν_i's are scaled harmonic frequencies.

(for a linear molecule)